# REVIEW OF DIAGNOSTICS FOR NEXT GENERATION LINEAR ACCELERATORS

M. Ross, Stanford Linear Accelerator Center, Stanford, CA 94309, USA


### *Abstract*

New electron linac designs incorporate substantial advances in critical beam parameters such as beam loading and bunch length and will require new levels of performance in stability and phase space control. In the coming decade, e- (and e+) linacs will be built for a high power linear collider (TESLA, CLIC, JLC/NLC), for fourth generation X-ray sources (TESLA FEL, LCLS, Spring 8 FEL) and for basic accelerator research and development (Orion). Each project assumes significant instrumentation performance advances across a wide front.

This review will focus on basic diagnostics for beam position and phase space monitoring. Research and development efforts aimed at high precision multi-bunch beam position monitors, transverse and longitudinal profile monitors and timing systems will be described.


## 1 INTRODUCTION

Next generation linacs have smaller beam sizes, increased stability and improved acceleration efficiency. They will be used for single pass free electron lasers (FEL) [1], linear colliders (LC) [2] and advanced accelerator research and development [3]. Table 1 shows the evolution of beam parameters from the SLAC Linear Collider (SLC) toward the next generation projects. Performance improvements of a factor 10 are typical. If we consider older, more conventional linacs, the relative changes in performance parameters are more impressive, often as much as a factor of 1000. In addition, there are special locations within the linac system where the beam requirements are much more stringent: for example at the LC interaction point or within the FEL undulator.

Table 1: Next generation linac parameter comparison for SLC (1985), the SLAC Linac Coherent Light Source (LCLS) and the Next Linear Collider (NLC).

| | SLC | LCLS | NLC |
|---|---|---|---|
| σ_x (μm) | 90 | 30 | 7 |
| σ_y (μm) | 50 | 30 | 1 |
| σ_z (μm) | 1300 | 30 | 100 |
| peak I (A) | 700 | 3400 | 1000 |
| power density ($W/m^2$) | 2e13 | 1e12 | 1e18 |

It is evident that new technology and different physical principles, such as diffraction radiation and Compton scattering, are needed in order to extend the performance of diagnostics to meet the challenge [4]. In this paper we will review ideas and tests of diagnostics for measuring electron beam position, profile (transverse and longitudinal) and loss.

## 2 POSITION

### *2.1 Purposes*

High peak current linacs require accurate, well referenced, beam position monitors (BPM's) to suppress the interaction between the RF structure and the beam. In addition, equally as important, the small beam must pass close to the center of each quadrupole magnet in order to avoid emittance dilution arising from the dispersion generated from a small dipole kick. Some LC designs include two separate BPM systems in each linac. Typical requirements are shown in table 2.

Table 2: NLC Linac quadrupole BPM performance requirements

| Parameter | Value | Conditions |
|---|---|---|
| Resolution | 300 nm rms | @ $10^{10}$ $e^-$ single bunch |
| Position Stability | 1 μm | over 24 hours |
| Position Accuracy | 200 μm | wrt the quad magnetic center |
| *x,y* dynamic range | ±2 mm | |
| Q dynamic range (per bunch) | $5\times10^8$ to $1.5\times10^{10}$ $e^-$ | |

The most challenging requirement is the long-term position stability, ~ $2\times10^{-4}$ $r_0$ ($r_0$=BPM radius). The planned resolution is ~ $6\times10^{-5}$ $r_0$; both are a factor of 50 improvement over BPMs used in the SLC.

The BPM's are in continual use by an automated steering loop that keeps the beam centered in the accelerating structure and the quadrupole magnets. The model for operation of the linac assumes that a second, presumably more intrusive, automatic quadrupole beam centering procedure is implemented once per day, as required by long term BPM drifts.

BPM system requirements for the FEL are tightest in the undulator itself. For full coherent emission saturation, the beam and the light it has generated must remain superimposed throughout the undulator. Surprisingly, longitudinal considerations rather than transverse set the steering tolerances. The difference between the x-ray

# Instrumentation and Diagnostics Using Schottky Signals

F. Nolden, GSI, Darmstadt, Germany

*Abstract*

Schottky signal measurements are a widely used tool for the determination of longitudinal and transverse dynamical properties of hadron beams in circular accelerators and storage rings [1]. When applied to coasting beams, it is possible to deduce properties as the momentum distribution. the $Q_{x,y}$ values and the average betatron amplitudes. Scientific applications have been developed in the past few years, as well, namely nuclear Schottky mass spectrometry and lifetime measurements.

Schottky signals from a coasting beam are random signals which appear at every revolution harmonic and the respective betatron sidebands. Their interpretation is more or less straightforward unless the signal is perturbed by collective effects in the case of high phase space density.

Schottky signals from bunched beams reveal the synchrotron oscillation frequency, from which the effective rf voltage seen by the beam can be deduced.

The detection devices can be broad-band or narrow-band. The frequency range is usually in the range between a few hundred kHz up to about 150 MHz. In connection with stochastic cooling, Schottky signals are used at frequencies up to 8 GHz. Narrow-band devices are needed if signal-to-noise problems arise, e.g. in the case of antiproton beams. Heavy ion beams require less effort, it is relatively easy to detect single circulating highly charged ions.

## 1 SCHOTTKY SPECTRA

### 1.1 Coasting beam current

Imagine a detector at some given location in the storage ring. The beam current at this given place is the sum of the currents from each charged particle passing by. Let us assume that the beam is composed of $N$ particles of a single species with charge $qe$. These particles are characterized in the longitudinal phase plane by their revolution period $T_n$ (which we assume to be constant). Secondly, they are ordered randomly along the ring circumference. One way to parameterize this random placement is to stop the time $t_n$ the particle passes by the detector during the revolution $k = 0$. The beam current is the sum over all particles $n$:

$$I(t) = qe \sum_{n=1}^{N} \sum_{k=-\infty}^{\infty} \delta(t - t_n - kT_n) \qquad (1)$$

The frequency spectrum, i.e. the Fourier transform of this current is an infinite train of delta functions, as well,

$$\tilde{I}(\Omega) = qe \sum_{n=1}^{N} \omega_n \sum_{k=-\infty}^{\infty} \delta(\Omega - k\omega_n) \exp(-i\Omega t_n) \qquad (2)$$

i.e. the current spectrum consists of peaks at each harmonic of the revolution frequency $\omega_n = 2\pi/T_n$ with a random phase. The mathematics of this Fourier correspondence can be found in most textbooks on signal theory. Because of the random phase, the expectation value of $\tilde{I}(\Omega)$ vanishes. However, the cancellation of the phases is never complete due to the finite number of particles in the beam. Therefore the power spectrum of the random process $I(t)$ can be detected, as we shall see. Before doing so, let us look at the distribution of the frequencies $\omega_n$. The variation of the revolution frequencies around their mean value $\omega_0$ is proportional the the deviation of the particle momenta $p$ from their mean $p_0$:

$$\frac{\delta\omega}{\omega_0} = \eta \frac{\delta p}{p_0} \qquad (3)$$

with the frequency dispersion

$$\eta = \gamma^{-2} - \alpha_p \qquad (4)$$

Here, $\gamma$ is the relativistic Lorentz factor, and $\alpha_p$ is the momentum compaction factor of the ring lattice. $\alpha_p$ is related to the transition $\gamma_t$ by $\alpha_p = \gamma_t^{-2}$. Once $\eta$ is known, it is possible to infer from the beam current frequency spectrum the momentum width of the beam. It is sufficient to measure the spectrum at one given harmonic. This is one of the main applications of Schottky diagnosis. If the momentum distribution is bounded by a momentum deviation $\pm\delta p_{\max}$, then there is a harmonic $k_{\max}$ above which the correspondence $\Omega(\delta p)$ ceases to be unique, i.e. where the Schottky harmonics begin to overlap:

$$k_{\max} > \frac{1}{2} \left| \eta \frac{\delta p_{\max}}{p_0} \right|^{-1} \qquad (5)$$

The width of the frequency distribution is proportional to the harmonic number.

Signal detectors are linear devices which respond to the beam with a voltage

$$u(t) = \frac{qeZ_L}{2} \sum_{n=1}^{N} \omega_n \sum_{k=-\infty}^{\infty} S(x_{kn}, y_{kn}, t) * \delta(t - t_n - kT_n) \qquad (6)$$

# DIAGNOSTICS AND INSTURMENTATION FOR FEL

M. E. Couprie, Service de Photons, Atomes et Molécules, Saclay, and Laboratoire d'Utilisation du Rayonnement Électromagnétique, Orsay, France

*Abstract*

*Free Electron Laser are coherent sources of radiation based on the interaction of a relativistic electron beam in an undulator field. According to the energy of the accelerator, they presently cover a wide spectral range, from the infra-red to the VUV. FELs combine the diagnostics of typical laser systems (for the measurement of spectral and temporal characteristics, the transverse mode pattern, the polarisation) and the diagnostics of relativistic electron beams. The electron beam is characterised in order to evaluate and control the FEL performances, but also in order to measure the effect of the FEL on the electron beam. The FEL characteristics are monitored with various types of detectors, depending mainly on the spectral range. Diagnostics for Linac based Infra Red FELs and storage ring FELs in the UV-VUV will be described. Particular instrumentation, required for FEL operation, such as the optical resonator, possible diagnostics inside the undulator will also be analysed.*

## 1 INTRODUCTION

The development of FELs followed the pioneering ideas [1] and experiment led by J. M. J. Madey in 1977 in the infra-red at Stanford on a linear accelerator [2]. The second FEL oscillation was then achieved in Orsay, on the storage ring ACO, in the visible range in 1983 [3]. Since then, a large number of simple and advanced undulators have been built and integrated into FELs. FEL facilities provide a fully coherent tuneable light in a wide spectral range for scientific applications in various domains.

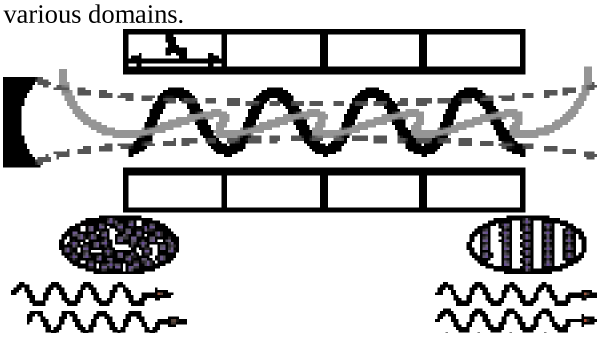

Fig.1 FEL principle

As illustrated in figure 1, Free Electron Laser (FEL) oscillation results from the interaction of an optical wave with a relativistic electron beam circulating in the periodic ppermanent magnetic field of an undulator (period $\lambda_o$ and peak magnetic field $B_o$ along the vertical direction y). The relativistic particles are transversely accelerated and emit synchrotron radiation, at the resonant wavelength $\lambda_r$ and its harmonics :

$$\lambda_r = \frac{\lambda_0}{2\gamma^2}\left(1+K^2/2\right) \qquad (1)$$

with the deflection parameter K = 0.94 $\lambda_o$(cm) $B_o$(T) and $\gamma$ the normalised energy of the electrons. The interaction between the optical wave and the electron bunch occurs along the undulator progression. Generally, an optical resonator, the length of which is adapted to the recurrence of the electron bunches, allows the radiation to be stored and the interaction to take place at each passage. The optical wave and the charged particles exchange energy, which can lead to a modulation of the electronic density at the wavelength of light (microbunching), phasing the emission and reinforcing the coherence of the produced radiation. An additional second order energy exchange between the optical wave and the electron beam leads to a non linear amplification of the stored towards saturation is reached (the gain of the system becomes equal to the cavity losses); meanwhile the spectral and temporal widths narrow. Through the system constituted by the relativistic electron beam in the undulator, coherent harmonics can be produced from an external laser source or from the FEL itself.

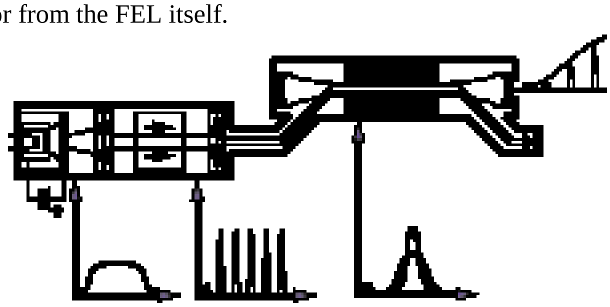

Fig. 2 : LINAC based FEL

By changing the deflection parameter K or the electron energy, one changes the resonant wavelength. As result, the FEL is intrinsically a tuneable source of radiation. The undulator period is typically a few cm long, therefore the higher the electron energy, the shorter the wavelength. FELs on low energy accelerators (MeV range) operate in the microwave and far infra red ranges, FELs on intermediate energy accelerators (50 MeV) cover the mid infra-red and ultra-violet ranges, and systems on higher energy accelerators (100 MeV-GeV) reach the UV, VUV and X-ray ranges. The gain is lower for higher energies, and optics are easily available in the infra-red. Therefore, the FEL was developed faster in the infrared (the first FEL oscillation was achieved in the UV in 1988 in

# REVIEW OF EMITTANCE AND STABILITY MONITORING USING SYNCHROTRON RADIATION MONITORS

K.Holldack, J.Feikes and W.B. Peatman, BESSY, Berlin, Germany

*Abstract*

Different techniques of emittance and stability monitoring using bend magnet and undulator radiation will be reviewed. Besides imaging methods for emittance monitoring , the problem of XBPM's used for the measurement of the centre of mass position of the undulator beams will be treated in detail. The key feature of these monitors is a careful electron optical design to take account of gap dependent changes of the shape and photon energy of the undulator beam as well as spurious signals from dipoles and high heat load. The reason for the fact that these monitors work well on low energy machines like BESSY II but often fail due in high energy machines will be demonstrated by experimental results obtained on different types of BESSY II insertion devices such as undulators, wavelength shifters, multipole wigglers and electromagnetic undulators. Experimental results of global and local orbit monitoring and a proof of principle of a XBPM-based local feedback will be shown.

## 1 INTRODUCTION

Experiments with Synchrotron Radiation (SR) which make use of the low emittance of the electron beam on third generation storage rings are closely related to stored beam parameters. Early predictions that orbit fluctuations of the order of 1/10 of the beam's emittance dimensions [1] can be significant have been confirmed also at BESSY II where the opening angle of the monochromatic photon beam in insertion device beam lines is dominated by the electron beam divergence rather than by the photon beam itself. For a nominal vertical opening angle of the electron beam of 25 µrad and 20µm beam size at 1% coupling in the BESSY II high beta straight sections an orbit stability of 2.5 µm and 2 µrad is required. Hence, vertical emittance changes of 5 pmrad can already be a problem in particular for high resolution monochromators, where the source is stigmatically imaged to a slit of the order of 10 µm or less. The horizontal stability is usually a factor of 10 more relaxed due to the larger horizontal beam shape and/or divergence and due to the fact that the monochromators usually work with vertical dispersion.

In order to measure and eventually to stabilise the beam to these small values, several types of optical monitors in addition to the usual machine diagnostics have been designed and used at other facilities. Here, after a short review, experiences with optical emittance monitors and a review of high heat load photon beam position monitors (XBPM) and their present status together with results obtained on BESSY II will be presented.

## 2 OPTICAL SOURCE SIZE AND EMITTANCE MONITORS

### *2.1 Basic designs*

The design parameters for the measurements of the beam cross section and divergence by means of SR can be estimated according to a theoretical work of Hoffmann and Meot [2]. Applying the formulas therein to third generation storage rings it becomes clear that a simple optical image of the beam in the visible is diffraction limited and yields only a blurred information for beam sizes less than about 100µm because of the angular aperture produced by the beam itself. In order to overcome the limit given by Fraunhofer diffraction one has to image the beam with shorter wavelengths to achieve a resolution of 10µm or less [3] or to use interference methods utilising the spatial coherence of SR to obtain the beam size indirectly [4]. For a fast direct X-ray imaging, however, the quality of the optics (slope errors), aberrations as well as the heat load stability of the optics has to be rather high to preserve the diffraction limited resolution which can be of the order of 1µm depending on the wavelength and the type of optics employed.

Several kinds of X-ray and VUV optics have been used for this purpose: Grazing incidence optics in a Kirkpatrick-Baez mirror scheme at the ALS diagnostic beamline [5], crystal based X-ray Bragg-Fresnel lenses at the ESRF [6-7]. X-ray transmission zone plates at the APS [8-9]. At BESSY, multilayer Bragg-Fresnel lenses have been tested at BESSY I and installed in the first diagnostic front end at BESSY II [10]. A monitor based on a transmission zone plate is being installed for the SLS storage ring [11]. Another type of X-ray optics, the pinhole camera , which was in operation at BESSY I from 1993 to 1999 [12] and since the first day of commissioning of BESSY II [13]. It has been successfully used at the ESRF [13] and at the APS [14] for a routine observation of the source point in a dipole and was used to determine the emittance from an undulator source [15]. At BESSY, the system was updated to a pinhole array such that a regular array of images of the dipole beam can be used to obtain the vertical divergence as well as the beam size simultaneously [10]. Presently, there are three such monitors at different source points in the BESSY II

# RESULTS WITH LHC BEAM INSTRUMENTATION PROTOTYPES

C. Fischer, CERN, Geneva, Switzerland


*Abstract*

The beam instrumentation foreseen to provide the necessary diagnostics in the transfer lines and in the main rings of the LHC was conceived in the past years. The requirements expected from the different systems are now being closely analyzed and specified. In a few cases, tests of prototypes have already been performed, profiting from the facilities offered by existing machines.

The beam position measurement system had to be tackled first, as the pick-ups had to be integrated into the cryogenic part of the machine. Over the last two years other topics started to be experimentally investigated in order to define the best way to meet the requirements for the LHC era. Amongst these different studies are luminosity monitoring devices, various instruments for the measurement of the transverse beam distributions, the use of head-tail sampling to measure the beam chromaticity and quadrupole gradient modulation to derive the local amplitude of the lattice function.

The paper discusses the results of these tests.


## 1 BEAM POSITON MEASUREMENT

Along the two LHC rings about 1000 position monitors will be distributed, one per ring and per quadrupole, each with four electrodes to provide the beam excursion in both the horizontal and the vertical planes. The signal treatment is based on a Wide Band Time Normalizer as sketched in Figure 1. More details are provided in [1]. After normalization, the signal is transmitted via optical link outside the machine tunnel, where it is digitised. The Digital Acquisition Board, (DAB), treats then the data. Three prototypes of the normalizer card have been tested in the laboratory and some results on linearity and reproducibility are presented in Figures 2 and 3.

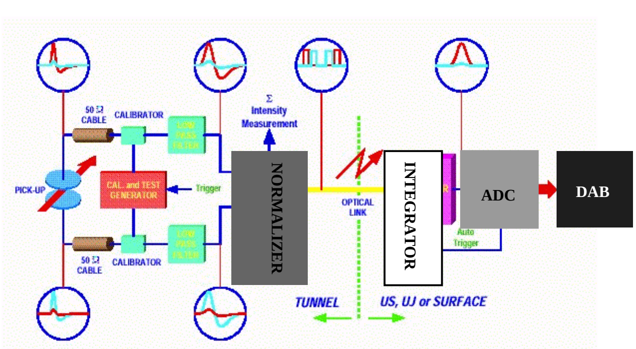


Figure 1: LHC BPM signal treatment block diagram.

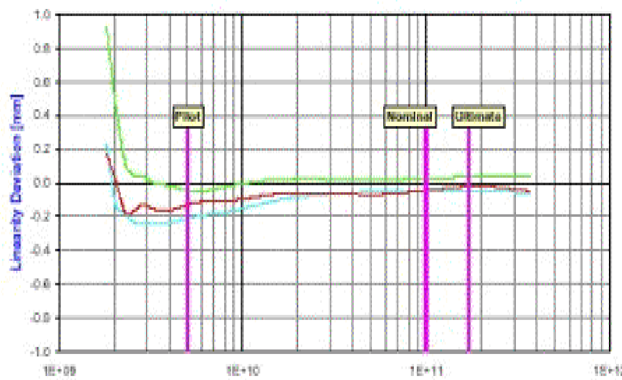


Figure 2: Normalizer card linearity vs bunch current at the LHC bunch frequency (40 MHz ).

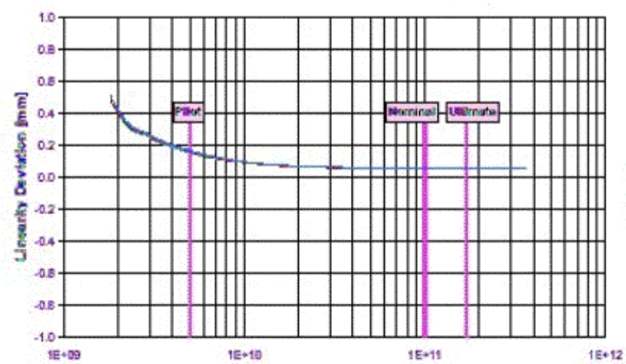


Figure 3: Signal rms deviation vs bunch current

Three bunch current levels are considered, first the pilot bunch intensity of 5. $10^{9}$ protons which will be used during the machine setting-up, and then the nominal and an ultimate bunch current levels of respectively 1.1 $10^{11}$ and 1.7 $10^{11}$ protons. At the nominal bunch current and above, the linearity is good for the three samples, whereas for the pilot bunch current, deviations up to 200 µm are observed, (Figure 2). These results are quite satisfactory. The measurement rms noise is 50 µm at nominal current and remains below 200 µm for pilot bunches, (Figure 3).

A prototype position monitor equipped with the complete LHC control system was tested last year in the SPS. Comparison with the data from a standard SPS MOPOS) monitor is made in Figure 4. The agreement is quite good. The prototype monitor was also used during a test on “AC dipole “ excitation [2], and results are presented in Figure 5. It is possible to appreciate the difference between this type of maintained beam oscillations and the more classical excitation from a classical kick, which is very quickly damped.

# MEASUREMENT OF SMALL TRANSVERSE BEAM SIZE USING INTERFEROMETRY

T. Mitsuhashi

High Energy Accelerator Research Organisation, Oho, Tsukuba, Ibaraki, 305-0801 Japan

*Abstract*

The principle of measurement of the profile or size of small objects through the spatial coherency of the light is known as the van Cittert-Zernike theorem. We developed the SR interferometer (interferometer for synchrotron radiation) to measure the spatial coherency of the visible region of the SR beam, and we demonstrated that this method is able to measure the beam profile and size. Since the small electron beam emits a SR beam which has a good spatial coherency, this method is suitable for measuring a small beam size. In this paper, the basic theory for the measurement of the profile or size of a small beam via the spatial coherency of the light, a design of the SR interferometer, and the results of beam profile measurement, examples of small beam size measurements and recent improvements are described.

## 1 INTRODUCTION

The measurements of beam profile and size are two of the most fundamental diagnostics in an electron storage ring. The most conventional method to observe the beam profile is known as a beam profile monitor via imaging of the visible SR beam[1]. The resolution of this monitor is generally limited by diffraction phenomena. In the usual configuration of the profile monitor the RMS size of diffraction (1σ of the point spread function) is no smaller than 50 μm. In the last 10 years, research and development in electron storage rings (especially in the area of emittance reduction) has been very remarkable. We can realise sub-diffraction-limited beam sizes in electron storage rings. So the above-mentioned profile monitor via imaging of the visible SR beam becomes useless in precise quantitative measurements of the beam profile and size. In the visible optics, opticians use an interferometer as the standard method to measure the profile or size of very small objects. The principle of measurement of the profile of an object by means of spatial coherency was first proposed by H.Fizeau [2] and is now known as the Van Cittert-Zernike theorem [3]. It is well known that A. A. Michelson measured the angular dimension (extent) of a star with this method [4]. Recently we developed the SR interferometer (an interferometer for SR beams) to measure the spatial coherency of the visible region of an SR beam, and as one of the results of investigations on the spatial coherence of SR beams, we demonstrated that this method is applicable to measure the beam profile and size at the KEK Photon Factory [5]. Since the SR beam from a small electron beam has good spatial coherency, this method is suitable for measuring a small beam size. The characteristics of this method are: 1) we can measure beam sizes as small as 3 and 4μm with 1μm resolution in a non-destructive manner; 2) the profile is easy to measure using visible light (typically 500 nm); 3) the measurement time is a few seconds for size measurement and few tens of seconds for profile measurement. In this paper we describe the van Cittert-Zernike theorem, the design of the SR interferometer and examples of the profile and the beam size measurements

e-mail: mitsuhas@mail.kek.jp

## 2 SPATIAL COHERENCE AND BEAM SIZE

According to van Citterut-Zernike's theorem, the profile of an object is given by the Fourier Transform of the complex degree of spatial coherence at longer wavelengths as in the visible light[3][6]. Let $f$ denotes the beam profile as a function of position $y$, $R$ denotes distance between source beam and the double slit, and $\gamma$ denotes the complex degree of spatial coherence as a function of spatial frequency $\upsilon$. Then $\gamma$ is given by the Fourier transform of $f$ as follows;

$$\gamma(\upsilon) = \int f(y) \exp(-2\pi i \upsilon \cdot y) dy , \quad \upsilon = \frac{2\pi D}{\lambda R} .$$

We can measure the beam profile and the beam size via spatial coherence measurement with the interferometer.

## 3 SR INTERFEROMETER

To measure the spatial coherence of SR beams, a wavefront-division type of two-beam interferometer using polarized quasi-monochromatic rays was designed as shown in Fig.1[6].

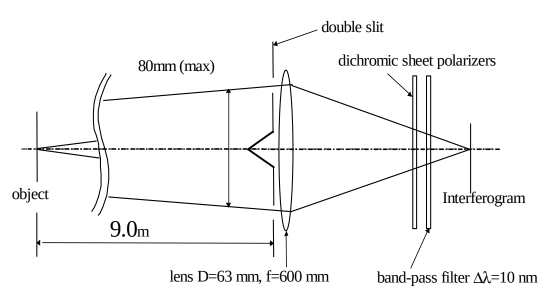


Fig.1 Outline of the SR interferometer.

# ACCELERATOR PHYSICS EXPERIMENTS WITH BEAM LOSS MONITORS AT BESSY

P. Kuske, BESSY, Berlin, Germany

*Abstract*

The extended use of beam loss monitoring has led to a better understanding of the linear and non-linear physics involved in the single and multiple particle dynamics at BESSY. This knowledge has been used for improving the performance of the light source in terms of lifetime, beam stability, and stability of the energy.

The key to these experiments are loss monitors placed at strategic locations of the ring with high sensitivity to Touschek or Coulomb scattered particles.

Coulomb-scattering depends strongly on the transverse dynamics which is determined by the magnetic guiding fields. Losses occur primarily at the vertical aperture restrictions imposed by the flat insertion device vacuum chambers. Tune scan measurements clearly show resonances produced by the lattice magnets and by some of the insertion devices.

Touschek scattering depends on the 3-dimensional electron density and the spins of the colliding particles. In transfer function type experiments these dependencies have been used to observe the effect of resonant transverse and longitudinal beam excitations. Loss monitors allow to detect excited head-tail and higher longitudinal modes which are invisible in the center of mass motion. Another application is the detection of the resonant destruction of the spin polarization of the ensemble of electrons. This is used routinely in order to determine the beam energy with high accuracy.

## 1 INTRODUCTION

The lifetime of the stored beam current, or its inverse, the decay rate of the intensity, is a very convenient measure of global particle losses. However, a fast and accurate determination of this quantity is difficult. The limited resolution of current monitors require long time intervals, $\Delta t$, in order to detect significant changes of the intensity, $\Delta I$, especially if the lifetime, $\tau$, is large since $\Delta I/I=-\Delta t/\tau$.

The alternative is the direct local detection of lost particles. When high energy particles are hitting the vacuum chamber, they produce a shower of many particles with low energy like photons, electrons, and positrons. These fragments are emitted into a small cone in the forward direction and they are easy to observe with different types of detectors[1]. With beam loss monitors (BLM) placed close to the vacuum chamber each lost electron at that location can be detected. Particles hit the chamber at specific locations depending on the loss mechanisms involved. With a system of strategically distributed loss monitors the detection is sensitive to the mechanisms causing the loss.

The high speed of the measurements and the information on the loss mechanisms have been exploited by correlating beam losses with parameters like external transverse and longitudinal excitations, the working point, different settings of machine parameters, the beam current, and further more.

## 2 PARTICLE LOSS MECHANISMS

Experiments have been performed at the second generation light source BESSY I, an 800 MeV electron storage ring, and the third generation source BESSY II operating at energies between 900 MeV and 1.9 GeV[2]. Dominating, unavoidable particle losses in this energy range stem from the electron-electron interactions within one bunch, the so called Touschek effect, and interactions of electrons with residual gas molecules, like elastic and inelastic Coulomb scattering[3]. Particle losses can occur just downstream the collision point at the next transverse or longitudinal aperture restriction or at any other location if particles are scattered close to, but not exceeding the aperture limits. This introduces a background of losses which can not clearly be attributed to a specific loss mechanism.

### *2.1 Detection of Touschek Scattered Particles*

Good locations for the detection of Touschek scattered particles are in the achromatic sections with the highest value of the dispersion function just behind straight sections where a high particle density is reached. Since the two colliding particles loose and gain an equal amount of momentum, they will hit the in- and outside wall of the vacuum chamber. In principle the selectivity of the detection to Touschek events can be improved by counting losses at these locations in coincidence.

### *2.2 Detection of Coulomb Scattered Particles*

Losses from elastic Coulomb scattering occur at locations where the beta functions are large and where apertures are small. Aperture restrictions are introduced either intentionally, like in the case of small gap insertion device (ID) vacuum chambers, in-vacuum IDs, the septum magnet, and by mechanical scrapers or unintentionally by burned RF fingers and other obstructions.

If, in an inelastic Coulomb collision, the energy carried away by the emitted photon is too large, the particle gets

# BREAKING NEW GROUND WITH HIGH RESOLUTION TURN-BY-TURN BPMS AT THE ESRF

L.Farvacque, R.Nagaoka, K.Scheidt, ESRF, Grenoble France

*Abstract*

This High-Resolution, Turn-by-Turn BPM system is a low-cost extension to the existing BPM system, based on the RF-multiplexing concept, used for slow Closed-Orbit measurements. With this extension Beam Position measurements in both planes, at all (224) BPMs in the 844 m ESRF Storage Ring, for up to 2048 Orbit Turns with 1 micrometer resolution are performed.

The data acquisition is synchronised to a single, flat 1 uS, transverse deflection kick to the 1µs beamfill in the 2.8µs revolution period. The high quality of this synchronisation, together with the good reproducibility of the deflection kick and the overall stability of the Closed Orbit beam allows to repeat the kick & acquisition in many cycles. The subsequent averaging of the data obtained in these cycles yields the 1um resolution.

The latter allows lattice measurements with high precision such as the localisation of very small focussing errors and modulation in Beta values and phase advances. It also finds an unique application to measure, model, and correct the (H to V) Betatron coupling which recently showed successfully the reduction of coupling and vertical emittance below respectively 0.3% and 12picometer.rad. This method takes full benefit from 64 BPM stations situated around 32 straight-sections (no focussing elements) of 6m length allowing the phase-space measurements in their centers.

## 1 EXTENSION TO THE EXISTING CLOSED-ORBIT BPM SYSTEM

### *1.1 The 'slow' BPM system for Closed Orbit*

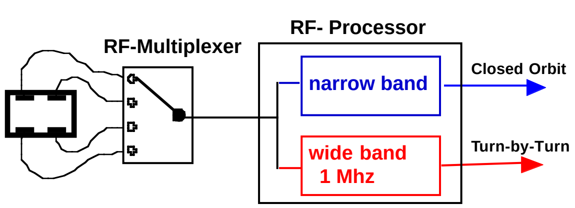


fig.1 the BPM RF-Mux concept with fast & slow output

The C.O. BPM system measures the electron beam Closed Orbit position in the Storage Ring at a slow rate of 1Hz at 224 individual BPM stations evenly distributed in the Storage Ring. This measurement is an average of many turns and taken on all the beam filling i.e. all bunches & electrons. This C.O. BPM system is at the heart of the slow Global Orbit correction scheme that attains the objective of serving the beamlines with a stable positioned beam over time periods of a few seconds to hours, days, weeks and longer [1].

The requirements of notably high reproducibility, low drift and low dependency on beam fill were fulfilled using the concept of RF-Multiplexing. [2,3] Each BPM station scans the 4 signals from the electrode buttons by an RF-Multiplexer device and performs all the signal conditioning operations (filtering, amplification, detection, digitization) on the 4 time-multiplexed signals by a single RF Processor. (see fig.1) This offers the advantage of high immunity to variations of characteristics (gain, linearity, offset) of the Processor electronics (since it affects the 4 signals equally). However, the drawback is that the slow scanning (millisec) does not allow to measure a beam position on a single beam turn (microsec).

Nevertheless, the Processor possesses 2 channels of signal conditioning : 1) a narrow band, low noise channel, and 2) a wide band (1MHz) for fast signals (1µs). With the latter a single turn can be detected, but only on one electrode at a time. Consequently a position measurement needs 4 separate cycles. It is in this way that First-Turn BPM measurements after injection have been performed to satisfaction with the existing system.

After careful analysis of the applications that the Turn-by-Turn BPM system would fulfil it was concluded that in a similar way the position data on a large number of turns could be obtained.

### *1.2 a 'pseudo' Turn-by-Turn beam position measurement system*

A wealth of information can be obtained on the beam characteristics and machine parameters by measuring the beam position on a turn-by-turn basis after the application of a single deflection kick. [4-15]

Note that the measurement is to be synchronised with this deflection kick. If this synchronisation is precise and if this kick is of good reproducibility then the measurement can be performed in 4 distinct cycles (1 for each of the 4 electrodes). Moreover, each cycle may itself be repeated a large number of times. The individual measurements can be averaged which then improves the resolution of the results. It is essential that the beam is otherwise stable during the whole measurement sequence. It is obvious that the system is a 'pseudo' turn-by-turn system since the data is acquired over many cycles during a time much longer then N x revolution time. However, this has no effect on the information that the system yields, i.e. turn-by-turn beam position after an applied beam excitation, since the beam excitation and the data

# OVERVIEW OF RHIC BEAM INSTRUMENTATION AND FIRST EXPERIENCE FROM OPERATION *

P. Cameron, P. Cerniglia, R. Connolly, J. Cupolo, C. Degen, K. A. Drees,
D. Gassner, M. Kesselmann, R. Lee, T. Satogata, B. Sikora, R. Witkover
Brookhaven National Laboratory, Upton, NY, USA

*Abstract*

A summary of the beam instrumentation tools in place during the year 2000 commissioning run is given including the technical layout and the appearance on the user level, here mainly the RHIC control room. Experience from first usage is reported as well as the lessons we have learned during RHIC operation so far. Upgrades and changes compared to the year 2000 systems are outlined. Described tools include beam position monitors (BPM), ionization profile monitors (IPM), beam loss monitors (BLM), bunch current measurements, luminosity monitors, tune meters and Schottky monitors.

## 1 INTRODUCTION

The **R**elativistic **H**eavy **I**on **C**ollider (RHIC) is the new accelerator flagship at Brookhaven National Laboratory on Long Island, NY (USA). The two super-conducting rings are built in the 3.8 km long tunnel originally constructed for the ISABELLE project. RHIC has 6 interaction regions where the two beams - “blue” circulating clockwise and “yellow” counter-clockwise - collide with zero crossing angle. Four are equipped with experiments. Table 1 summarizes some of the major collider parameters.

One of the major goals of the RHIC project is to discover and study the quark-gluon plasma, a very hot and dense state of matter believed to have existed a fraction of a second after the Big Bang. For this purpose, RHIC is designed to operate with various ions, from gold to lighter species such as copper, oxygen or silicon. In addition RHIC can accelerate polarized proton beams. The combination of polarization, luminosity, and beam energy to be found in RHIC will open exploration of a new and theoretically interesting regime in high energy spin physics.

RHIC instrumentation systems [1, 2] monitor diverse beams of up to 60(120) bunches in each of the two collider rings. Intensities range from low-intensity commissioning and pilot bunches to $10^{11}$ protons/bunch at 250 GeV and $10^9$ $Au^{+79}$ ions/bunch at 100 GeV/nucleon.

The major challenge to Instrumentation during the year 2000 commissioning run was to provide adequate diagnostic information during the acceleration ramp. While the main dipole and quad bus power supplies were well behaved, there were regulation problems in the shunt supplies (these problems grew out of late vendor deliveries, and are corrected for the year 2001 run) that caused tune and orbit to drift up the ramp. The effect of orbit drift at the beginning of the ramp was aggravated by poor sextupole power supply regulation at the extreme low currents required at injection, as well as by the compensation required for snapback. In addition, during acceleration of Gold the beam must pass thru transition. Transition crossing was complicated by the absence of power supplies for the gamma jump, which led to the use of a radial jump for transition crossing, and tune shifts proportionate to chromaticity. All of the above suffered the additional complication that the machine was not fully repeatable, that ramps with apparently identical initial conditions often produced radically different results. Despite these difficulties, but not without considerable effort, the machine was successfully commissioned and good experimental physics data was gathered.

* Work performed under the auspices of the U.S. Department of Energy

| Parameter | Value | Unit |
|---|---|---|
| Circumference | 3833.845 | m |
| Beam energy (Au) | 10.2 - 70 (100) | GeV/u |
| Beam energy (p) | 28.3 - (250) | GeV |
| Revolution Frequency | 78 | kHz |
| Revolution Time | 12.8 | $\mu$s |
| RF frequency | 28 (200) | MHz |
| # of filled buckets | 60 | |
| Bunch separation | 220 | ns |
| Luminosity | 0.2 (2) $10^{26}$ | $cm^{-2}sec^{-1}$ |
| Betatron tunes (x/y) | 0.22/0.23 (0.19/0.18) | |
| horiz. $\epsilon_{nor}$ (*) | 10-20 | $\pi$ mm mrad |
| vert. $\epsilon_{nor}$ (*) | 10-15 | $\pi$ mm mrad |
| $\beta^*$ | 3,8 (1,10) | m |
| Number of ions/bunch | 5 $10^8$ (1 $10^9$) | |

Table 1: *Basic RHIC parameters during the year 2000 commissioning run. Design values, if different from commissioning run values, are added in brackets.( (*): measured)*

## 2 BEAM POSITION MONITORS

The BPM electrode assemblies [3] operate at 4.2 K. The collider ring contains 480 BPM assemblies plus additional units for spin rotators, Siberian snakes, and beam dumps. Tight constraints on orbit relative to quadrupole centers are imposed during polarized proton acceleration, to minimize the strength of spin resonances. The relative locations of BPM electrical centers and quadrupole magnetic centers

# 6-D ELECTRON BEAM CHARACTERISATION USING OPTICAL TRANSITION RADIATION AND COHERENT DIFFRACTION RADIATION

M. Castellano, V. Verzilov, INFN-LNF, Italy
L. Catani, A. Cianchi, INFN-Roma2, Italy
G. D'Auria, M. Ferianis, C. Rossi, Sincrotrone Trieste, Italy

*Abstract*

The development of non-intercepting diagnostics for high charge density and high energy electron beams is one of the main challenge of beam instrumentation.

Diffraction Radiation based diagnostics, being non-intercepting, are among the possible candidates for the measurements of beam properties for the new generation linacs.

At the 1 GeV Sincrotrone Trieste linac, we are performing the first measurements of beam transverse parameters using Diffraction Radiation emitted by the electron beam passing through a 1 mm slit opened on a screen made of aluminium deposited on a silicon substrate.

The analysis of the angular distribution of the Diffraction Radiation for a given wavelength, slit aperture and beam energy gives information about the beam size and its angular divergence.

## 1 INTRODUCTION

The usefulness of Optical Transition Radiation (OTR) for electron beam diagnostics was demonstrated in 1975 by L. Wartski [1], but it took more than ten years before becoming a real instrument usable for beam measurement [2]. For the first time, in the design of the TESLA Test Facility (TTF) linac, OTR was considered as the main beam diagnostics tool, with the intent of fully exploit its many properties. In these years, we have used OTR to measure all the 6D phase space beam parameters. Some of the most interesting measurements will be described in this paper. More recently we started some experiments with the Diffraction Radiation (DR), that is emitted when the beam crosses a hole in a metallic screen. This radiation open the possibility of a non-intercepting diagnostics, required for high power beams or strongly focalised ones, as those designed for short wavelength FELs or Linear Colliders. On the TTF beam we have proved that coherent DR can give the same result as coherent Transition Radiation for bunch length measurement, while on the Sincrotrone Trieste linac an experiment is running to demonstrate the possibility of measuring beam size and angular spread with near-infrared DR.

Transition Radiation has many advantages over more traditional imaging devices, being completely linear and free from source saturation, but its spatial resolution has some peculiar aspects that can create some limits in the details that can be extracted from an image. So a very brief presentation of the space resolution of OTR will precede the illustration of the experimental results.

## 2 OTR RESOLUTION

Few years ago, some concern aroused about the spatial resolution reachable with OTR, especially at very high energy. The reason was the collimating of the radiation, with its peak cone at an angle of $1/\gamma$, that could produce an auto-diffraction limit increasing with the energy. This argument has been fully studied in [3-5], and now we know that the only real limitation arises from the collection optics diffraction, independently from energy, but with peculiar features due to the nature of this radiation. In particular, the radial polarisation produces a zero in the centre of the image, resulting in a FWHM larger than that of a standard scalar point source. On the other hand, the extension of the source (the e.m. field of the particle) increases with energy, and this produces a long tail which contain most of the optical intensity. This means that some caution must be used in defining the OTR spatial resolution, depending on how this long tail is managed. Figure 1, taken from Ref. [4], shows the normalised radial distribution for a single particle OTR image with different angular acceptance.

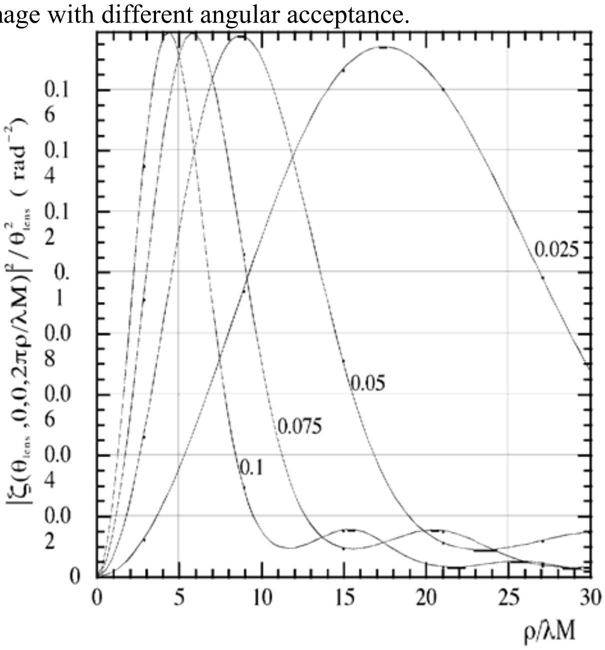


Figure 1: Normalised OTR angular distribution for different acceptance of the collection optics.

# POSSIBLE SPIN-OFFS FROM LHC PHYSICS EXPERIMENTS FOR BEAM INSTRUMENTATION

R. Jones, CERN, Geneva, Switzerland

*Abstract*

This paper aims to introduce some of the new technology and materials used in the construction of the LHC physics experiments into the domain of the beam instrumentalist. The development of radiation hard fibre-optic technology, for example, can equally well be applied to beam instrumentation systems for the direct transmission of analogue or digital signals from high to low radiation environments. Many electronics techniques such as a system developed for the fast integration of photomultiplier signals could also prove very useful in the construction of new beam diagnostic instruments for bunch-to-bunch measurements. Other topics covered will include a fast beam synchronous timing system based on laser technology and a look at pixel detectors as a possible replacement for CCD cameras in imaging applications.

## 1 INTRODUCTION

The Accelerator and High Energy Physics (HEP) Experiment domains of large laboratories are often separated, with very little interaction taking place between the two. Accelerators are generally maintained by on-site staff, while the HEP Experiments are designed and built by a multitude of world-wide institutions. This makes it difficult to exchange ideas and foresee common applications for any development work. However, many of the new techniques investigated by the HEP Experiments can equally well be applied to beam instrumentation. With the ever-increasing demands on beam diagnostics requiring new and innovative solutions, coupled with decreasing staff numbers, such collaborations can prove to be very useful. In the following sections I will highlight a few techniques derived from the LHC Physics Experiments that are already being investigated for beam instrumentation purposes.

## 2 RADIATION HARD FIBRE-OPTIC TECHNOLOGY

Acquiring data in the front-end systems of HEP experiments necessitates the use of radiation resistant electronics. The detector itself is also crowded with equipment, severely limiting the amount of space available. Hence, in order to minimise the amount of electronics located in these high radiation regions, the LHC experiments have been investigating ways to transmit the data as soon as possible to the outside world. Described in this section is a way in which analogue signals can be extracted with limited very-front-end electronics.

### *2.1 CMS Analogue Signal Transmission*

The CMS tracker is comprised of pixel, silicon and gas microstrip detectors, located in the centre of the experiment, right next to the beam pipe [1,2]. The silicon and gas microstrip detectors are read-out by charge sensitive amplifiers. The resulting signal, from some 12 million detector channels, has to be transmitted to the counting room on the outside of the CMS detector. The requirements for this link is as follows:

- Full scale dynamic range ~ 200:1 (46dB)
- < 2% deviation from linearity
- Overall rms link noise < 0.2% of full scale.
- Operation in magnetic field of up to 4T
- ~10kGy/year integrated radiation dose and $10^{13}$ (1Mev neutron equivalent)/$cm^2$ hadronic fluence.

The solution adopted by the CMS tracker team[1] makes use of analogue fibre-optic transmission [3,4]. A 1310nm, edge emitting, MQW semiconductor laser diode is directly modulated by a transconductance amplifier, with the light produced passing into a single-mode optical fibre. This fibre, some 150m in length, carries the analogue signal to the digitisers in the counting room, where it is converted back into an electrical signal by PIN photodiodes. Using this technique, the requested linearity was obtained, with a link noise of less than 0.2%. The overall bandwidth was limited by the laser driver to 172MHz.

Since radiation hardness was of great concern, many tests were carried out on the influence of radiation on the laser characteristics [5,6,7] and on the fibre-optic cable [8]. In conclusion, it was found that a variety of commercially available 1310nm lasers and single-mode fibres could meet the stringent radiation requirements for operation in the CMS tracker environment.

### *2.2 Example Application for Beam Instrumentation*

This type of fibre-optic transmission is already being investigated for possible use in beam instrumentation. In

[1] http://cms-tk-opto.web.cern.ch/cms-tk-opto/default.htm

# INVESTIGATIONS OF THE LONGITUDINAL CHARGE DISTRIBUTION IN VERY SHORT ELECTRON-BUNCHES

Markus Hüning, III. Phys Inst RWTH Aachen, Sommerfeldstrasse 26-28, 52056 Aachen, Germany
current address: DESY, Notkestrasse 85, 22603 Hamburg, Germany

*Abstract*

Electro-optical-sampling is a powerful technique to measure the longitudinal charge distribution of very short electron bunches. The electrical field moving with the bunch induces an optical anisitropy in a ZnTe crystal which is probed by a polarized laser pulse. Two measurement principles are possible. In the first one a short laser pulse of lengths $< 50$ fs is used directly to scan the time varying optical properties of the crystal. In the second method the laser pulse is frequency chirped and the temporal information is encoded into the time ordered frequency spectrum, which can be recovered by an optical grating and a CCD camera.

A resolution in the 100 fs regime can also be achieved with longitudinal phase space tomography. Acceleration on the slope of the rf wave at different phases and measurements of the energy profiles are sufficient for a reconstruction algorithm based on maximum entropy methods. The longitudinal phase space distribution can be obtained without artefacts due to the limited angular range of the projections.

## 1 INTRODUCTION

Linear electron positron colliders or free electron lasers (FEL) require electron bunches of subpicosecond bunch length. Measurement techniques have been developed in recent years to provide diagnostics in this parameter regime.

One possibility is to measure the coherent radiation emitted by the bunches under certain circumstances: Coherent transition radiation (CTR), diffraction radiation, or synchrotron radiation (CSR). By analysis of the radiation spectrum one can determine the longitudinal bunch profile. In most cases the phase information is lost and has to be reconstructed for example with the Kramers-Kronig-Relation. This kind of analysis can be considered as well established [3][4][5] and will be used as a reference in this paper.

The development of Ti:sapphire lasers with ultra-short pulses of FWHM $< 50$ fs led to the concept of electro-optic sampling and imaging in THz-spectroscopy [17][20]. At the FEL Laboratory for Infrared Experiments (FELIX) in Rijnhuizen near Utrecht, NL electro-optic sampling (EOS) has been successfully applied to measure bunch lengths [19][7]. Similar measurements are being prepared at several accelerators and as well at the TESLA Test Facility (TTF)[2][8].

Many experiments have been carried out to measure longitudinal beam profiles by means of the rf acceleration in the linac themself [3][16]. Using off-crest acceleration in the rf cavities an energy deviation is induced depending on the longitudinal position of the electrons in the bunch. This can be measured with a spectrometer dipole. One of the problems with this kind of measurement is the entanglement with the initial energy spread, which often is in the same order of magnitude. Using magnetic chicanes followed by an acceleration section, it is possible to rotate the phase space by $90°$ so that the longitudinal position is projected onto the energy [13][4]. In general tomographic methods can be used to get a reconstruction of the full longitudinal phase space.

## 2 ELECTRO-OPTIC METHODS

Exposed to a strong electric field some optical crystals exhibit the Pockels effect: The electric field distorts the lattice of the crystal and the material becomes birefringent. Linearly polarized light with its polarisation oriented $45°$ to the optical axis is transformed into elliptically polarised light with the fraction of circularly polarized light proportional to the strength of the electrical field.

Compared to the oszillation of the laser even THz-fields can be considered as slowly varying and so the Pockels Effect can be applied to measure the electric field strength in THz pulses with a resolution governed by the width of the laser pulse used to sample. There are Ti:Sapphire lasers available which deliver pulses shorter than 20 fs FWHM. For the EOS often ZnTe is used because it provides good sensitivity and good optical properties for THz frequencies as well as for the light from Ti:sapphire lasers. The Phonon resonances with the lowest frequency in ZnTe can be found at 5.6 THz, but their influence on the measurement can be modelled precisely. Electro-optical Sampling has been demonstrated with ZnTe up to frequencies of 37 THz [18].

In contrast to many applications in THz-Spectroscopy where the same laser pulse is utilized for generation of the THz-pulse as well as for probing the electrical field, in a linac the bunches and the ultra-short laser pulses are generated by different sources. A demanding task in the adaption of EOS to accelerator diagnostics is therefore the synchronisation of the Ti:Sapphire laser to the master clock of the accelerator. This can be accomplished by building a phase locked loop which synchronizes a harmonic of a photodiode signal from the laser with the rf-reference from the master clock. In this way phase noise can be reduced by a factor of 10. The residual noise translates into a timing

# BPM READ-OUT ELECTRONICS BASED ON THE BROADBAND AM/PM NORMALISATION SCHEME

M. Wendt, DESY, Hamburg, Germany

*Abstract*

Recently developed circuit modules, used for the processing of position signals of electrostatic ("button"-type) pickups are presented. The concept is based on the broadband ("monopulse") AM/PM normalisation technique. The short integration time ($\approx$ 10 ns) makes this read-out electronics suitable for single-bunch position measurements nearby interaction areas and in linear accelerators. Details on circuit design and technology, as well as the practical realization are shown. The results discussed include beam position and orbit measurements made with a set of 40 units at the FEL-undulator sections of the TESLA Test Facility (TTF) linac.

## 1 INTRODUCTION

Each *beam position monitor* (BPM) (Figure 1) basically consists out of a *pickup* station for the signal detection and a set of *read-out electronics* (often 2 channels for horizontal and vertical plane) for signal processing and *normalisation*.

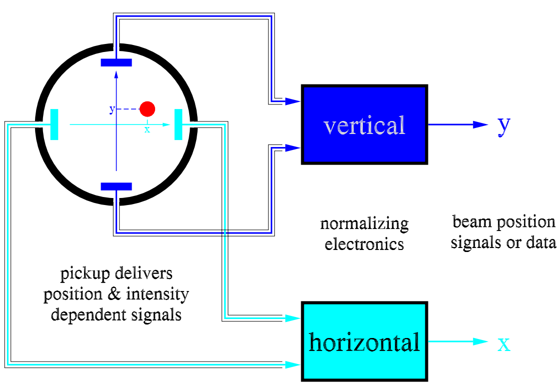


Figure 1: BPM principle.

A single electrode of a BPM pickup delivers a signal voltage

$$V_{\text{elec}}(\omega, x, y) = s(x, y)\, Z(\omega)\, I_{\text{beam}}(\omega) \qquad (1)$$

which is proportional to the beam intensity $I_{\text{beam}}(\omega)$ (e.g. bunch charge) and to the beam-to-electrode distance $(x, y)$ (e.g. tranverse beam displacement) or coupling which is covered by a sensitivity function $s(x, y)$. In case of high energy electron accelerators the frequency spectra of $I_{\text{beam}}(\omega)$ is of no concern; for the BPM system the bunches behave like dirac impulse excitation signals. The transfer impedance $Z(\omega)$ of the pickup electrode (centred beam) depends on the type of BPM pickup (e.g. button, stripline, cavity-BPM, etc.) and its geometry. It also fixes (roughly) the frequency range of the following signal processing system.

The BPM read-out electronics extracts the beam position (displacement) information from the analogue signals of the pickup electrodes. In order to simplify the normalisation procedure and to reduce the nonlinearities of $s(x, y)$ two symmetrically arranged electrode are sensed in each plane (see Figure 1). The read-out electronics *normalises* the electrode signals and therefore performs a beam intensity independent beam position measurement.

For each plane (horizontal or vertical) the corresponding BPM pickup electrodes supplies two signals ($A$ and $B$). For symmetry reasons the *amplitude-ratio* $\hat{a}/\hat{b}$ is a beam-intensity independent function of the beam displacement:

$$\text{beam-position} = f(\frac{\hat{a}}{\hat{b}}) \qquad (2)$$

which is processed by the presented broadband AM/PM technique [1]. The read-out system outputs an analogue pulse signal, from which the flat peak value is proportional to the beam displacement. Further data acquisition techniques are required to digitise the signal for use in the control system.

## 2 THE AM/PM PRINCIPLE

The amplitude-ratio, and such the beam-position, is measured with the *AM/PM signal processor* by converting the ratio into a phase-difference – the *amplitude modulation* (AM) converts into a *phase modulation* (PM). Practically the conversion is realized by a $90^0$ hybrid junction, which is extended at one output port with a $90^0$ delay-line.

For the analysis it is sufficient to simplify the two sine-wave burst ("ringing") shaped input signals of the pickup electrodes to stationary sine-wave voltage functions $v_A$ and $v_B$:

$$v_A(t) = \hat{a}\, e^{j\omega t} \qquad (3)$$

$$v_B(t) = \hat{b}\, e^{j\omega t} \qquad (4)$$

They have same frequency and are in phase, but the amplitudes $\hat{a}$ and $\hat{b}$ differ due to the beam displacement and are bunch charge dependent. At the outputs $C$ and $D$ of the hybrid-with-delay circuit the signals:

$$v_C(t) = \sqrt{\frac{\hat{a}^2 + \hat{b}^2}{2}} \arctan\left[\frac{\hat{a}\sin(\omega t) + \hat{b}\cos(\omega t)}{\hat{a}\cos(\omega t) - \hat{b}\sin(\omega t)}\right] \qquad (5)$$

$$v_D(t) = \sqrt{\frac{\hat{a}^2 + \hat{b}^2}{2}} \arctan\left[\frac{\hat{a}\sin(\omega t) - \hat{b}\cos(\omega t)}{\hat{a}\cos(\omega t) + \hat{b}\sin(\omega t)}\right] \qquad (6)$$

[1] For an overview of normalisation schemes see [1, 2]

# FIRST COMMISSIONING RESULTS OF THE ELETTRA TRANSVERSE MULTI-BUNCH FEEDBACK

D. Bulfone, C. J. Bocchetta, R. Bressanutti, A. Carniel, G. Cautero, A. Fabris, A. Gambitta, D. Giuressi, G. Loda, M. Lonza, F. Mazzolini, G. Mian, N. Pangos, R. Sergo, V. Smaluk, R. Tommasini, L. Tosi, L. Zambon, Sincrotrone Trieste, Trieste, Italy
M. Dehler, R. Ursic, Paul Scherrer Institut, Villigen, Switzerland

*Abstract*

A wide-band bunch-by-bunch Transverse Multi-Bunch Feedback, developed in collaboration with the Swiss Light Source (SLS), has been installed at ELETTRA. After a description of the main hardware/software components, the first commissioning results and the present status of the system are given.

## 1 INTRODUCTION

The ELETTRA Transverse Multi-Bunch Feedback (TMBF) [1] consists of a wide-band bunch-by-bunch system where the positions of the 432 bunches, separated by 2 ns, are individually corrected. After combining and demodulating the wide-band signals from a standard ELETTRA electron Beam Position Monitor (BPM), the X (Y) baseband signal (0-250 MHz) is sampled by an eight-bit 500 Msample/s Analog-to-Digital Converter (ADC). The resulting 500 Mbyte/s data flux is first de-multiplexed into six 32 bit FDPD (Front Panel Data Port) channels. The data from each of them is then distributed by means of a programmable switch to the four TI-TMS320C6201 programmable Digital Signal Processors (DSP) housed in one VME board. In the present configuration all of the data coming from one FPDP channel, which correspond to 72 bunches, are passed to one DSP for on-line diagnostics and concurrently split over the remaining three DSPs for the execution of the feedback algorithm. A detailed description of the digital processing electronics is given in [2]. The calculated corrective kick values are recombined following a symmetric multiplexing scheme and transmitted to an eight-bit 500 Msample/s Digital-to-Analog Converter (DAC), amplified by an RF power amplifier and applied to the beam by a stripline kicker. A flexible timing system provides the necessary synchronization signals.

## 2 CLOSED-LOOP RESULTS

Commissioning has focussed on the vertical plane since the instabilities are stronger and users are more sensitive to vertical emittance. The TMBF loop has been characterized and successfully closed on beams of increasing current and energy, up to 320mA@2GeV and 130mA@2.4GeV, which are the typical target values during users' shifts. Figure 1 shows the effect of the TMBF as seen on the synchrotron radiation profile monitor image of a 200 mA stored beam affected by vertical transverse coupled-bunch instabilities.

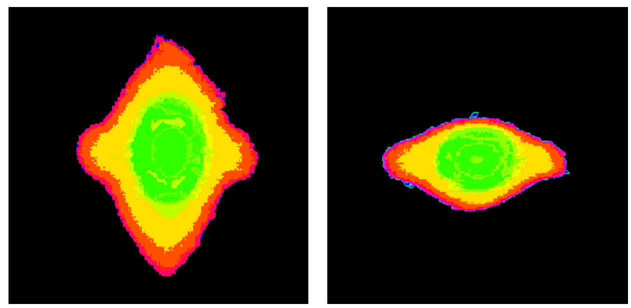

Figure 1: Synchrotron radiation profile monitor images of a 200 mA beam affected by vertical transverse coupled-bunch instabilities with TMBF off (left) and on (right).

The developed DSP software allows the adoption of Finite Impulse Response (FIR) filters with up to 5 taps for the feedback algorithm. However, the presently used filter is a 3-tap FIR that provides rejection of the closed orbit signal while ensuring the right phase and gain at the betatron frequency. The total closed-loop delay is four revolution periods plus the BPM-to-kicker delay. One RF amplifier per plane powers the downstream port of a single kicker stripline.

## 3 DIAGNOSTIC TOOLS

In parallel to the closed loop functionality, the digital implementation of the TMBF system opens the way for additional diagnostic features that can be built by appropriate programming of the system. A number of them have been developed starting from the commissioning phase.

### *3.1 Bunch-by-Bunch Data Acquisition*

As already mentioned, one of the four DSPs on each VME board is dedicated to data acquisition for on-line diagnostics and 16 Mbytes of Synchronous Dynamic RAM are available for this purpose. The whole system made up of six boards allows 96 Mbytes of bunch-by-bunch continuous data at 500 Msample/s, corresponding

# PERFORMANCE OF THE DIGITAL BPM SYSTEM FOR THE SWISS LIGHT SOURCE

V. Schlott, M. Dach, M. Dehler, R. Kramert, P. Pollet, T. Schilcher, PSI, Villigen, Switzerland;
M. Ferianis, R. DeMonte, Sincrotrone Trieste, Italy;
A. Kosicek, R. Ursic, Intrumentation Technologies, Slovenia.

*Abstract*

The accelerator complex of the Swiss Light Source (SLS) is presently under commissioning at the Paul Scherrer Institute (PSI) in Villigen, Switzerland. The newly developed digital beam position monitor (DBPM) system has been successfully used to determine beam positions in the pre-injector LINAC, the transfer lines, the booster synchrotron and the storage ring. Instant and free selection of operation modes through the EPICS-based SLS control system allows to choose between single turn, turn-by-turn and closed orbit measurements. The operational experience and performance of the DBPM system is presented, based on measurements, taken during SLS commissioning. A monitoring system (POMS), which measures the horizontal and vertical mechanical positions of each BPM block in reference to the adjacent quadrupole magnets has been installed and first results, indicating transverse movements of the BPM blocks as a function of current in the storage ring will be presented.

## 1 INTRODUCTION

The DBPM system played a vital role during the commissioning of the SLS accelerator complex, which started in March 2000 and is still continuing until August 2001 [1]. The implementation of all available operation modes [2] from the beginning delivered beam position measurements in the LINAC, the transfer lines, the booster synchrotron and in the storage ring. In addition to simply visualizing the positions in the control room, the DBPM system is constantly delivering data to SLS beam dynamics applications [3]. This data transfer is arranged through a batch process consisting of up to 8192 x- and y-position and intensity readings, synchronized to the 3 Hz repetition rate of the SLS injector. The full programmability of the quad digital receiver (QDR) [2] as well as the complete integration of the DBPM electronics in the EPICS based control system, allows remote switching of operation modes for each sector of the booster synchrotron and storage ring individually. Optimization of injection and beam optics studies like measurement of tunes and chromaticities as well as “beta scans” have been performed in the high speed / medium resolution *turn-by-turn mode*. For determination of closed orbits, the system has been switched to lower bandwidth and therefore higher resolution. The application of a pilot signal in the RF front end [2] provides calibration of the electronics for any chosen gain setting. A self test mode can be applied to exclude mal-functioning of BPM stations and therefore improves reliability. Using the features and flexibility of the DBPM system resulted in a fast and efficient commissioning and provided complete understanding of the SLS accelerator optics.

## 2 PERFORMANCE CHARACTERISTICS

The following measurements have been taken in the laboratory and during SLS commissioning to determine the DBPM systems performance, to demonstrate first operational experience and to present some results from the SLS accelerators.

### *2.1 Resolution and Beam Current Dependence*

While an AGC loop is presently not yet implemented, the full dynamic range of the DBPM system is covered through downloading of specific sets of pre-calibrated gain levels which correspond to pre-defined beam current ranges. These ranges are large enough to guarantee standard storage ring operation between adjacent injection (re-filling) cycles. The gain settings are chosen in such a way that the signal levels in the RF front end are always kept within the linear regimes of all electronics components and that the RF front end output is not exceeding 70% of the QDRs analog-to-digital converters input range (1 Vpp for presently used 12 bit AD9042 from Analog Devices). Minimum *turn-by-turn* resolution, which corresponds in case of SLS to 1 MS/s, has been measured to be in the order of 20 μm over a dynamic range of 5 mA to 700 mA. The minimum resolution at 15 kHz bandwidth corresponding to a so called "*ramp-250 ms*" mode, which was especially implemented for the booster synchrotron, has been determined to be < 3 μm and the resolution in the *closed orbit / feedback* mode, which operates at 4 kS/s, is < 1.2 μm. The increase of resolution from *turn-by-turn* mode over the "*ramp-250ms*" mode to the *closed orbit / feedback* mode goes - as can be expected - with the square root of bandwidth. In the latter two modes however, some low bandwidth noise floor can still be observed, which may be caused by phase noise in the RF front end. This issue needs be addressed (and solved) before the global closed orbit feedback [4] will be implemented. The sudden decreases of resolution whenever the gain levels of DBPM system are changed is

# FIBRE OPTICAL RADIATION SENSING SYSTEM FOR TESLA

H. Henschel, Fraunhofer-INT, Euskirchen, Germany
M. Körfer, DESY, Hamburg, Germany
F.Wulf, HMI, Berlin, Germany

*Abstract*

High energy accelerators generate ionising radiation along the beam-line and at target places. This radiation is related to beam losses or dark currents. The in-situ measurement of this ionising dose that is distributed over long distances or large areas requires a new monitor system. This paper presents first results and the concept of such a monitor system at the Tesla Test Facility.

## 1 MOTIVATION

Field emission electrons are coming out of the RF laser gun and accelerator cavities. Particles based on this dark current can leave the cavity when they are emitted in a proper phase and will be accelerated together with the bunched beam. The dark current is not well-matched to the magneto optics so that most of it will hit the vacuum chamber, cavities and collimators in front of the undulators/detectors. This mechanism produces high energetic X-rays and electromagnetic showers. The regular bunched beam can also be lost during the accelerator commissioning or standard beam operation due to power supply failures. For a long and complex accelerator system like TESLA [1] it will be advantageous to monitor and measure on-line the local dose in sections of interest, especially at radiation sensitive equipment like fast signal processing units (PCs), superconducting components, collimators and permanent undulator magnets . A new in-situ sensing system could be realised by optical fibres combined with an Optical Time Domain Reflectometer (OTDR).

## 2 MEASUREMENT

### 2.1 General Layout

The most obvious effect of ionising radiation in optical fibres is an increase of light attenuation. The radiation penetrates the fibre and creates additional colour-centres which cause a wavelength-dependent attenuation that can be measured with an OTDR (Fig.1). A short laser pulse is launched into the fibre. A fraction of the signal reaches the photo-detector by Rayleigh back-scattering and Fresnel-reflections. The light coming from fibre sections behind the exposed fibre part suffers absorption leading to an attenuation step on the OTDR trace. The height of the step is proportional to the radiation dose. Differentiation of the OTDR curve results in peaks with dose-proportional height.

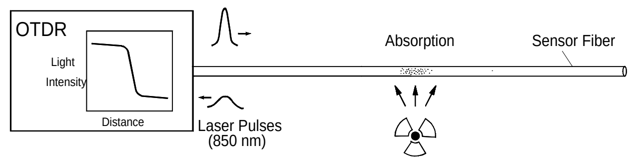


Figure 1: Principle of radiation dose measurement with optical fibres: OTDR-solution (= "distributed" sensor with local resolution). The radiation produces absorbing "colour centers". Propagation time and intensity of the back-scattered laser pulses allow determination of radiation intensity (= dose) and location of the radiation exposure.

With the known speed of light (~ 0.66 c), the measured pulse propagation time can be converted into distance, allowing the localisation of dose deposition. The shorter the laser pulse length, the better the local resolution. But reducing the pulse length leads to a reduction of the light intensity and thus of the dynamic range of the OTDR. As a consequence, the maximum sensor fibre length and/or the maximum measurable dose are reduced. The multimode fibre module of the chosen OTDR (Tektronix TFP2A) is equipped with a 850 nm laser of pulse widths (PWs) ≥ 1 ns as well as a 1300 nm laser (PWs ≥ 10 ns). Due to the wavelength dependence of the radiation-induced attenuation, the dynamic range at 1300 nm is about a factor of five higher than at 850 nm. The local resolution is also limited by the pulse broadening (= mode dispersion) that reduces the bandwidth (BW) of the selected multimode gradient-index (MM GI) fibre of 50 µm core diameter. The table below shows the broadening of laser pulses of different width by fibres with different BW along fibre sections with a length of 0.33, 1 and 5 km, respectively. To avoid excessive pulse broadening, the BW for the Tesla Test Facility (TTF; [2]) should be at least 800 MHz.

# BEAM-PROFILE INSTRUMENTATION FOR A BEAM-HALO MEASUREMENT: OVERALL DESCRIPTION, OPERATION, AND BEAM DATA•

J. D. Gilpatrick, D. Barr, L. Day, D. Kerstiens, M. Stettler, R. Valdiviez, Los Alamos National Laboratory
M. Gruchalla, J. O'Hara, Honeywell Corporation
J. Kamperschroer, General Atomics Corporation

*Abstract*

The halo experiment presently being conducted at the Low Energy Demonstration Accelerator (LEDA) at Los Alamos National Laboratory (LANL) has specific instruments that acquire horizontally and vertically projected particle-density beam distributions out to greater than 105:1 dynamic range. We measure the core of the distributions using traditional wire scanners, and the tails of the distribution using water-cooled graphite scraping devices. The wire scanner and halo scrapers are mounted on the same moving frame whose location is controlled with stepper motors. A sequence within the Experimental Physics and Industrial Control System (EPICS) software communicates with a National Instrument LabVIEW virtual instrument to control the movement and location of the scanner/scraper assembly. Secondary electrons from the wire scanner 33-µm carbon wire and protons impinging on the scraper are both detected with a lossy-integrator electronic circuit. Algorithms implemented within EPICS and in Research Systems' Interactive Data Language (IDL) subroutines analyse and plot the acquired distributions. This paper describes the beam profile instrument, describes our experience with its operation, compares acquired profile data with simulations, and discusses various beam profile phenomenon specific to the halo experiment.

## 1 HALO INSTRUMENTATION

At LEDA a 100-mA, 6.7-MeV beam is injected into a 52-quadrupole magnet lattice (see fig. 1). Within this 11-m FODO lattice, there are nine wire scanner/halo scraper/wire scanner (WS/HS) stations, five pairs of steering magnets and beam position monitors, five loss monitors, three pulsed-beam current monitors, and two image-current monitors for monitoring beam energy (2). The WS/HS instrument's purpose is to measure the beam's transverse projected distribution. These measured distributions must have sufficient detail to understand beam halo resulting from upstream lattice mismatches. The first WS/HS station, located after the fourth quadrupole magnet, verifies the beam's transverse characteristics after the RFQ exit. A cluster of four HS/WS located after magnets #20, #22, #24, and #26 provides phase space information after the beam has debunched. After magnets #45, #47, #49, and #51 reside the final four WS/HS stations. These four WS/HS acquire projected beam distributions under both matched and mismatched conditions. These conditions are generated by adjusting the first four quadrupole magnets fields so that the RFQ output beam is matched or mismatched in a known fashion to the rest of the lattice. Because the halo takes many lattice periods to fully develop, this final cluster of WS/HS are positioned to be most sensitive to halo generation.

Figure 1. The 11-m, 52-magnet FODO lattice includes nine WS/HS stations that measure the beam's transverse projected distributions.

As the RFQ output beam is mismatched to the lattice, the WS/HS actually observe a variety of distortions to a properly matched gaussian-like distribution (1,3). These distortions appear as distribution tails or backgrounds. It is the size, shape, and extent of these tails that predicts specific type of halo. However, not every lattice WS/HS observes the halo generated in phase space because the resultant distribution tails may be hidden from the projection's view. Therefore, multiple WS/HS are used to observe the various distribution tails.

## 2 WS/HS DESCRIPTION

Each station consists of a horizontal and vertical actuator assembly (see fig. 2) that can move a 33-µm-carbon monofilament and two graphite/copper scraper sub-

# THE MEASUREMENT OF Q' AND Q'' IN THE CERN-SPS BY HEAD-TAIL PHASE SHIFT ANALYSIS

R. Jones, H. Schmickler, CERN, Geneva, Switzerland

*Abstract*

A so-called "Head-Tail" chromaticity measurement system has recently been installed in the CERN-SPS, which allows the chromaticity (Q') to be calculated from several hundred turns of data after transverse excitation. The measurement relies on the periodic dephasing and rephasing that occurs between the head and tail of a single bunch for non-zero chromaticity. By measuring the turn-by-turn position data from two longitudinal positions in a bunch it is possible to extract the relative dephasing of the head and the tail, and so to determine the chromaticity. In addition, by changing the orbit of the circulating beam this technique allows the variation of chromaticity with radial position (Q'') to be measured with a much higher resolution than is currently possible using RF modulation. This paper describes this "Head-Tail" measurement technique and discusses some recent results obtained using prototype LHC beam (25ns spacing) in the CERN-SPS.

## 1 INTRODUCTION

The tight tolerances on beam parameters required for successful LHC operation implies a good knowledge of the chromaticity throughout the cycle. However, many of the methods currently used to measure chromaticity in circular machines (see [1] and references therein) are likely to be incompatible with LHC high intensity running. For example, the most common method, of measuring the betatron tune as a function of beam energy, might be difficult to implement due to the tight tolerances imposed on the betatron tune itself and the limited momentum acceptance of the LHC. Chromaticity can also be calculated from the amplitude of the synchrotron side-bands observed in the transverse frequency spectrum. This method, however, suffers from resonant behaviour not linked to chromaticity and the fact that the low synchrotron tune of the LHC would make it difficult to distinguish these side-bands from the main betatron tune peak. The width of the betatron tune peak itself, or the phase response of the beam transfer function also give a measure of chromaticity, but require a knowledge of how the momentum spread in the beam changes with energy.

In this paper we describe the first results from an alternative method, tested during 2000 on the CERN-SPS. This so-called "Head-Tail" chromaticity technique does not rely on an accurate knowledge of the fractional part of the betatron tune and, for a machine operating well above transition, the calculated chromaticity is virtually independent of beam energy.

## 2 THE HEAD-TAIL PRINCIPLE

Assuming longitudinal stability, a single particle will rotate in longitudinal phase-space at a frequency equal to the synchrotron frequency. During this longitudinal motion the particle also undergoes transverse motion, which can be described by the change in the betatron phase, θ(t), along the synchrotron orbit. If the whole bunch is kicked transversely, then the resulting transverse oscillations for a given longitudinal position within the bunch can be shown to be given by

$$y(n) = A\cos[2\pi nQ_0 + \omega_\xi \hat{\tau}(\cos(2\pi nQ_S) - 1)] \quad \mathbf{(1)}$$

where n is the number of turns since the kick, $Q_0$ is the betatron tune, $Q_S$ is the synchrotron tune, $\hat{\tau}$ is the longitudinal position with respect to the centre of the bunch, and $\omega_\xi$ is the chromatic frequency and is given by

$$\omega_\xi = Q'\omega_0 \frac{1}{\eta} \quad \mathbf{(2)}$$

Here Q' is the chromaticity, $\omega_0$ is the revolution frequency and $\eta = 1/\gamma^2 - 1/\gamma_{tr}^2$. If we now consider the evolution of two longitudinal positions within a single bunch separated in time by Δτ, then from Eq. 1 it follows that the phase difference in the transverse oscillation of these two positions is given by

$$\Delta\Psi(n) = -\omega_\xi \Delta\tau(\cos(2\pi nQ_S) - 1) \quad \mathbf{(3)}$$

This phase difference is a maximum when $nQ_S$ = ½, i.e. after half a synchrotron period, giving

$$\Delta\Psi_{MAX} = -2\,\omega_\xi\,\Delta\tau \quad \mathbf{(4)}$$

The chromaticity can therefore be written as

$$Q' = \frac{-\eta\,\Delta\psi(n)}{\omega_0\,\Delta\tau(\cos(2\pi nQ_s) - 1)}$$

$$Q' = \frac{\eta\,\Delta\psi_{MAX}}{2\omega_0\,\Delta\tau} \quad \mathbf{(5)}$$

## 3 THE SPS HEAD-TAIL MONITOR

A schematic layout of the SPS Head-Tail monitor set-up is shown in Fig. 1. A straight stripline coupler followed by a 180° hybrid is used to provide the sum and difference signals for a given measurement plane. These

# Excitation of Large Transverse Beam Oscillations Without Emittance Blow-up Using the AC-Dipole Principle

O. Berrig, W. Hofle, R. Jones, J. Koopman, J.P. Koutchouk, H. Schmickler, F. Schmidt,
CERN, Geneva, Switzerland

*Abstract*

The so-called "AC-Dipole" principle allows the excitation of transverse oscillations to large (several $\sigma$) excursions without emittance blow-up. The idea was originally proposed and tested at BNL for resonance crossing with polarized beams, using an orbit corrector dipole with an excitation frequency close to the betatron tune, hence "AC-Dipole". This method of beam excitation has several potential applications in the LHC, such as phase advance and $\beta$-measurements, dynamic aperture studies and the investigation of resonance strengths. The technique was recently tested in the CERN SPS using the transverse damper as an "AC-Dipole" providing the fixed frequency excitation. results from this experiment are presented, along with an explanation of the underlying principle.

## 1 INTRODUCTION

The measurement of transverse beam parameters requires either kicking the beam or exciting a coherent oscillation. In both cases the emittance of hadron beams increases in the absence of a significant radiation damping. Furthermore the decoherence due to the incoherent betatron tune spread and head-tail damping perturbs the measurement in a complicated way in the presence of non-linearities.

In LHC, the latter are expected to be significant, requiring corrections of the geometric and chromatic sextupole, octupole, decapole and dodecapole field perturbations. The emittance budget for nominal performance is only 7%. The blow-up due to beam measurements integrated over a machine cycle should therefore be limited to $\approx 1\%$.

Another requirement is the understanding of the non-linearity. If it is significant, the transverse signal due to a kick decoheres very rapidly. The number of possible sources is too large for an empirical optimization. The emittance blow-up can be tolerated at injection energy as the machine can be refilled rapidly. At collision energy, however, the measurement of the non-linearity by kicking the beam would become very costly in time, on top of being very delicate if quenching the machine is to be avoided.

There is therefore a strong motivation to explore other means of transverse beam measurements for small and large transverse amplitudes.

## 2 PRINCIPLE OF THE AC DIPOLE EXCITATION

The emittance-conserving beam excitation was studied at BNL for adiabatic resonance crossing with polarized hadron beams [1]. It was realized that the same principle can be used to diagnose the linear and non-linear transverse beam dynamics [2] [4] [3]. The principle is as follows: the beam is excited coherently at a frequency close but outside its eigenfrequencies by an oscillating dipolar field. Hence the name of AC dipole given to the excitor. In the simplified model of a linear oscillator, the beam is expected to oscillate at the excitor frequency with a phase shift of $\pi/2$. The energy of the coherent oscillation does not couple with the incoherent oscillations of the individual beam particles. There is therefore no change of the beam emittance. The amplitude of the forced oscillation is given by, e.g. [2]:

$$z(s) \approx \frac{1}{4\pi|Q_z - Q_e|}\frac{B_e l}{B\rho}\sqrt{\beta(s)\beta_e} \qquad (1)$$

where $z$ stands for $x$ or $y$, $Q_z$ the eigentune of the $z$-mode, $Q_e$ the tune of the excitor (frequency divided by the revolution frequency), $B_e l/B\rho$ the kick angle and $\beta$ the usual focusing function.

There is no constraint which would prevent selecting a rational excitor frequency of the form $Q_e = n/p$. The beam can then be seen to circulate on a dc closed orbit which closes after $p$ turns.

## 3 ADIABATICITY CONDITION

The field of the AC dipole must be turned on and off in such a way that no beam blow-up occurs during these phases. The adiabaticity condition can be calculated by integrating the equation of the motion for a simple linear ramp. The results (Figure 1) show that a ramp duration in the few ms range is enough to guarantee a blow-up less than 1% up to amplitudes of the order of $100\sigma$. This adiabaticity condition may be understood qualitatively in two ways:

- Considering that the beam circulates on a $p$-turn closed orbit, the usual criterion of bumping the beam closed orbit can be used. The orbit increment on each turn shall be small compared to the beam size, giving a blow-up of the order of this increment. This criterion explains why the ramp rate must be reduced when the tune difference $|Q_z - Q_e|$ decreases. The orbit increment per turn indeed increases like $1/|Q_z - Q_e|$.

# MEASURING BETA-FUNCTIONS WITH K-MODULATION

O. Berrig, C. Fischer, H. Schmickler CERN, Geneva, Switzerland

*Abstract*

The precise measurement of the local value of the beta-function at the place of a beam size monitor is necessary for the precise determination of the beam emittance. We developed a new method for the measurement of the beta-function by using of continuous square-wave modulation of the force of the quadrupole and by continuous tune tracking. Measurements were performed at LEP in order to evaluate the precision that can be achieved with this method in the LHC.

The paper describes the method and discusses in details the results obtained at LEP for colliding and non-colliding beams.

## 1 EMITTANCE MEASUREMENT

The emittance can be obtained from the measurement of the beam size from the following formula:

$$\sigma(s) = \sqrt{\varepsilon\beta(s)}$$

where σ(s) is the transverse beam size, ε is the emittance, β(s) is the beta-function and s is the longitudinal distance.

Therefore, in order to determine the emittance with high precision, the beta-function must also be known to high precision. We aim at a precision of 1%.

## 2 BETA-FUNCTION MEASUREMENT

The general principle of the beta-function measurement can be seen in fig.1. By changing the strength ( k ) of the quadrupole, the accelerator optics change, and therefore the tune change. The bigger the change of the strength, the bigger the tune change. The two are linked via the average value of the beta-function in the quadrupole:

$$\beta_{average} \approx 4\pi \frac{\Delta Q}{\Delta k \cdot l}$$

where $\Delta Q$ is the tune change, $\Delta k$ is the change in quadrupole strength and $l$ is the length of the quadrupole. The measurement of the tune is done by a PLL [1]. We could also have measured the tune with a continuous FFT, but chose not to, because a FFT has a quantization error of 1/(NΔT).

Apart from the internal noise in the PLL, the measurement of ΔQ is subjected to noise from various sources, like:

- A change in the closed orbit.
- Beam-beam interactions.

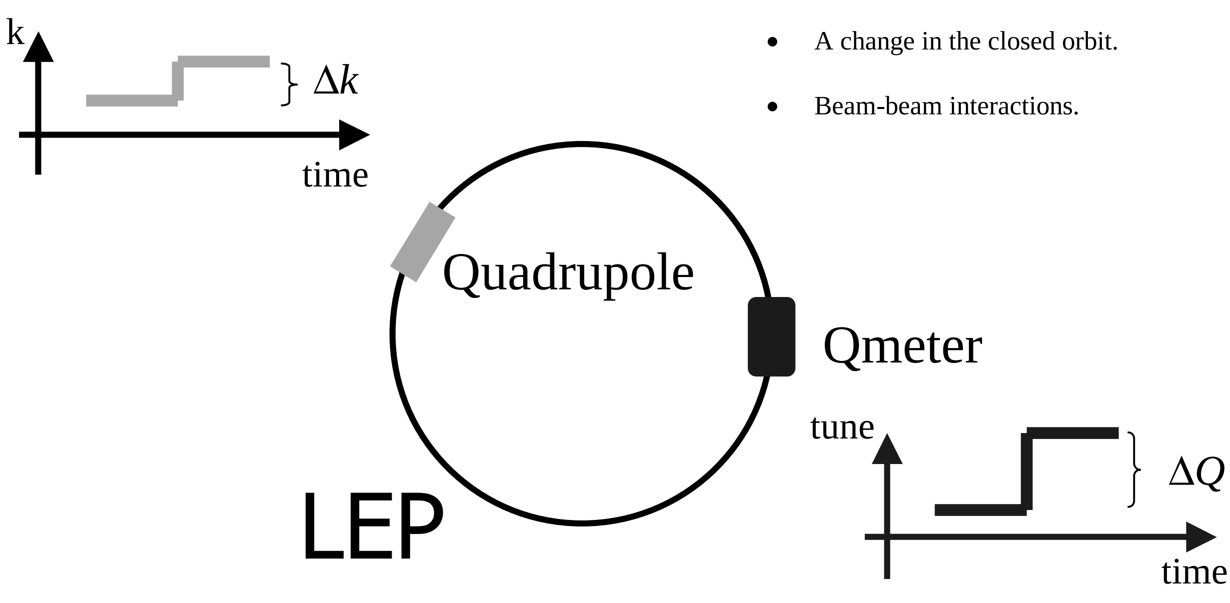


Figure 1: Static-k measurement. By changing the strength (=Δk) of the quadrupole, the tune (=ΔQ) change. The ratio between them is determined by the value of the beta-function at the place of the quadrupole.

# X-RAY INTERFERENCE METHODS OF ELECTRON BEAM DIAGNOSTICS

O.Chubar, A.Snigirev, S.Kuznetsov, T.Weitkamp, ESRF, Grenoble, France
V.Kohn, Russian Research Center “Kurchatov Institute”, Moscow

*Abstract*

Electron beam diagnostics methods based on interference and diffraction of synchrotron radiation (SR) in hard X-ray range will be discussed. Two simple optical schemes providing X-ray interference patterns highly sensitive to transverse size of the emitting electron beam, will be considered. For each scheme, the visibility of fringes in the pattern depends on transverse size of the electron beam. However, the pattern is also determined by the scheme geometry, shape and material of diffracting bodies. Therefore, for correct interpretation of the experimental results, high-accuracy computation of SR emission and propagation in the framework of physical optics should be used. Examples of practical measurements and processing of the results are presented.

## 1 INTRODUCTION

Visible light interference methods have proved to be very efficient for diagnostics of relativistic charged particle beams emitting synchrotron radiation in magnetic fields of accelerators [1-6]. Nevertheless, since 3rd-generation SR sources are mainly dedicated for X-rays, the use of X-rays for electron beam diagnostics in these accelerators can be advantageous. Such diagnostics can be based on the same equipment that is used in other experiments; besides, it may offer higher resolution.

A number of X-ray experimental techniques benefiting from high spatial coherence of the SR, e.g. phase-contrast imaging, holography, interferometry, have been developed [7-11]. These techniques require characterisation and “in-place” control of the source coherence, which makes the X-rays based beam diagnostics further important.

This paper considers two very simple diffraction/ interference schemes, which can be readily used for beam diagnostics at any X-ray beamline (not necessarily fully dedicated for the diagnostics). One is the well-known Fresnel diffraction at a slit, and the other is a wavefront-splitting interference scheme where a thin fiber is used as an obstacle and phase-shifting object. As different from previous considerations made for isotropic source with finite transverse size [12-14], the current paper takes into account peculiarities of synchrotron (undulator) radiation emitted by an electron beam with finite transverse emittance (i.e., not only with the size, but also with angular divergence).

## 2 BASICS OF THE METHODS

### *2.1 Isotropic Source with Finite Transverse Size*

Let us recall that in the case when a source has finite transverse size, and different points of the source emit incoherently, the resulting intensity of the radiation passed through an optical system to a detector plane is obtained by summing up intensities of emission from all points of the source [15]:

$$I(x,y) = \iint I_0(x,y;x_s,y_s)\, B(x_s,y_s)\, dx_s dy_s \, , \qquad (1)$$

where $(x,y)$ are transverse coordinates in the detector plane, $(x_s,y_s)$ transverse coordinates at the source, $I_0$ intensity from a point source (referenced below as point-source intensity), and $B$ the source brightness.

For many simple diffraction and interference schemes with a source emitting spherical waves, in small-angle approximation, Eq. (1) is a convolution-type integral, i.e.:

$$I_0(x,y;x_s,y_s) \approx \tilde{I}_0(x - mx_s, y - my_s)\, , \qquad (2)$$

where $m = -r_d/r_s$ is a “magnification” factor, with $r_s$ being distance from the source to an obstacle, and $r_d$ distance from the obstacle to the detector (see Fig. 1). We note that this effect is used in pinhole cameras (which are successfully applied for electron beam diagnostics [16]).

If Eq. (2) is valid, $\tilde{I}_0(x,y)$ is known, and the resulting intensity $I(x,y)$ is measured to a sufficient accuracy, one can try to reconstruct $B(x_s,y_s)$ using the Wiener filtering [17] or a regularization technique [18].

The resolution of an optical scheme at the source size measurement depends on the point-source intensity $\tilde{I}_0(x,y)$. In the case of Fresnel diffraction at a slit, $\tilde{I}_0$ possesses fringes with the widths on the order of $\lambda r_d/a$, where $\lambda$ is the radiation wavelength and $a$ the slit size. This can be compared with the source image size $\sigma r_d/r_s$. However, the resolution of this scheme can be much better, because $\tilde{I}_0$ has also smaller details originating from “interaction” of the slit edges (see Fig. 2).

Figure 1: Interference pattern formation from a source with finite transverse size.

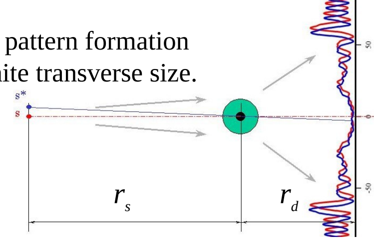

# Beam Charge Asymmetry Monitors for Low Intensity Continuous Electron Beam*

Chris Cuevas, Jean-Claude Denard, Arne P. Freyberger, Youri Sharabian
Jefferson Lab, 12000 Jefferson Avenue, Virginia, 23606 USA

*Abstract*

Experimental Hall B at Jefferson Lab (JLAB) typically operates with CW electron beam currents in the range of 1 - 10 nA. This low beam current coupled with a 30 Hz flip rate of the beam helicity required the development of new devices to measure and monitor the beam charge asymmetry. We have developed four independent devices with sufficient bandwidth for readout at 30 Hz rate: a synchrotron light monitor (SLM), two backward optical transition radiation monitors (OTR) and a Faraday Cup. We present the results from the successful operation of these devices during the fall 2000 physics program. The reliability and the bandwidth of the devices allowed the control of the current asymmetry at the source laser by means of a feedback loop.

## 1 POLARIZED BEAM AT JLAB AND HALL B REQUIREMENTS

The JLAB polarized source generates three CW electron beams for the experimental halls (A, B & C). Two of these halls, A & C, house two-arm spectrometers and operate with beam currents between $50\mu$A and $100\mu$A. Hall B houses a large acceptance spectrometer which is luminosity limited to beam currents of 1 to 10nA. This small CW beam current is a challenge for beam diagnostics.

The electron beam polarization is toggled between the $h^+$ helicity state and the $h^-$ helicity state at a 30Hz rate. The relative beam charge for each state must be accurately measured in order to correctly extract the physics cross sections. The measured physics asymmetries are of the order of a few percent, which was used to place a desired limit on the beam charge asymmetry; $A_Q = \frac{N^+_{e^-} - N^-_{e^-}}{N^+_{e^-} + N^-_{e^-}} < 0.1\%$.

## 2 BEAM CHARGE ASYMMETRY MONITORS

To monitor the relative amount of beam charge in each helicity state requires devices that are linear with respect to beam current, fast enough to be recorded at the 30Hz time scale and independent of other possible helicity dependent effects (like beam motion).

Prior to fall 2000, the Hall-B beam current instrumentation consisted of the Faraday Cup and beam position/current RF cavities. Both were of insufficient bandwidth to measure the beam charge at a 30Hz rate. Three new devices were installed along the beam-line, a synchrotron light monitor (SLM) and two backward optical transition radiation monitors (OTR), prior to the fall 2000 physics run. The Faraday Cup electronics was upgraded to work at a higher bandwidth at this time as well. The following sections describe these developments.

### 2.1 Synchrotron Light Monitor

The electron beam is transported from the “switch-yard” to Hall-B via a vertical “S” bend. The bending radius of the last dipole is 33m. Downstream of this dipole a mirror reflects the synchrotron light through an optical port. From there the synchrotron light goes through an aperture and is split, with one half of the light incident on a CCD camera and the other half is focussed via a lens onto a photomultiplier tube (PMT). The PMT current output is proportional to the beam current and is used to measure $A_Q$. The lens is used to focus the light onto the photo-cathode so that the synchrotron light position on the photo-cathode is independent of beam position. Beam motion in the bend plane changes the geometrical acceptance. Details of the PMT and electronics chain is found in a later section.

### 2.2 Optical Transition Radiation Monitors

Two OTR monitors were installed; each use $0.8\mu$m Al foils[1] as the source of OTR. OTR-1 consists of a foil 2.54cm in diameter mounted at a $45^0$ angle with respect to the beam and an optical port. OTR-1 is installed just upstream of the Hall-B Møller polarimeter target and is used only during Møller runs. OTR-2 consists of a foil mounted at $60^0$ with respect to the beam. The foil resides just inside of an integrating sphere[2], and uniformly illuminates the photo-cathode. The integrating sphere is used to minimize reflective variations in the OTR foil and to minimize the position dependence of the light on the photo-cathode. OTR-2 is located ∼5m upstream of the experimental target. The electron beam in this region is rastered in a spiral pattern approximately $1.5$cm in diameter.

### 2.3 Faraday Cup

After the electron beam traverses the experimental target it is transported to the Faraday Cup. With a capacitance of

* Work supported the Southeastern Universities Research Association (SURA) which operates the Thomas Jefferson National Accelerator Facility (JLAB) for the United States Department of Energy under contract DE-AC05-84ER40150

[1]Goodfellow Cambridge Limited, Cambridge, CB4 4DJ, England

[2]Oriel Instruments, 150 Long Beach Boulevard, Stratford, CT 06615-0872

# NEW DEVELOPMENT OF A RADIATION-HARD POLYCRYSTALLINE CdTe DETECTOR FOR LHC LUMINOSITY MONITORING

E. Rossa, H. Schmickler, CERN, Geneva, Switzerland,
A. Brambilla, L. Verger, F. Mongellaz, LETI, Grenoble, France

*Abstract*

Detectors presently considered for monitoring and control of the LHC luminosity will sample the hadronic/electromagnetic showers produced by neutrons and photons in copper absorbers designed to protect the superconducting magnets from quenching. At this location the detectors will have to withstand extreme radiation levels and their long term operation will have to be assured without requiring human intervention. For this application we have successfully tested thick polycrystalline-CdTe detectors. The paper summarizes the results obtained on rise-times, sensitivity and resistance to neutron irradiation up to a dose of $10^{15}/cm^2$.

## 1 - INTRODUCTION

The requirements on the LHC luminosity monitors can be summarised as:

- Possible counting rate of 40 MHz, i.e. rise and fall times below 10 ns
- Resistance to radiation damage up to doses of $10^{18}$ neutrons/$cm^2$ and $10^{16}$ protons/$cm^2$
- Good signal to noise ratio even for single minimum ionisation particles, such that in the shower sample statistically multiple events per bunch crossing can be destinguished from single events.

Cadmium telluride (CdTe) photo-conductor material used for nuclear radiation detectors and opto-electronic devices. A single Minimum Ionising Particle (MIP) creates about 50 000 electron-hole pairs in a 300 μm thick CdTe layer. In comparison about 53 000 pairs will be created in GaAs, but only 32 200 in Si and 11 850 in diamond [1].

The CdTe samples used for our tests have been produced by LETI (part of CEA) in Grenoble. These prototype detectors consist of discs of polycrystalline-CdTe about 16-mm in diameter with gold electrodes of 7 by 7 mm on both sides.

An ionisation chamber is currently as well under study to meet the above requirements [2]. References on the luminosity project are given in [3] and some others applications of CdTe are in [4-5].

## 2 - SPEED TESTS

### *2.1 Tests with a picosecond laser*

The speed tests of the polycrystalline-CdTe output signal were undertaken at the Laboratoire de Sciences et Ingénierie des surfaces at the Université Claude Bernard-Lyon 1, [7]. A laser pulse (35 ps FWHM, 1060 nm wavelength) was onto one of the gold plated electrodes. The electrodes are porous enough to allow photons to reach the main bulk of the photoconductor. The photon transmission through the 0.5 mm thick sample was close to 50% at 1060 nm. Such a pulse is a good simulation of the ionisation track produced by a high energy particle going through the detector parallel to the electric field.

The signal produced by the laser pulse was very large and easy to measure on a single shot, fast-sampling oscilloscope. The measured rise time was limited to a fraction of nanosecond by the oscilloscope bandwidth.

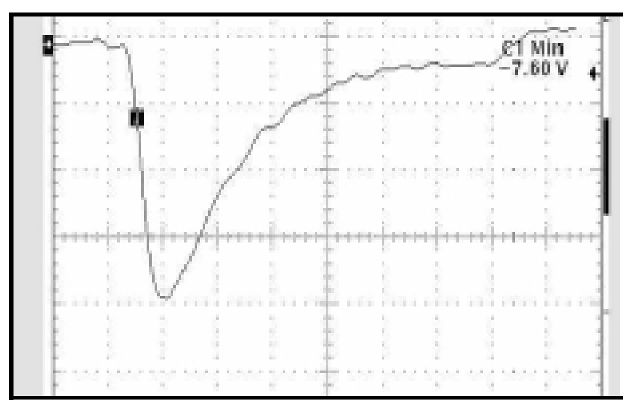


Figure 1: Example of a CdTe output signal terminated directly into 50Ω on the oscilloscope. The vertical scale is 2 Volts/division and the horizontal 2.5 ns/division. The applied bias voltage was 100 Volts.

## 3 - TESTS WITH MIP

The sensitivity was measured using a charge sensitive amplifier with a shaping time of 2 μs. The set-up used is described in reference [8]. The sample was irradiated by a radioactive source ($^{90}Sr$) and the particles traversing the sample were detected by a diode and triggered the

# REAL-TIME TUNE MEASUREMENTS ON THE CERN ANTIPROTON DECELERATOR

M.E. Angoletta, M. Ludwig, N. Madsen, O. Marqversen# and F. Pedersen,
CERN, Geneva, Switzerland

*Abstract*

A novel system for real-time tune measurement during deceleration of a low-intensity particle beam is presented. The CERN Antiproton Decelerator decelerates low intensity (2 x $10^7$) antiproton beams from 3.5 GeV/c to 100 MeV/c. Because of the eddy-currents in the magnets, a tune-measurement during a pause in the deceleration would not be representative. One must thus be able to measure the tune in real time during the deceleration. The low intensity of the antiproton beam prevents the use of standard Schottky techniques, and swept Beam Transfer Function (BTF) measurements are too slow. A system was therefore developed which uses an M-shaped power spectrum, exciting the beam in a band around the expected frequency of a betatron side-band. Excitation at the betatron frequency, where beam response is highest, is thus minimized and measurements of BTF, and therefore the tune, can be made with much reduced emittance blow-up.

## 1 INTRODUCTION

The CERN Antiproton Decelerator (AD) decelerates low intensity (15 µA to 0.2 µA) antiproton beams from 3.5 GeV/c to 100 MeV/c. The low intensity in the AD results in very weak transverse Schottky signals from 0.5 pA/√Hz at 3.5 GeV/c down to 0.025 pA/√Hz for an uncooled beam at 100 MeV/c measured around 5.6 MHz (The resonance frequency of the pick-up (PU)). The Schottky signals are not large enough to measure the tune, so it is therefore necessary to use BTF-measurements. To measure the AD tune during deceleration without pausing (due to eddy-currents in the magnets, a paused measurement will not be representative) we needed a technique faster than a swept BTF (although swept BTF on plateaux has been used during the start up phase). A system was therefore developed which uses an M-shaped power spectrum, exciting the beam in a band around the expected frequency of a betatron side-band.

## 2 THE TUNE MEASURING SYSTEM

The system, see Figure 1, consists of the Schottky system, which measures the beam response, and the M-shaping filters that generate the stimulation. The Schottky system consists of a resonant PU and an ultra- low-noise pre-amplifier followed by a level adaptation system (to lift the signal over the quantization noise of the digital system). The amplified signal enters a Digital Receiver Board (DRX) after being analog to digital converted, where the data are hardware pre-processed in up to 8 Digital Down Converters (DDC). By this digital translation (down-mixing) the frequency window of interest is from DC and upwards. This will enable a Digital Signal Processor (DSP) perform the processing i.e. find the BTF. This is then passed on to the control system. The control system sets up the wanted analysis including the hardware control. The stimulation centre frequency is set as a factor n±q of the revolution frequency, where n is

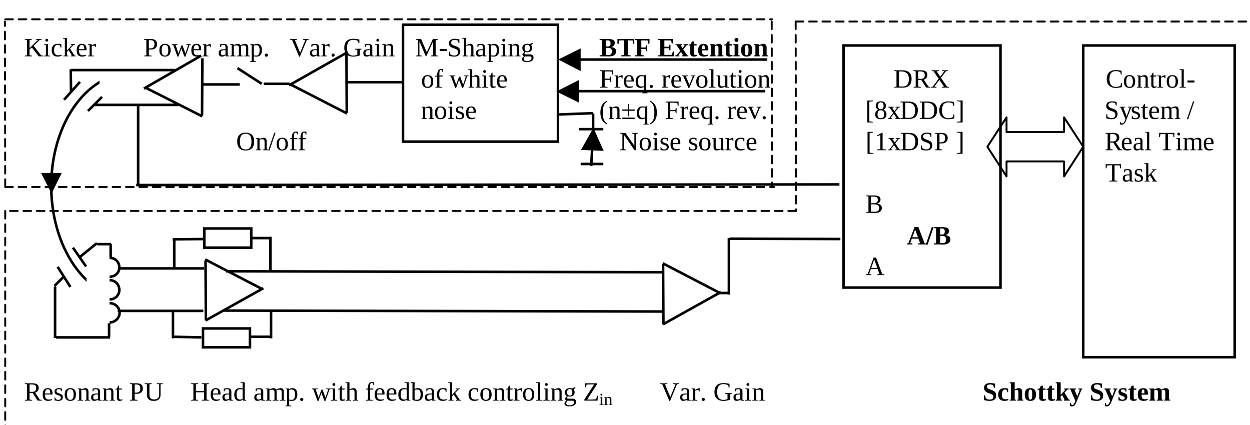


Figure 1: System block diagram.

# BENCH TEST OF A RESIDUAL GAS IONIZATION PROFILE MONITOR (RGIPM)[1].

W. C. Sellyey, J. D. Gilpatrick, LANL, Los Alamos NM, USA
Ralph Senior, General Atomics, San Diego CA, USA

*Abstract*

An RGIPM has been designed[1], constructed and bench tested to verify that all components are functioning properly and that the desired resolution of about 50 μm rms can be achieved. This paper will describe some system details and it will compare observed results to detailed numerical calculations of expected detector response.

## 1 BEAMLINE COMPONENTS

Figure 1 shows a top view horizontal cross section of the primary beam line components. It is set up to measure a vertical beam profile. The magnet (1) is a split H configuration with a gap of 24.6 cm. The coils (2) can produce a 0.12 T field at the center of the magnet. The electrostatic vacuum box (3) contains an 8 mm thick high voltage (HV) plate (4) 39 by 38 cm. One cm above the plate (towards the bottom of the page) is a set of 100 μm gold coated wires (not seen) running across the page. These are separated by 30 mm. High voltage feedthrough (5) is used to supply up to -15 kV to the plate and (6) supplies voltage to the grid wires. The vacuum box is at ground potential. Not seen is a 100 μW Krypton light and collimator on the top of the box. It shines a 5° wide beam on the wires near the center of the box. Its spectrum consists of 20% 10.64 eV photons and 80% 10.03 eV photons. On the left and right side of the box are flanges (not shown) to connect to 10 cm diameter beam tubes.

A removable "hat" (7) contains a mechanism that moves a scintillation detector (8) across the wires (in and out of the page). A quartz fibre (9) carries scintillation photons through an optical vacuum feedthrough (10). A motion feed through under the hat (not visible) connects the moving mechanism to a worm gear driven by a stepper motor. The worm gear shaft was rigidly connected to an LVDT.

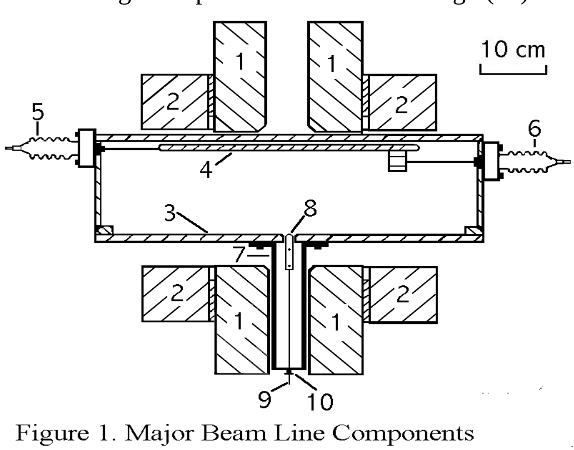

Figure 1. Major Beam Line Components

Some details of the scintillation detector are shown in figure 2. The limiting aperture (1) was a 125 μm hole in a 1 mm thick Aluminum piece. The electrons that pass through this hit a 0.5 mm thick, 2X2 mm square scintillator (2). A 500 μm gold coated quartz optical fibre (3) caries some of the resulting photons to a photomultiplier (PM) tube outside the vacuum. The detector moves in a 1.8 cm by 10 cm slot in the top of the vacuum box. The total distance from the HV plate to the scintillator is 14 cm.

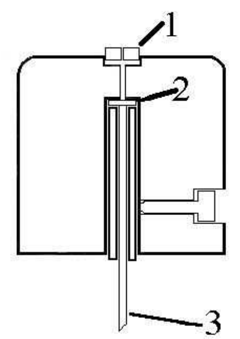

Figure 2. Scintillation Detector

## 2 DATA ACQUISITION SYSTEM

The single photon PM output pulses are amplified, shaped and sent as TTL pulses to a counter/timer on a National Instruments (NI) PCI-MIO-16XE-10 board. This board is installed in a Micron PC. A/D's and D/A's on the NI board are used for controlling and measuring most voltages and currents in the system.

High voltages are generated by analogue control of Glassman MJ series power supplies. A high precision resistive high voltage divider system is used to produce a stable ratio of voltages to the plate and grid. The exact ratio of the grid to plate voltage is fine tuned by a manually controlled potentiometer.

The stepper motor is controlled by a set of output bits on the NI board. The LVDT electronics is interfaced to the PC by a serial port. Software closes the loop between the stepper motor and the LVDT. The detector position is reproducible to about 3 μm on a short term basis (hours

[1] This work supported by U.S. Department of Energy.

# OPTICAL BUNCH-BY-BUNCH BEAM DIAGNOSTIC SYSTEM IN KEK-PF

T. Kasuga, A. Mochihashi, T. Obina, Y. Tanimoto
High Energy Accelerator Research Organization (KEK), Japan

*Abstract*

An optical bunch-by-bunch beam diagnostic system, which can detect oscillations of individual bunches in a multi-bunch operation, has been developed. The system is composed of a high-speed light shutter and an optical beam-oscillation detector. The shutter that consists of a pockels cell and polarizers can be opened or closed in a bunch spacing time (2ns in KEK-PF) and it can select a light pulse corresponding to a certain bunch in a bunch train. The beam oscillation detector can detect oscillations of the picked-out bunch with a spectral analysis method. The diagnostic system has been installed in KEK-PF Beamline-21, and observed vertical oscillation of individual bunches due to an instability in the multi-bunch operation.

## 1 INTRODUCTION

An analog switch method is usually adopted for a bunch-by-bunch beam diagnostic system. In the method, a pulse corresponding to a certain bunch in a pulse train from a beam monitor (a button type electrode is usually chosen) is selected by a fast electronic switch [1]. A bunch-by-bunch and turn-by-turn beam diagnostics with a digital memory system has also been developed [2]. However, ringing that commonly occurs in a fast electronics degraded the detection capability. Moreover, the electronic detection has an unavoidable problem that the BPMs detect not only the beam signal but also wake fields. To avoid these problems, we have adopted an optical beam detection method and developed an optical switch called a "high-speed light shutter"[3]. One of its merits is that the optical system is free from harmful effect caused by ringing, and has an excellent tolerance to electronic noise. Moreover, it is the most important strong point that the system is not affected by wake fields propagating in vacuum ducts. We have developed an optical bunch-by-bunch beam diagnostic system with the shutter, and have been observing vertical oscillation of individual bunches due to an instability in a multi-bunch operation in KEK-PF with the system.

## 2 OPTICAL BEAM DIAGNOSTIC SYSTEM

### 2.1 High-Speed Light Shutter

Basically, the shutter system is composed of a pair of polarization filters and a pockels cell [3]. The pockels cell (Fastpulse Technology, 1044-FW) is placed between the polarization filters whose polarization angles are perpendicular to each other. The incident light can pass through the shutter while a high voltage pulse is applied to the cell because the cell rotates the polarization plane. Since the time response of the cell is fast enough, the operation speed of the shutter is mainly determined by the rise and fall time of the pulser. We have used the pulser whose output pulse has a width (FWHM) of 1.7 ns, which is shorter than the bunch spacing of 2 ns, and a height of 550 V. We operate the shutter with a repetition rate of $f_{shutter}$= 534 kHz which is one third of a revolution frequency ($f_{rev}$=1.60 MHz in the KEK-PF) because of the limitation of the repetition rate of the high voltage pulser (max. 600 kHz) and a reason described below.

### 2.2 Operation of High Speed Light Shutter

In order to observe the time structure of the shutter we made use of a photon counting method [4] and used a CW-laser (Spectra Physics, $\lambda = 488$ nm) as a light source. A block diagram of the shutter, including the optical setup, is shown in Fig. 1. To improve the polarization of the incident light on the cell we used a couple of polarizers. A signal generator generates a signal with a frequency equal to the RF acceleration frequency ($f_{RF}$=500 MHz in the KEK-PF). A divider generates a signal with a repetition frequency of $f_{rev}/3$. We used the divided signal as a trigger for the high voltage pulser. To eliminate electronic noise caused by the high voltage pulse, we carefully shielded the whole of the cell and cables that feed the pulse to the cell.

The light from the shutter passes through a pair of lenses. To eliminate stray light due to multiple scattering between optical devices, an iris diaphragm is set at the focal position of the first lens of the pair. The light from the lenses is attenuated by a neutral density filter (ND filter) and a slit, and detected by a microchannel-plate type photomultiplier (MCP-PMT, Hamamatsu Photonics, R3809U-52), which has an excellent time resolution (rise time of 0.15 ns, transit time spread of 25 ps). The output signal of the MCP-PMT is processed by a constant fraction discriminator (CFD, TENNELEC, TC454) to generate the start signal of the time-to-amplitude converter (TAC, ORTEC 467). On the other hand, a signal synchronized with the trigger for the pulser is used as a stop signal for the TAC. The output signals of the TAC are amplified and analyzed with a multichannel analyzer (MCA, Laboratory Equipment). An extinction ratio, which is defined as the ratio of intensity of singled-out light by the shutter to that of the leaked one, sensitively depends on a direction of an axis of the cell. Therefore, it is important to align the axis of the cell precisely with the direction of the light to operate the shutter system properly. To adjust the angle of the cell minutely

# DESIGN OF A MAGNETIC QUADRUPOLE PICK-UP FOR THE CERN PS

A. Jansson, L. Søby and D.J. Williams, CERN, Geneva, Switzerland

*Abstract*

A quadrupole pick-up is sensitive to the quantity $\sigma_x^2 - \sigma_y^2$, where $\sigma_x$ and $\sigma_y$ are the horizontal and vertical r.m.s. beam sizes. Since it is a non-invasive device, it is potentially very useful for matching and emittance measurements. A magnetic quadrupole pick-up has been developed for the CERN PS. By coupling to the radial component of the magnetic field around the beam, it was possible to eliminate the common-mode problem, which is usually a limiting factor in the use of quadrupole pick-ups. This paper presents the final pick-up design, which is the result of a series of simulations and test prototypes. The performance of the pick-up and its associated electronics is discussed. Preliminary results from the two pick-ups recently installed in the PS machine are also presented.

## 1 INTRODUCTION

A quadrupole pick-up measures the quadrupole moment of the transverse beam distribution

$$\kappa = \sigma_x^2 - \sigma_y^2 + \bar{x}^2 - \bar{y}^2, \tag{1}$$

by probing the quadrupole component of the field that the beam induces inside the vacuum chamber. Here, $\sigma_x$ and $\sigma_y$ are the r.m.s. beam dimensions in the $x$ and $y$ directions, while $\bar{x}$ and $\bar{y}$ denote the beam position.

An electrostatic pick-up measures the charge collected on electrodes around the beam. The charge is proportional to the electric field in the radial direction, which in polar coordinates $(r, \theta)$ is

$$E_r \propto \frac{i_b}{r}\left(1 + 2\left[\frac{\bar{x}}{r}\cos\theta + \frac{\bar{y}}{r}\sin\theta + \frac{\kappa}{r^2}\cos 2\theta + \dots\right]\right) \tag{2}$$

if the pick-up is round. Here, $i_b$ is the beam current. To measure the $\kappa$ component, four electrodes at $0°$, $90°$, $180°$ and $270°$ are used. A problem with this setup is that the $\kappa$ component is a very small part of the signal on each electrode, which requires extremely good common-mode rejection and a large dynamic range in the electronics. To bypass this problem, a new design was proposed [1], where the radial magnetic field is measured instead. If the conducting boundary is at $r_0$, this field is

$$B_r \propto \frac{i_b}{r}\left[\left(\frac{\bar{x}}{r}\sin\theta - \frac{\bar{y}}{r}\cos\theta\right)\left(1 - \frac{r^2}{r_0^2}\right) + + \frac{\kappa}{r^2}\sin 2\theta\left(1 - \frac{r^4}{r_0^4}\right) + \dots\right] \tag{3}$$

where there is no constant term causing a common-mode signal. For such a pick-up, four antenna loops at $45°$, $135°$, $225°$ and $315°$ are needed to measure the quadrupole field component (see Fig. 1). A prototype tested in the machine produced encouraging results [2]. Based on the prototype experience, laboratory tests and simulations, a final design has been produced [3].

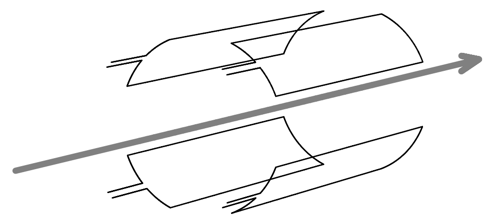

Figure 1: Schematic quadrupole pick-up measuring radial magnetic field. The arrow symbolises the beam.

## 2 PICK-UP DESIGN

### 2.1 Bandwidth and Transfer Impedances

The bunch spectrum at injection into the PS normally covers about 20 MHz, with the lowest interesting frequency component at about 75 kHz (betatron frequency). The pick-up was therefore built with a low-frequency cut-off at 75 kHz. On the high frequency end, the usefulness of the pick-up is limited by reduced common-mode rejection at frequencies above 25 MHz (due to standing waves in the loop). The transfer impedances of the pick-up have a flat frequency characteristic in the pass-band and are 35 $\mu\Omega$/mm$^2$ for the quadrupole signal and 1.5 m$\Omega$/mm for the position signals. These values are for a single antenna loop.

The final pick-up has a length of 508 mm, and a (circular) aperture of 145 mm diameter.

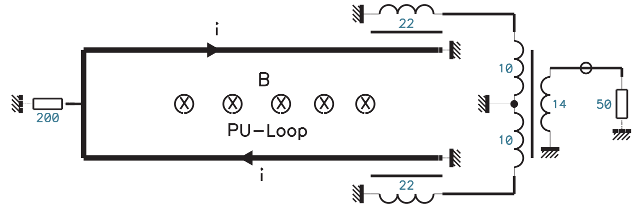


Figure 2: Schematic layout of one antenna loop

### 2.2 Common-Mode Rejection

Although theoretically a pick-up measuring the radial magnetic field has a perfect common-mode rejection, in prac-

# MEASUREMENT OF THE TIME-STRUCTURE OF THE 72 MEV PROTON BEAM IN THE PSI INJECTOR-2 CYCLOTRON

R. Dölling, Paul Scherrer Institut, Villigen, Switzerland

*Abstract*

The time-structure monitor at the last turn of the 72 MeV Injector-2 cyclotron has been improved in order to meet the stringent time-resolution requirement imposed by the short bunch length. Protons scattered by a thin carbon-fibre target pass through a first scintillator-photomultiplier detector and are stopped in a second one. The longitudinal bunch shape is given by the distribution of arrival times measured with respect to the 50 MHz reference signal from the acceleration cavities. From a coincidence measurement, the time resolution of the detectors has been determined to be 51 ps and 31 ps fwhm. Longitudinal and horizontal bunch shapes have been measured at beam currents from 25 µA to 1700 µA. Approximately circular bunches were observed with diameter increasing with current. The shortest observed proton bunch length was 38 ps fwhm.

## 1 INTRODUCTION

Time-structure measurement has been used at PSI since 1974 and has delivered valuable information during the commissioning of Injector 2 and at the introduction of the buncher in the injection line to Injector 2 [1 - 6]. Due to the buncher, the bunch length inside the cyclotron was reduced from ~15° fwhm of RF period to below 5° and it was not clear if the resolution of the time-structure monitor was still sufficient to resolve the bunch shape. In the end of 2000 a new double detector set-up based on NE111 scintillators and Hamamatsu R7400 metal package PMTs with custom divider circuits was tested, which allowed for the determination of the time resolution.

## 2 EXPERIMENTAL SET-UP

The monitor is located half a turn in front of the beam extraction in the space between two sector magnets. A carbon fibre of 30 µm diameter is moved transversally through the beam by a motorised feedthrough (Fig. 1). The detectors are located above, behind a 0.5 mm stainless steel window and a stainless steel aperture of 4.5 mm diameter. Scintillator A (a 8x8x16 mm$^3$ piece of NE111) is separated from scintillator B (8x8x40 mm$^3$ from the same piece of raw material) by a 12 µm aluminium foil which also covers the surface opposite to PMT A in order to enhance light collection. Both PMTs are coupled to the scintillators by silicon grease.

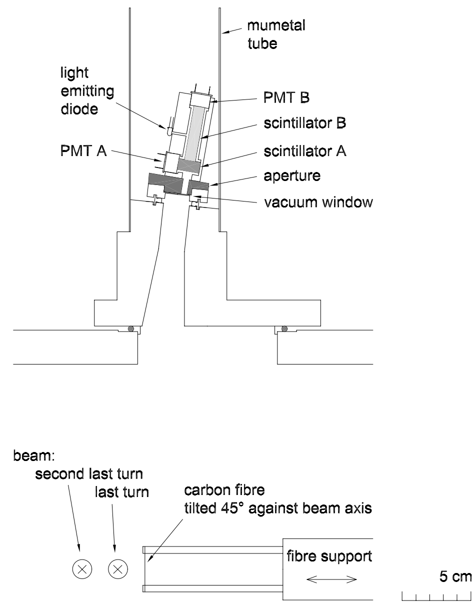


Fig. 1: Detector geometry.

An overview of the electronic set-up and modes of operation is given in Fig. 2. The output signals from the PMTs are transmitted through approximately 80 m of 50 Ω Cellflex LCF ½" cable to the control room. After passing an ohmic divider, one part of the signal is fed to an Elscint STD-N-1 snap-off timing discriminator (SOD) [7] and the other part is used for pulse height discrimination. Besides the elastically scattered protons, there are protons with lower energy from inelastic scattering at the carbon fibre and from scattering at the aperture, which arrive later. Hence, only the highest pulses at PMT B correspond to the correct timing information, and pulse height discrimination is necessary. This is provided by a SIN-FDD100 leading edge discriminator (LED). For a time-structure measurement with PMT B, the fast timing signal of SOD B is allowed to proceed as the start signal to a Canberra 2043 time-to-amplitude converter (TAC) if the pulse height of PMT B surpasses a defined high level. Gating is provided by a SIN-FC107B logic module. The stop signal is derived from the 50 MHz RF-reference signal by a SIN ZCD100A zero-crossing detector and gated in the same way. If the probe is positioned at the centre of a 1600 µA beam, the rate of accepted pulses is of the order of 250 cps.

If the time structure is measured with PMT A, pulse height discrimination is done also with the PMT B signal.

# LASER PROFILE MEASUREMENTS OF AN H$^-$ BEAM

R. Connolly, P. Cameron, J. Cupolo, M. Grau, M. Kesselman,
C-J. Liaw, and R. Sikora
Brookhaven National Lab, Upton, NY, USA

*Abstract*

A non-intercepting beam profile monitor for H$^-$ beams is being developed at Brookhaven National Lab. An H$^-$ ion has a first ionization potential of 0.75eV. Electrons can be removed from an H$^-$ beam by passing light from a near-infrared laser through it. Experiments have been performed on the BNL linac to measure the transverse profile of a 750keV beam by using a Nd:YAG laser to photoneutralize narrow slices of the beam. The laser beam is scanned across the ion beam neutralizing the portion of the beam struck by the laser. The electrons are removed from the ion beam and the beam current notch is measured.

## .1. INTRODUCTION

The Spallation Neutron Source (SNS) under construction at Oak Ridge National Lab consists of a 1GeV H$^-$ linear accelerator (linac), a storage ring, target, and connecting beam-transport lines [1]. The linac delivers a 1.04 ms macropulse which is chopped into $10^3$ pulses of $10^{11}$ protons each. As this pulse enters the storage ring from the linac each chopped pulse lines up longitudinally with all proceeding pulses forming a single 550-ns bunch and a 250-ns gap. After stacking beam in the storage ring for 1000 turns the proton beam is dumped onto a metal target producing a 550 ns pulse of neutrons.

Profiles of the H$^-$ beam will be measured in the medium energy transport line (MEBT) between the radio frequency quadrupole (rfq) and the linac entrance, along the linac, and in the linac-ring transport line. Stepped carbon-wire scanners are the primary profile diagnostic. However beam heating will limit wire scanners to tuning and matching applications with either the beam pulses shortened or the current reduced. Also there are concerns about placing wires near the superconducting cavities where wire failure can cause cavity damage.

We are developing a laser beam profile monitor (LPM) which is non-invasive and suitable for continuous profile monitoring. The technique selects a transverse slice of an H$^-$ beam by photoneutralization by a laser beam [2,3]. An H$^-$ ion has a first ionization potential of 0.75eV and can be neutralized by interacting with a photon with wavelength<1500 nm, fig.1. The 1064-nm light from a Nd:YAG laser is very near the peak of the cross section.

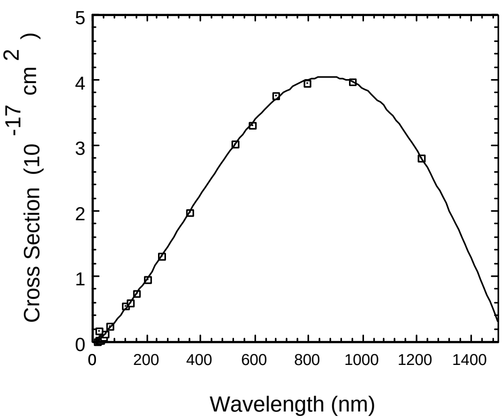


Figure 1: Calculated cross section for H$^-$ photoneutralization as a function of photon wavelength. Data are from a table in ref. [4].

## 2. LINAC EXPERIMENT

Figure 2 shows the experiment on the BNL linac. A light pulse from a Q-switched Nd:YAG passes through the 750 keV H$^-$ beam from the linac rfq neutralizing most of the beam the light passes through. A downstream current transformer measures a dip in the beam current which is proportional to the fraction of the beam hit with the light, fig. 3. The laser beam is stepped across the ion beam and the profile is constructed by plotting the depth of the current notch vs. laser beam position.

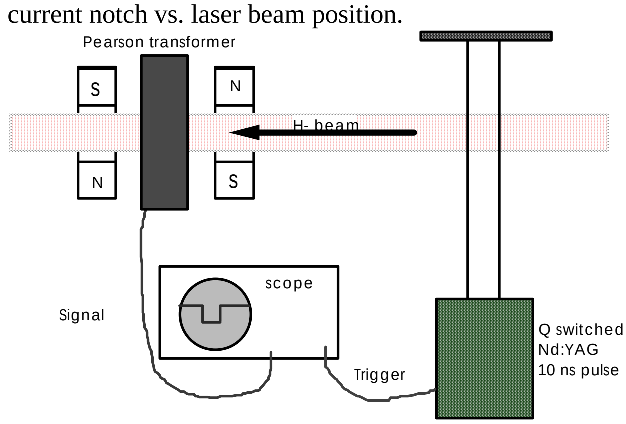


Figure 2: Laser scanner experiment on BNL linac. The first of two 10 Gm dipole magnets removes the free

# NEW SCHOTTKY- PICKUP FOR COSY - JÜLICH

I.Mohos, J. Bojowald, J. Dietrich and F.Klehr
Forschungszentrum Jülich GmbH, Germany

*Abstract*

A new Schottky-pickup for the Cooler Synchrotron COSY [1] at the Forschungszentrum Jülich was developed, tested and installed. The new pickup with four diagonally arranged plates replaces the two 1 m long Schottky–pickups used until now in COSY. The previous ones were removed mainly to gain space for new installations (e.g. rf-cavity, experimental devices), but also to increase the horizontal aperture. The available space for the new pickup is only 0.8 m. The pickup plates can be combined by means of relays to measure either in the horizontal or in the vertical plane. The pickup can also be used either as a sensitive broadband beam position monitor or as a tuneable narrowband pickup for Schottky-noise analysis with ultahigh sensitivity. A new method for resonant tuning of the Schottky-pickups for transversal measurements was developed. The differentially excited resonant circuitry enhances the sensitivity by about a factor of 30. The pickups are also used for dynamical tune measurements (tune meter) in the acceleration ramp [2].

## 1 INTRODUCTION

The Schottky-noise is preferably measured in the 10 to 60 MHz frequency range. This is due to the fact that the line widths in the Schottky-noise spectrum are proportional to the harmonic number with equal noise power per line. The narrow longitudinal lines are measured in the upper part of this frequency range, but the generally much broader transversal lines at lower frequencies because here the line structures do not yet overlap and, in particular at higher frequencies, the amplitudes can vanish in the noise level.

Because of the low power of the transversal signals an especially sensitive monitor is required whose sensitivity will be enhanced further by resonant tuning. Despite of the gain of 20 to 30 dB by resonant tuning, the sensitivity itself is very important and also its frequency dependence. Both sensitivity and frequency dependence are influenced by the layout and the mode of operation.

Three monitor types are at disposal: inductive, capacitive and stripline monitors. In the frequency range of 10 to 60 MHz the capacitive monitor is well suited, but the inductive monitor less so. This is due to the fact that the azimuthal magnetic field of the beam and hence the induced signal power is proportional to $ß^2$, and Schottky-noise measurements at COSY also must be performed at low ß-values. The stripline monitor can be operated at high frequencies and it is able to separate the signals of particles travelling opposite to each other (directivity), a very useful feature in storage rings. This cannot be used at COSY, however, the great disadvantage is the sinusoidal frequency dependence. The maximal sensitivity, obtained at frequencies with $\lambda/4$ corresponding to the monitor length, would be with 0.8m length at 94 MHz. In the 10 to 60 MHz range the sensitivity diminish drastically.

The amplitudes of the transversal Schottky signals are dependent on the square root of the ß-function. A suitable position in COSY with high ß-function values should therefore be chosen. In monitor design, attention must be payed to save the total aperture. For this reason the electrodes must be arranged far outside, at best with beam tube diameter.

## 2 MONITOR DESIGN AND TRANSFER IMPEDANCE

The capacitive monitor with high impedance preamplifier has the particular advantage of a flat frequency response within a pass band. The lower cut-off frequency is determined by the electrode capacity and the preamplifier input impedance, and can be realized to 10kHz. The upper cut-off frequency is determined by the bandwidth of the preamplifier and is larger than 100MHz, the proper frequency range.

The sensitivity or transfer impedance of one electrode with beam centred is given by

$$Z_{tr} = \frac{A_{el}}{2\pi r} \cdot \frac{1}{\beta c \cdot C_{el}} = \frac{\alpha_{el}}{2\pi} \cdot \frac{L}{\beta c \cdot C_{el}}$$

where: $A_{el}$ = electrode plane, r = beam tube radius, L = monitor length and $\alpha$ = azimuthal angle of electrode. The first term is a geometrical factor, corresponding to the ratio of electrode plane to total monitor cylinder plane. The transfer impedance is maximized if all electrodes together entirely enclose the beam, i.e. if $\Sigma\alpha_{el} = 2\pi$. For high sensitivity the electrode capacity $C_{el}$ must be small, i.e. the distance to the beam tube cannot be too small.

# CURRENT TRANSFORMERS FOR GSI'S KEV/U TO GEV/U ION BEAMS - AN OVERVIEW

H. Reeg, N. Schneider
Gesellschaft fuer Schwerionenforschung (GSI), Darmstadt, Germany

*Abstract*

At GSI's accelerator facilities ion beam intensities usually are observed and measured with various types of current transformers (CT), matched to the special requirements at their location in the machines.

In the universal linear accelerator (UNILAC), and the high charge state injector (HLI) as well, active transformers with 2nd-order feedback are used, while passive pulse CTs and two DC-CTs based on the magnetic modulator principle are implemented in the heavy ion synchrotron (SIS) and the experimental storage ring (ESR). In the high energy beam transfer lines (HEBT) the particle bunch extraction/reinjection is monitored with resonant charge-integrating types.

Since more than 10 years number and significance of beam current transformers for operating GSI's accelerators have grown constantly. Due to increased beam intensities following the last UNILAC upgrade, transmission monitoring and beam loss supervision with CTs have become the main tools for machine protection and radiation security purposes.

All CTs have been constructed and developed at GSI, since no commercial products or were available, when solutions were needed.

## 1 INTRODUCTION

In GSI's various accelerators a large range of ion species are handled, from protons to uranium, including a lot of isotopes and nearly all possible charge states. The peak beam currents in the SIS in the meantime have grown up to nearly 1 Ampere, reaching the space charge limit with $Ne^{+10}$, while still experiments with less than one μA are performed with low energy beams in the UNILAC. The time structures of the different beams spread from $10^{-9}$ to more than 10 seconds, and often have to be resolved and displayed.

CTs built from high permeability tape-wound ring cores have replaced most of the faraday cups in the UNILAC, because they do not destroy or even influence the beam, and do not suffer from beam power load. Their output exhibits no dependence to the beam's position or extent.

Their most important characteristic feature is their inherent and reliable calibration, if careful design and construction are applied.

## 2 LINAC TRANSFORMERS

### *2.1 Electronic and magnetic layout*

Up to 15 different machine settings with respect to ion energy or species can be treated in a periodically pulsed sequence. Typical macropulse duration of the ion sources and linacs between 50 μs and 8 ms demand rise times about 1 μs, and negligible pulse droop losses to guarantee accurate measurements. The RF cavities are operated at 36 and 108 MHz, with bunch widths of about 1 ns FWHM, respectively. As this would require more than 1 GHz bandwidth, beam energy (Time-Of-Flight), energy spread, longitudinal emittance and beam position measurements are performed with a system of capacitive pick-ups installed along the machines, so transformer bandwidth can be kept around 500 kHz. At present 38 CTs are installed in the linac sections and the low energy experimental areas.

Each CT's crossed-differential winding is connected to the front electronics, mounted as close as possible to the beam pipe. By those means excessive noise or hum pickup is reduced. A current-to-voltage converter with a second-order current feedback network [1], range selection and a switched clamp for baseline restoration are installed in the front box. The analogue output signals are then transmitted via differential and terminated twisted pair lines to their associated integrating digitizers [2]. These again are installed in a central control station outside the linac tunnel, keeping the cable lengths below 100 meters. Via special interfaces, a multiplexer and a PC equipped with an ADC plug-in, 2 of 64 CT pulse signals can be selected for display on the PC screen.

This feature enables the machine operators to observe any modulations on the macropulse, like plasma fluctuations in the ion source, or settling problems of the RF cavity amplitude controllers induced by beam loading.

A/D-conversion of the CT signals is performed by an U/F-converter with 8 MHz maximum frequency, feeding a 16-bit digital counter. In the lowest current range one count equals a charge amount of 0.6 pC. By gating the counter with a trigger interval congruent to the beam pulse, the pulse charge can be read as the counter end value. This is transferred to the control system together with the gate length value (measured simultaneously), and a simple calculation returns the

# TRANSVERSE BEAM PROFILE MEASUREMENTS USING OPTICAL METHODS

A. Peters, P. Forck, A. Weiss, A. Bank
Gesellschaft für Schwerionenforschung (GSI), Darmstadt, Germany
e-mail: A.Peters@gsi.de

*Abstract*

Two different systems are currently under development at GSI's heavy ion facility to measure transverse beam profiles using optical emitters.
At the GSI-LINAC for energies up to 15 MeV/u residual gas fluorescence is investigated for pulsed high current beams. The fluorescence of $N_2$ is monitored by an image intensified CCD camera.
For all ion species with energies above 50 MeV/u slowly extracted from the synchrotron SIS a classical viewing screen system is used. Three different target materials have been investigated and their behavior concerning efficiency, saturation and timing performance is evaluated.
Both systems (will) use CCD cameras with a digital readout using the IEEE 1394 standard.

## 1 RESIDUAL GAS FLUORESCENCE MONITORS

The traditional determination of transverse beam profiles by secondary emission grids can not be applied at the high current heavy ion LINAC at GSI [1] due to the high beam power. Alternatively a non-intersecting residual gas monitor can be used or the fluorescence of the residual gas can be detected. The latter has the advantage that no mechanical parts and therefore no extra apertures are installed in the vacuum pipe, leading to a compact and cost efficient design. The method of residual gas fluorescence was applied to a proton LINAC [2] and recently also at a synchrotron [3]. Here a first test at a pulsed heavy ion LINAC is done.

The residual gas at the LINAC has a typical pressure of $10^{-7}$ mbar containing mainly Nitrogen. We use an additional gas inlet to increase the pressure up to $10^{-4}$ mbar. The $N_2$ is excited by the accelerated ions and the fluorescence from neutral or ionized molecules at wavelengths between 350 and 470 nm is dominant [2, 4]. The excited states have lifetimes of 40 ns and 60 ns, short enough to prevent broadening due to the movement of $N_2^+$ in the space charge potential of the beam.

For the detection we used an intensified camera (Proxitronics NANOCAM HF4 [5]), yet with a video signal output which is digitized using a PC frame-grabber. The photo-cathode is made of S20/Quartz, having a quantum-efficiency of $10 - 15\%$ at the interesting wavelength interval and a low dark current. A two-fold MCP amplified the photo-electrons with a gain of $10^6$ and a P46 fast phosphor screen is used. The gating of the camera is done by switching the voltage between photo-cathode and the MCP within 5 ns.

A first test was performed with an 5.8 MeV/u $Ar^{11+}$ beam with an electrical current of 700 $\mu$A and a pulse length of 200 $\mu$s. This corresponds to $\sim 10^{11}$ particles per macro-pulse passing the 35 mm diameter view-port for the camera. An example is given in Fig. 1 for one macro-pulse recorded at a pressure of $10^{-5}$ mbar having a relatively large vertical width of 13.6 mm FWHM. The projection of the 2-dim. plot with the 'single photon counting' pixels onto the axis of interest shows sufficient statistics. This can by easily improved by binning, in particular for a large width. The measurement is background-free, even without using any optical filters.

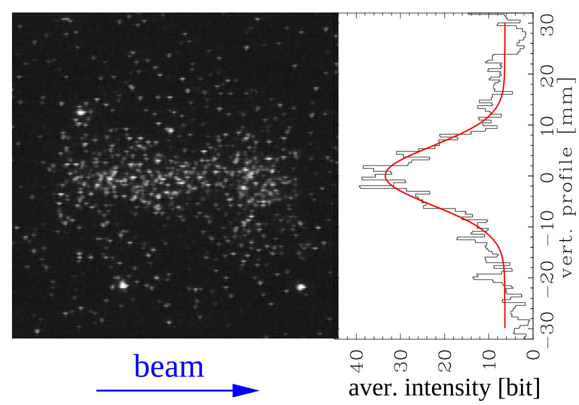


Figure 1: Fluorescence image and projection of a 5.8 MeV/u $Ar^{11+}$ beam

It is shown, that for beams behind the stripper, like tested here, the method can be applied with a moderate pressure bump. While for beams at the first section of the LINAC, before the stripper, the particle current is an order of magnitude higher as well as the energy deposition, therefore a pressure bump is not needed. Using the switching of the photo cathode voltage, movement of the beam within the macro-pulse can be detected easily.

## 2 IMPROVEMENT OF VIEWING SCREEN SYSTEM

Up to now the viewing screens used at GSI to observe the slowly extracted ion beams from the heavy ion synchroton are equipped with Chromox targets [6], which have a good sensitivity, a high radiation hardness and are UHV-compatible as well. But a major disadvantage is their long-

# CONTROL AND DATA ANALYSIS FOR EMITTANCE MEASURING DEVICES

T. Hoffmann, D.A. Liakin[1]
Gesellschaft für Schwerionenforschung (GSI), Planckstr. 1, 64291 Darmstadt, Germany
E-Mail: T.Hoffmann@gsi.de, Liakin@vitep5.itep.ru

*Abstract*

Due to the wide range of heavy ion beam intensities and energies in the GSI linac and the associated transfer channel to the synchrotron, several different types of emittance measurement systems have been established. Many common devices such as slit/grid or dipole-sweep systems are integrated into the GSI control system. Other systems like the single shot pepper pot method using CCD-cameras or stand-alone slit/grid set-ups are connected to personal computers. An overview is given about the various systems and their software integration. Main interest is directed on the software development for emittance front-end control and data analysis such as evaluation algorithms or graphical presentation of the results. In addition, special features for improved usability of the software such as data export, project databases and automatic report generation will be presented. An outlook on a unified evaluation procedure for all different types of emittance measurement is given.

## 1. INTRODUCTION

The GSI linear accelerator provides ion acceleration of all chemical elements from p up to U and allows various energies in a range from 120 keV/u to 15 MeV/u[1]. Therefore in ion source development, ion type changing activities, regular beam optimisation and for commissioning purposes emittance measurement is required. Since the foundation of the GSI facility in 1970 a lot of different types of emittance measurement devices have been installed. Slit/grid systems, dipole-sweep systems but also slit/sandwich systems, a special type of detector using 32 isolated layers with a thickness of 0.15 mm are operated with the GSI control system. However, different types of control software are used within the control system leading to manifold data outputs and evaluation processes. Newer emittance measurement systems like the pepper pot [2,3] or the stand-alone slit/grid device are operated with personal computers and are based on various types of Windows and DOS control and evaluation software. All types of the emittance soft- and hardware components are working properly but reorganisation to a unitary graphical user interface (GUI) and evaluation procedure is mandatory due to improved usability and comparability of the results.

## 2. STRUCTURE OF THE SOFTWARE

The new designed control and evaluation software, first used for pepper pot emittance measurement, is a bundle of subprograms, which are combined together using unified data structures and Windows Component Object Model (COM) technology. Due to this not only pepper pot emittance measurement devices but also other types could

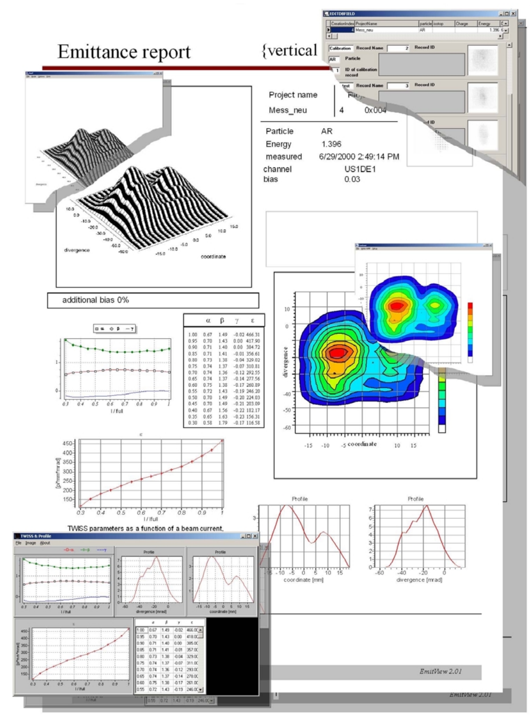


Fig.1. All 'independent' software parts are merged into the hardcopy report generation.

be connected without code recompilation. To provide flexibility in data computation few output data formats are realized. Independent data analysis algorithms may be used if they are available as special dynamic libraries.

The software consists of data acquisition, evaluation and visualization tools.

An extensive description of the software on the basis of the pepper pot method is given in [2]. The possibilities of the visualisation part of the software are shown in fig.1. The calculated emittance data is illustrated with various visualisation tools such as contour plot and three-

[1] ITEP-Moscow, work done at GSI.

# TEST OF DIFFERENT BEAM LOSS DETECTORS AT THE GSI HEAVY ION SYNCHROTRON

P. Forck and T. Hoffmann
Gesellschaft für Schwerionenforschung GSI, Darmstadt, Germany.
e-mail: p.forck@gsi.de

*Abstract*

For the sensitive process of slow extraction from a synchrotron a reliable control of the beam losses is needed. We have tested several types of particle detectors mounted at the extraction path of the SIS: A $BF_3$-tube for pure neutron detection, a liquid and a plastic scintillator detecting neutrons, gammas and charged particles and an Ar filled ionization chamber mainly sensitive to charged particles. While the count rate is quite different, the time evolution of all detector signals during the spill are similar, but the plastic scintillator has the highest dynamic range. This type is going to be used for beam alignment.

## 1 DEMAND FOR LOSS MONITORS

To control the beam losses during the beam alignment and operation of an accelerator it is an important issue to prevent permanent activation. At the GSI heavy ion synchrotron SIS all heavy ions can be accelerated from 11.4 MeV/u to a variable final energy up to $\sim$ 1.5 GeV/u. During the last years a large increase of beam current up to a factor of 100 in particular for heavy specious was possible due to the installation of an electron cooler and an upgrade of the LINAC [1]. Most of the experiments are using third order resonance extraction having an extraction time of several seconds. Most of the losses occur during this extraction, some of them are unavoidable, others should be minimized by careful setting of the accelerator parameters like tune changes, focusing, steering angles, in particular of the septa etc. The highest activation is measured around the electrostatic septum (mostly due to 'unavoidable' losses for slow extraction), the following dipole magnet inside the SIS and the magnetic septa due to their small acceptance (here the right orientation of the transverse emittance is needed). Compared to other large accelerators there are some differences concerning the loss: Firstly the currents in terms of particles per second are relatively low due to the long cycle time using slow extraction. Secondly different ions with a wide span of current and final energy are accelerated. Thirdly the detectors should be used for the alignment procedure and not for creating an emergency interlock (like used elsewhere for quench-protection of superconduction magnets).

The cross section of the production of secondary particles is not well known for heavy ions. The energy of the colliding nuclear system is comparable to the energy of it constituents leading to a more complex reaction mechanism, as used e.g. for high energy protons [2]. Moreover, the penetration depth is in the order of several cm, and the assumption of a 'thick target' can not be applied for particles hitting the vacuum chamber. Some investigations using heavy ions have been made to measure the cross section, scaling laws and angular distribution [3], but not all needed parameters (ion specious and energy) are covered. In addition the charged primary or secondary particles loose a noticeable amount of energy in the target due to electronic stopping. Therefore the main secondary particles reaching the detector are expected to be neutrons from fragmentation and spallation processes. The angular distribution is peaked in forward direction inside a cone having an opening angle of several degrees with a strong depending on the primary ion's energy [3]. Due to all these dependences, an absolute dose cannot be generated from the data.

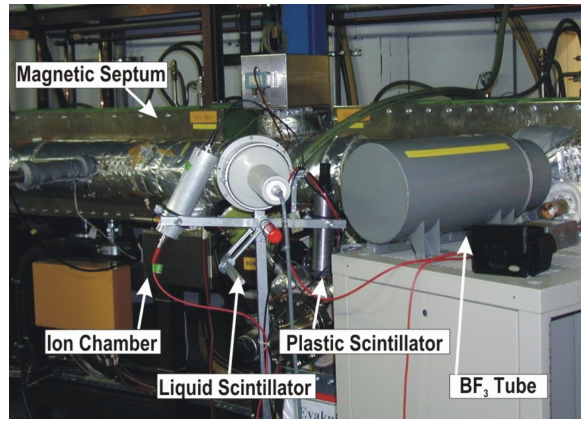


Figure 1: The detectors installed at the SIS-extraction.

## 2 TYPES OF DETECTORS

Different detectors have been tested at the SIS in a distance of $\sim$3 m and an angle of $\sim 20^o$ from the magnetic septa, see Fig. 1. One of them is only sensitive to neutrons, while the others have different sensitivity to other secondary particles, see below. For the purpose of beam alignment, a high dynamic range i.e. large count-rate capability and a background free operation is needed. General demands are an easy and hazard-free installation and a stable operation.

**Liquid scintillator:** An older device form Nuclear Enterprise containing NE 213 liquid scintillator (decay time 3.2 ns [4]) in a cylinder container of 1 l was installed. The light generation is based on collisions of the neutrons with hydrogen atoms of the polymers (elastic n+p-reaction), the

# SOURCE IMAGING WITH COMPOUND REFRACTIVE LENSES

O. Chubar, e-mail: chubar@esrf.fr
M. Drakopoulos, A. Snigirev, T. Weitkamp
ESRF, European Synchrotron Radiation Facility, Grenoble, France

**NO PAPER SUBMITTED**

## References

B. Lengeler, C. Schroer, J. Tümmer, B. Benner, M. Richwin, A. Snigirev, I. Snigireva & M. Drakopoulos, "Imaging by parabolic refractive lenses in the hard X-ray range", J. Synchrotron Rad., 1999, vol.6, p. 1153.

T. Weitkamp, M. Drakopoulos, A. Souvorov, I. Snigireva, A. Snigirev, F. Günzler, C. Schroer & B. Lengeler, "Direct imaging of high-energy synchrotron radiation sources using X-ray lenses", in Free Electron Lasers 1999, edited by J. Feldhaus and H. Weise, 2000 Elsevier Science B.V., p. II-117.

T. Weitkamp, O. Chubar, M. Drakopoulos, I. Snigireva, A. Snigirev, C. Schroer, F. Günzler & B. Lengeler, "Electron beam size and profile measurements with refractive X-ray lenses", Proc. of EPAC 2000, p. 1824.

T. Weitkamp, O. Chubar, M. Drakopoulos, A. Souvorov, I. Snigireva, A. Snigirev, F. Günzler, C. Schroer & B. Lengeler, "Refractive lenses as a beam diagnostic tool for high-energy synchrotron radiation", to appear in NIMA (Proc. of SRI 2000).

# A ZONE PLATE BASED BEAM MONITOR FOR THE SWISS LIGHT SOURCE

C. David, Laboratory for Micro- and Nanotechnology, Paul Scherrer Institute, CH-5232 Villigen

V. Schlott, A. Jaggi, Swiss Light Source, Paul Scherrer Institute, CH-5232 Villigen, Switzerland

*Abstract*

At the Swiss Light Source, a source imaging set-up is planned on a dedicated dipole magnet beam-line. A transmission Fresnel Zone Plate will be used to generate a demagnified image of the source at a photon energy in the 1.8 keV range. The image will be acquired by scanning a pinhole in the image plane. A diffraction limited spatial resolution of approximately 2 microns can be anticipated. The concept has the advantage of having no components operated in reflection, and no components inside the front-end.

## 1 PRINCIPLE OF OPERATION

Source imaging can provide valuable information about the size, shape, position, and stability of 3rd generation synchrotron radiation sources, and allows for an optimisation of the brilliance by minimizing the coupling parameter [1-3]. At SLS, a bending magnet beamline (12-B) is reserved for diagnostics purposes. At this location electron beam size, emittance and coupling measurements are planned. Apart from that, bunch purity and bunch length measurements have to be performed at the same beamline using visible synchrotron radiation. For beam size measurements we are expecting 1-sigma horizontal beam size of 45 µm and 1-sigma vertical beam size of 40 µm for 1% emittance coupling. The horizontal emittance is expected to be 4.8 nmrad at 2.4 GeV beam energy. However, the storage ring design allows much smaller coupling values for different lattice modes. Emittance coupling of 0.1% would already lead to vertical 1-sigma beam size of 13 µm. Thus, a resolution in the micron range is necessary.

Apart from the required resolution, some practical constraints have to be taken into account. Firstly, it is desirable to have no reflective components in the imaging system that could introduce aberrations and thus affect the source size measurements. Secondly, it is advantageous to have no components inside the beamline's front end. This allows for easier access and alignment and it is possible to remove the set-up from the beam without complications to use the beamline for other experiments. In our case this means, that the first component of the monitor has a distance from the source of at least $g$=10 m. Generating a magnified image of the source would thus require a very long, potentially unstable set-up. To keep the set-up short, we chose a demagnifying geometry.

The separation of two distant point sources that can be distinguished according to the Rayleigh-criterion is generally limited by the diffraction of the optics aperture [4]. This means that the distance between the images of two distinguishable source points is limited to: $B= 0.61\cdot\lambda\cdot f/r \approx 0.61\cdot\lambda\cdot b/r$, where $\lambda$ is the light wavelength, $f$ the focal length, and $b$ the image distance. This corresponds to a source size that could be resolved of $G = B \cdot g/b = 0.61 \cdot\lambda\cdot g/r$. If we introduce the solid angle $\alpha$ = 2r/g collected by the optics, we see that

$$G=1.22\cdot\lambda/\alpha. \tag{1.0}$$

The angular divergence of the bending-magnet beam line 12-B is in the order of 0.5 mrad, which limits the useful optics diameter to 5 mm at 10 m source distance. According to eq. (1.0) this results in a resolution of 1.7 µm at 1.8 keV photon energy (0.7 nm wavelength). However, it should be noted that the resolution criterion applied in this calculation is very conservative. The size of a source which is larger than the diffraction limit of the set-up can be determined with much better accuracy by deconvolution with the point spread function of the optical system. This is especially true if the function describing the source profile is known and e.g. only the position and width of a gaussian have to be determined.

Fresnel zone plates have been successfully applied for focusing and high resolution imaging in the x-ray range. As a good approximation the radius $r_n$ of the $n^{th}$ ring follows the law

$$r_n = \sqrt{n\cdot\lambda\cdot f} \tag{1.1}$$

where f is the first order focal length. The outermost (smallest) zone width $dr_n$ the total zone number n and the total radius r are linked by the following equations:

$$dr_n = r / 2n \tag{1.2}$$

$$f = 2r\cdot dr_n / \lambda \tag{1.3}$$

$$f = r^2 / (n\cdot\lambda) \tag{1.4}$$

The following properties of zone plates are of importance in the context of the presented set-up:

# MICROWAVE PICKUPS FOR THE OBSERVATION OF MULTI GHZ SIGNALS INDUCED BY THE ESRF STORAGE RING ELECTRON BUNCHES

E. Plouviez, ESRF, Grenoble, France

*Abstract*

The length of the bunches stored in ESRF lies in the 30 ps to 120 ps range (FWHM). The observation of single bunch phenomena like transverse or longitudinal oscillations or bunch length variation requires the acquisition and analysis of signals at frequencies higher than 10 GHz. A set of microwave cavity pick ups operating at 10 GHz and 16 GHz together with the appropriate electronics has been implemented on the ESRF storage ring; it detects the wall currents on the vacuum chamber due to the electron beams circulation. We describe the design of these cavities, give the result and analysis of measurements performed with the pick ups and indicate how we plan to use these devices as beam diagnostics

## 1 SINGLE BUNCH SIGNALS

Some examples of single bunch oscillation simulations are shown in the figure 1 (longitudinal oscillation) and 2 (transverse oscillation).

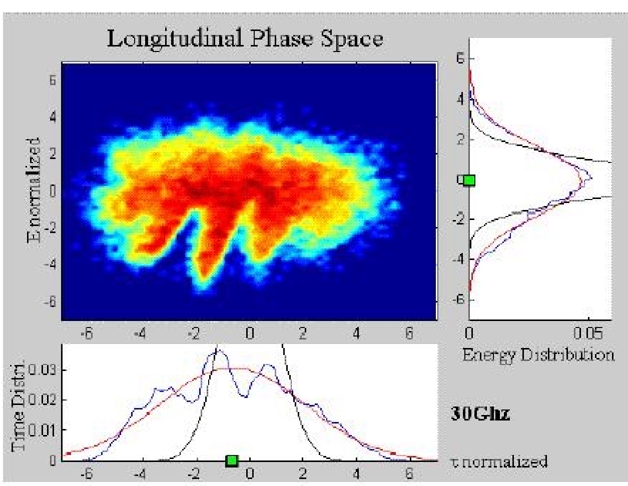


Figure 1: simulation of a microwave longitudinal instability caused by a 30 GHz broadband impedance [1]

For bunch lengths in the 30 ps to 120 ps range, the spectrum of the image currents of the bunch on the vacuum chamber will extend up to tens of gigahertz. However, especially in single bunch filling, the pattern of this spectrum is very repetitive: the parameters of interest are usually the frequency offset of the side bands of the harmonics of the revolution frequency ; So the analyze of an oscillation will only require the study of a narrow span of the total spectrum, in a part of the spectrum where the line amplitudes will be sufficient to be properly detected. An advantage of detecting the beam signal in a narrow span of its total spectrum is also to reduce the large peak/average level of a single bunch signal, avoiding the saturation of the detection electronics. In order to acquire this narrow bandwidth signals, we have developed and implemented dedicated pick ups on the ESRF storage ring

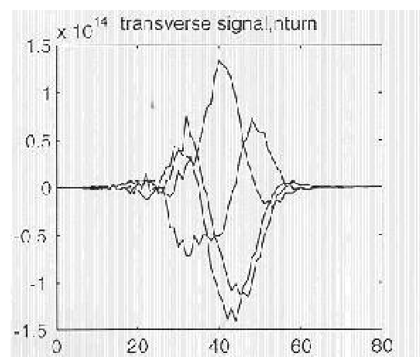


Figure 2: time domain simulation of a short rise time single bunch vertical instability [2] (horizontal scale:1ps/div)

## 2 PICK UP DESIGN

### 2.1 General Layout

The pick up principle and mechanical design is shown in the figure 3. The pick up is a 7mm diameter-2mm thick vacuum tight cylindrical iris filled with ceramic. The iris couples the beam image current to the TM010 mode of a pill box cavity. The frequency of this mode is the Nth harmonic of $f_{rev}$=352.2 MHz, revolution frequency of the beam. The iris diameter and thickness sets the coupling of the cavity to the image current. Two sets have been designed with TM010 mode frequency equal to 29 X $f_{RF}$ = 10.213 GHz and 45 and 45 X $f_{RF}$ = 16.2 GHz. The choice of these frequencies is consistent with the spectrum expected of signals induced by bunches with lengths ranging from 30 ps to 120 ps. The design was optimised using the Agilent HFSS high frequency electromagnetic simulator. By using cavities with different resonating

# A NEW WIRESCANNER CONTROL UNIT

M. Werner, K. Wittenburg, DESY, Hamburg, Germany

*Abstract*

Wires scanners are standard instruments for beam size measurements in storage rings: A wire is crossing the beam at a given speed and the secondary emission current of the wire and/or the photomultiplier signals produced from Bremsstrahlung or particles scattered at the wire are recorded together with the wire positions. The control unit described here is based on a previous CERN design [1]. It now has additional features:

- Triggered fast scans (1m/s) with a trigger uncertainty below ± 30µs (mechanics + electronics) used at the TTF Linac and at the proton synchrotron DESY III,
- Slow scans (e.g. 50µm/s) for the TTF Linac,
- Positioning of the wire within ± 3µm for tail scans at the storage rings PETRA and HERA,
- A 10.5MHz data acquisition rate for bunch-by-bunch acquisitions in the accelerators at DESY.

Another important design goal was the compatibility with CERN scanners; it is foreseen to operate them at LHC with the new control unit. First measurements with the new control unit at TTF and HERA will be presented.

## 1 OVERVIEW

The system is based on a special 19" 6HE VME crate controlled by a Motorola CPU running VxWorks. One crate controls 4 Wirescanners, one at a time. The concept is based on an earlier wire scanner control unit designed by J. Koopman, CERN and redesigned for new demands.

## 2 NEW FEATURES

### *2.1 Fast Scan with delayed Trigger*

A scan can be triggered in synchrotrons (to get a profile for a certain energy) or linacs (to cross the beam exactly while it is present) during a "Fast scan". A trigger delay up to 4 sec can be selected and the real time between trigger and reaching the desired acquisition start position is measured internally. So all time relations between trigger and acquisition data are defined. For storage rings the scan trigger can be disabled. The average trigger uncertainty is below ± 30µs (mechanics + electronics).

### *2.2 Slow Scan and Tail scans*

Slow scans are useful for linacs: a data array (all bunches, all photo multiplier signals) is recorded for each linac pulse while the wire is moving slowly (e.g. 20..100µ/sec) across the beam. For tail scans in circular accelerators the wire can be moved to a given position within ± 3µm. In this mode (useful for the range 3..6σ around the beam) the "statistical" low rate photo multiplier pulses are counted during several seconds per position point.

### *2.3 Data acquisition*

The 8-channel data acquisition for the photo multiplier signals or secondary emission signals from the wire now work up to 10.5 Msample/sec with 14 bits with a maximum of 128k datasets, using a low cost VME ADC card from DESY/Zeuthen.

### *2.4 Other improvements*

The position resolution was improved to 1µm. The positions of all wires are remote accessible at any time. Hardware trimming is no longer necessary. The wire motion is now controlled by a programmable function generator, allowing any movement, only limited by the maximum acceleration. The four-channel system fits into a single crate now.

## 3 HARDWARE CONFIGURATION

### *3.1 General*

The main system components are:

- The Motorola VME CPU with 4 IP Module sockets, one is occupied by an IP module (TIP570, 8-channel ADC + 8-channel DAC) to control voltage and current of up to 4 high voltage supplies for the photo multipliers
- The photo multiplier signal integration card
- The VME 8-channel 14 bit ADC card (designed by F. Tonisch, DESY/Zeuthen)
- The VME "motion control card" (in-house)
- The "motor driver" module and the ±48V/12A power supply (in-house)

### *3.2 Motion control card*

The motion control card contains:

- A quadrature decoder to read out the 4 optical position encoders including error recognition, connected to a memory for fast position recording
- A delay unit for delayed fast scans
- A time / frequency measurement unit for remote tests of the external clock signals and to check the time between scan trigger and reaching of a given position
- A programmable function generator to generate any motion function

# BEAM SIZE MEASUREMENT OF THE SPRING-8 STORAGE RING BY TWO-DIMENSIONAL INTERFEROMETER

M. Masaki and S. Takano
Japan Synchrotron Radiation Research Institute, SPring-8, Hyogo 679-5198, Japan

*Abstract*

Two-dimensional interferometer using visible synchrotron radiation was developed in order to measure beam sizes at a source point in a bending magnet of the SPring-8 storage ring. The theoretical background of this method is described in the framework of wave-optics. Assuming designed optics parameters, transverse emittance was evaluated from measured beam size.

## 1 INTRODUCTION

Electron beam imaging using visible synchrotron radiation (SR) is a conventional method of beam size measurement. In the case of SPring-8 storage ring, the resolution of vertical beam imaging is limited by diffraction effect [1] due to collimation of SR in a narrow vertical divergence angle. Interferometric technique has superior resolution than beam imaging. A visible SR interferometer with a double slit was first applied to KEK-PF and a small vertical beam size was successfully measured [2]. The similar technique was applied to the SPring-8 storage ring in order to measure the vertical beam size [3]. As an improvement of the interferometer, we newly developed a two-dimensional interferometer with a quad slit having four apertures, which has an advantage that horizontal and vertical beam sizes can be simultaneously measured by observing visibility of a two-dimensional interference pattern.

## 2 TWO-DIMENSIONAL SR INTERFEROMETER

### 2.1 Principle

When a monochromatic light is diffracted by a quad slit with four apertures located rectangularly, a two-dimensional interference pattern appears on an observation screen. The interference pattern of a spherical wave from a point source can be calculated by Rayleigh-Sommerfeld diffraction formula using a paraxial approximation. If the source is a group of incoherent point sources distributed in Gaussian shape with width $\sigma_x$ and $\sigma_y$ (1$\sigma$), the interference pattern is expressed as,

$$I(x_s, y_s) = I_0 \left[ \frac{\sin\left(\frac{\pi x_s a}{2\lambda L}\right)}{\frac{\pi x_s a}{2\lambda L}} \right]^2 \left[ \frac{\sin\left(\frac{\pi y_s b}{2\lambda L}\right)}{\frac{\pi y_s b}{2\lambda L}} \right]^2 \left[ 1 + V_x \cos\left(\frac{4\pi x_a x_s}{\lambda L}\right)\right]\left[ 1 + V_y \cos\left(\frac{4\pi y_a y_s}{\lambda L}\right)\right] \quad (1)$$

where $L$, $a$, $b$ and $\lambda$ are distance from the source to quad-slit, horizontal and vertical slit aperture sizes and wavelength of light, respectively. Parameters $V_x$ and $V_y$ are called as visibility. We have approximated that a are Gaussian convolution integral of envelope expressed by a sinc function can be neglected when the envelope width becomes far larger than the light source size by the use of a quad-slit with small aperture sizes. The relationships between the source size, namely electron beam size, and the visibility expressed by,

$$\sigma_x = \frac{\lambda}{2\pi\theta_x}\sqrt{-2\ln\left(V_x\right)}, \quad \sigma_y = \frac{\lambda}{2\pi\theta_y}\sqrt{-2\ln\left(V_y\right)} \quad . \quad (2)$$

### 2.2 Effect of aspherical features of SR wavefront

The wavefront of SR from an orbiting electron is not spherical in a strict sense. The relative phase relation of SR at each aperture of the quad-slit depends on the electron orbit angle, and an interference fringe shifts with respect to the overall envelope depending on the orbit angle. Therefore, a visibility generally depends not only on electron beam size but also on beam angular divergence. Deviation of SR phase from that of spherical wave on the transverse plane of the quad-slit of the SPring-8 interferometer is shown in Fig.1, which was calculated by Fourier transforming a radiation field derived from Lienard-Wiechart potentials of an electron orbiting in a bending magnet [1]. Wavelength $\lambda$ is 441.6nm. The aspherical feature of SR is apparent in the horizontal direction, however the deviation of SR phase

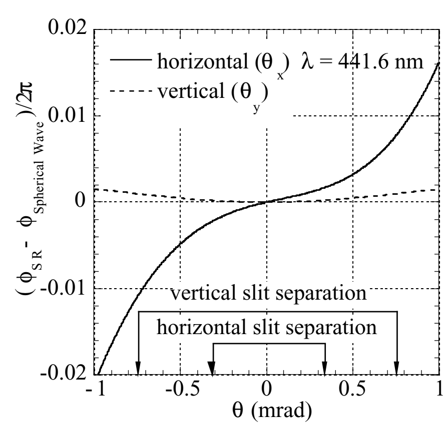


Figure 1:Difference of phase distributions between an ideal spherical wave and realistic radiation field derived from Lienard-Wiechart potentials of an electron orbiting in a bending magnet. Wavelength is 441.6nm.

# PLANNED X-RAY IMAGING OF THE ELECTRON BEAM AT THE SPRING-8 DIAGNOSTICS BEAMLINE BL38B2

M. Masaki, H. Ohkuma, S. Sasaki, M. Shoji, S. Takano*, and K. Tamura
Japan Synchrotron Radiation Research Institute, SPring-8, Hyogo 679-5198, Japan

*Abstract*

X-ray imaging observation of the electron beam is planned at the SPring-8 storage ring diagnostics beamline BL38B2 to evaluate small vertical emittance. The resolution target is 1 micron of electron beam size (1σ). The synchrotron radiation from a dipole magnet source will be imaged by a single phase zone plate. Monochromatic X-ray with energy of 8keV will be selected by a double crystal monochromator. The magnification factor of the zoneplate is 0.27, and an X-ray zooming tube will be used as a detector to compensate for demagnification.

## 1 INTRODUCTION

Measurement of small vertical size of electron beam is among the most challenging subjects of accelerator beam diagnostics of low emittance synchrotron radiation sources. At the SPring-8 storage ring, the high energy of electrons, 8 GeV, collimates synchrotron radiation in a narrow vertical divergence angle, and diffraction effect severely limits the resolution of conventional electron beam imaging with visible light[1].

The resolution is significantly improved by utilizing synchrotron radiation in shorter wavelength regions. X-ray imaging observation of the electron beam is planned at the SPring-8 storage ring diagnostics beamline BL38B2 to evaluate small vertical emittance.

## 2 DIAGNOSTICS BEAMLINE BL38B2

The beamline BL38B2 is dedicated for accelerator beam diagnostics and R&D of accelerator components. It has a bending magnet light source, and wide band spectral availability including visible/UV light, and soft and hard X-rays is anticipated. The beamline consists of a front end in the accelerator tunnel, an optics hutch in the experiment hall, a visible light transport line transporting visible/UV light from the optics hutch to a dark room, and an X-ray transport line in the optics hutch. The visible light transport line was completed in 2000, and longitudinal diagnostics of the electron beam such as bunch length and single bunch impurity are available.

Installation of the X-ray transport line is now under way. It has a double crystal monochromator, which can be moved off the beam axis when use is made of white, including both soft and hard, X-rays. Electron beam imaging with monochromatic X-ray is planned to evaluate small vertical emittance of the SPring-8 storage ring. The X-ray transport line as well as the front end has no windows, which potentially could distort wavefront and degrade imaging resolution, or obstructs soft X-ray and visible/UV light.

## 3 BEAM IMAGING WITH X-RAY

### *3.1 Why Phase Zone Plate ?*

The resolution target of the beam size measurement is 1 micron (1σ). Assuming the vertical betatron function $\beta_y$ of 30m at the source point, it corresponds to the resolution of vertical emittance $\varepsilon_y$ of 33 fm•rad.

In the initial stage of the design study of the diagnostics beamline BL38B2, an X-ray pinhole camera was proposed. The positions of the pinhole and the camera were 17.2m (front end) and 34.4 m (X-ray transport line), respectively, from the source point. In order to optimize the observing photon energy and the size of the pinhole, we calculated an image of a single electron numerically and concluded that the diffraction limited resolution of the X-ray pinhole camera is no smaller than 10 µm (Fig. 1).

The alternative is to use an imaging optical element. If the electron beam is imaged by utilizing full vertical divergence of synchrotron radiation, it is necessary to

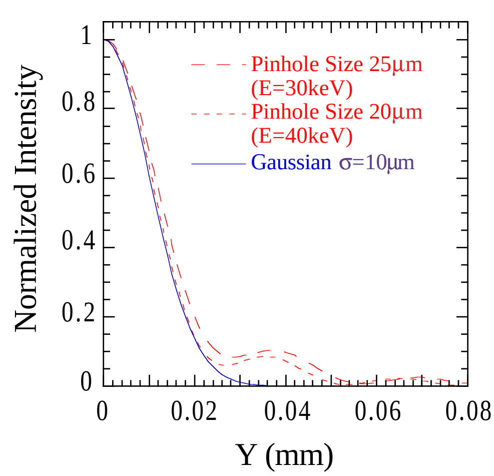


Figure 1: Computed intensity distributions of a single electron imaged by X-ray pinhole camera. The magnification factor is one.

* Email:takano@spring8.or.jp

# STATUS OF THE DELTA SYNCHROTRON LIGHT-MONITORING-SYSTEM

U. Berges, K. Wille, DELTA, Institute for Accelerator Physics and Synchrotron Radiation,
University of Dortmund, 44221 Dortmund, Germany

*Abstract*

Synchrotron radiation sources like DELTA need an optical monitoring system to measure the beam size at different points of the ring with high resolution and accuracy. An investigation of the emittance of the storage ring can also be done by these measurements.

Scope of this paper is the investigation of the resolution limit of the different types of optical synchrotron light monitors [1] at DELTA, a third generation synchrotron radiation source. At first the normal synchrotron light monitor is analysed. The minimum measurable electron beamsize at DELTA is about 80 µm. Emphasis is then put on a special synchrotron light interferometer, developed for DELTA, which has been built up and tested. This interferometer uses the same beamline and can measure beamsizes down to about 8 µm. So its resolution is about ten times better and sufficient for the expected small vertical beamsizes at DELTA. Measurements of the electron beamsize and emittance were done with both (synchrotron light monitor and interferometer) at different energies.

The image processing system based on a PC Framegrabber generates a gaussian fit to the images from different synchrotron light-monitors and calculates the beamsizes and positions.

An investigation of possible reasons of beam movements will be appended, because the theoretical values of the present optics are smaller than the measured emittance.

## 1 INTRODUCTION

The **D**ortmund **El**ectron **T**est **A**ccelerator facility DELTA consists of a 35 – 100 MeV LINAC, the 35 – 1500 MeV ramped storage ring called **Bo**oster **Do**rtmund (BoDo) and the electron storage ring called Delta (300 – 1500 MeV) [2].

Both transverse beamsizes of the electron storage ring Delta are measured by optical monitoring using synchrotron radiation from bending magnets and commercial CCD-cameras. We installed two optical synchrotron radiation monitors at different points of the ring (see Figure 1). One monitor is completely inside the radiation shielding. The other one allows use of synchrotron radiation outside the shielding, but not during injection time. We are able to measure the horizontal beamsize down to about 80 µm with a normal optical synchrotron light monitor. Because of the not optimal orbit due to not optimal alignment of the magnets at the moment the measured beamsize and emittance is larger than the theoretical values. Another reason are high frequent beam oscillations. Therefore the better resolution of a synchrotron light interferometer, which has been built up and tested, is not necessary at the moment, but will be used in near future.

## 2 OPTICAL SYNCHROTRON LIGHT MONITORING SYSTEM

The design of the optical synchrotron light monitors inside and outside the shielding at Delta have been described in DIPAC 1999 [3]. These monitors work reliable in a routine way. The video signal of the CCD-cameras can permanently be displayed on TV screens in the control room. The image processing system has been changed to a PC frame grabber DT 3155 and a new graphical surface, adapted from DESY software [4]. This allows a faster analysis of the beamsize by a gaussian fit to a chosen part of the image and determination of the position of the beam center than our old system [5]. The software enables subtraction of a background image.

Necessary corrections of the calculated beamsize are done by this software due to diffraction, curvature, depth of field and resolution of the CCD-chip. The experimental setups of the monitors are equipped with apertures to minimize the necessary corrections of the measured beamsize. This limits the achievable resolution to about 80 µm @ 500 nm with even an optimised horizontal or vertical opening angle.

The correction due to diffraction has been measured in an experimental setup (see Figure 2). A Siemensstar is illuminated by monochromatic light (LED with 660 nm) and used as a source instead of the electron beam. The image is digitized and analysed to determine the resolution. The experiment gives $\sigma = (34 \pm 2)$ µm as minimal measurable beam size due to diffraction only in this setup. The result is in good agreement with the theoretical value ($\sigma = 0.61 * \lambda / \Theta = 33.55$ µm).

The influence of the opening angle of the synchrotron radiation concerning the measured beam size has been investigated at DELTA synchrotron light monitors by variation of the horizontal and vertical aperture. After subtraction of the necessary corrections due to different opening angles, the real beam size was in good agreement at the different opening angles (see Figure 3).

# BEAM DIAGNOSTIC FOR THE NEXT LINEAR COLLIDER

Stephen R. Smith, Stanford Linear Accelerator Center, Stanford, CA 94309, USA

*Abstract*

The Next Linear Collider (NLC) is proposed to study e+ e- collisions in the TeV energy region. The small beam spot size at the interaction point of the NLC makes its luminosity sensitive to beam jitter. A mechanism for aligning the beams to each other which acts during the bunch-train crossing time has been proposed to maintain luminosity in the presence of pulse-pulse beam jitter[1]. We describe a beam-beam deflection feedback system which responds quickly enough to correct beam misalignments within the 265 ns long crossing time. The components of this system allow for a novel beam diagnostic, beam-beam deflection scans acquired in a single machine pulse.

## 1. INTRODUCTION

The beam-beam deflection feedback consists of a fast position monitor, kicker, and feedback regulator which properly compensates for the round-trip time-of-flight to the interaction point (Figure 1). A system consisting of conventional components may be effective at reducing the loss of NLC luminosity in the presence of vertical beam jitter many times larger than the vertical beam size.

Table 1: Beam Parameters at the IP

| Parameter | Value | Comments |
|---|---|---|
| CM Energy | 490 GeV | Stage 1 |
| Bunch Charge | $0.75 \times 10^{10}$ | $e^{+/-}$ / bunch |
| Bunches / train | 95 / 190 | |
| Bunch Spacing | 2.8 / 1.4 ns | |
| Repetition rate | 120 Hz | |
| $\sigma_y$ / $\sigma_x$ | 2.7 nm / 245 nm | At IP |
| $\sigma_z$ | 110 µm | |
| $D_y$ | 14 | Disruption |
| Deflection slope | $20 \times 10^{-6}$ /nm | Head-on |

## 2. POSITION MONITOR

### *2.1. Transducer*

We propose a stripline-type position monitor pickup, located about 4 meters from the IP. The strips are 50 Ohm lines and are assumed to be 10 cm long, peaking the response at the 714 MHz bunch spacing frequency. A 20 mm diameter BPM diameter is modelled here. Care must be taken to minimize radiation hitting the BPM, and to keep RF from propagating into the BPM duct.

Table 2: Beam Position Monitor Parameters

| Parameter | Value | Comments |
|---|---|---|
| Distance to IP | 4 m | |
| Duct diameter | 2 cm | |
| Stripline length | 10 cm | |
| Impedance | 50 Ohms | |
| Frequency | 714 MHz | Center |
| Bandwidth | 360 MHz | |
| Input filter | 4-pole bandpass | Bessel |
| Bandwidth | 200 MHz | Base band |
| Base band filter | 3-pole low pass | Bessel |
| Rise time | 3 ns | 0-60% |

### *2.2. Processor*

The position processor produces an analog output proportional to beam position. This signal must be fast to be useful in intra-pulse feedback. We propose to demodulate a 360 MHz band width around the 714 MHz BPM center frequency. The processor consists of an RF hybrid, band pass filter, and mixer driven by 714 MHz from the timing system, followed by a low pass filter. See Figure 2. This produces an amplitude proportional to the product of beam position and beam current.

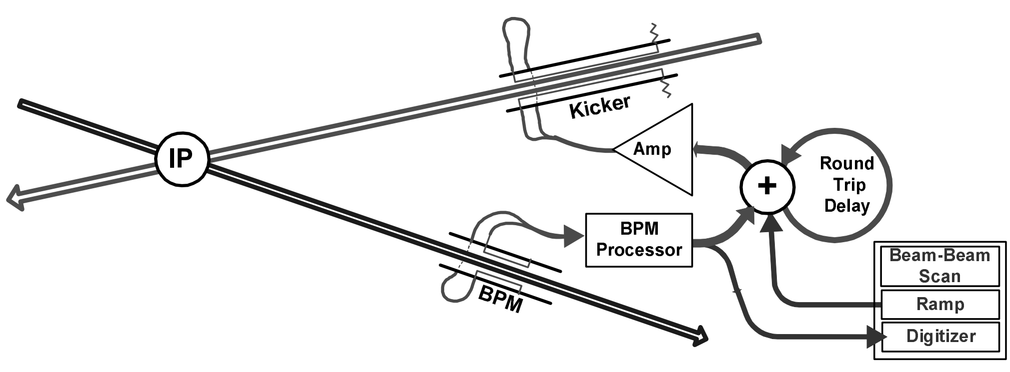


Figure 1: Intrapulse Feedback Block Diagram

# DIAGNOSTICS FOR THE PHOTOINJECTOR TEST FACILITY IN DESY ZEUTHEN

J. Bähr*, I. Bohnet, D. Lipka, H. Lüdecke, F. Stephan, Q. Zhao, DESY, Zeuthen, Germany
K. Flöttmann, DESY, Hamburg, Germany
I. Tsakov, Inst. for Nucl. Res. and Nucl. Energy of the Bulgarian Acad. of Sci. (NRNE), Sofia

*Abstract*

A **P**hoto **I**njector **T**est facility (PITZ) is under construction at DESY-**Z**euthen. The aim is to develop and operate an optimized photo injector for future free electron lasers and linear accelerators. This concerns especially minimal transverse emittances and proper longitudinal phase space. The commissioning of the photo injector will take place in summer 2001. In the first phase the energy of the produced electrons is about 5 MeV. A short description of the setup and beam parameters are given. Optimization of an electron gun is only possible based on an extended diagnostics system. The diagnostics system for the analysis of the transversal and longitudinal phase space will be described. It consists of a measurement system of the transversal emittance, a TV-based image measurement system, a streak-camera measurement facility, a spectrometer using a dipole magnet and further detectors. Problems of the measurement of the longitudinal phase space are discussed in detail.

## 1 INTRODUCTION

A Photo Injector Test Facility (PITZ) is under construction in DESY Zeuthen and will be commissioned in summer of 2001. The project was originated by a collaboration of the following institutions: BESSY (Berlin), DESY (Hamburg and Zeuthen), Max-Born Institut Berlin, Technical University (Darmstadt) and is funded partially by the HGF-Vernetzungsfonds.

The goal of PITZ is to operate a test facility for laser driven RF guns and to optimize photo injectors for the operation of Free Electron Lasers (FEL) and the TESLA linear collider. Comparisons of detailed experimental results with simulations are foressen. The setup will be used for conditioning of optimized cavity resonators for subsequent operation at the TESLA Test Facility - FEL. New developed components (for example lasers, cathodes) will be tested under realistic conditions. Later questions related to the production of flat beams for linear colliders and the development of polarized electron sources will be addressed.

At present, the mounting and commissioning of different subsystems (laser, interlock systems, control system, diagnostics systems) is going on. The vacuum system including cathode section, cavity section and diagnostics section is under vacuum. The commissioning of the RF system and conditioning of the cavity are the next steps. First photoelectrons will be produced in autumn 2001 followed by the commissioning of the full setup. An upgrade with a booster cavity is foreseen in the next years.

## 2 DESCRIPTION OF PITZ

The schematic layout of the PITZ facility is seen in Fig. 1. It consists of the following main components:

- the photo cathode based on $Cs_2Te$ [1])
- the copper cavity with a 1.5 cell geometry
- the laser system with output wavelength 263 nm
- the 1.3 Ghz RF-system with a klystron of 5 MW (later 10 MW)
- the control system based on DOOCS (Distributed Object-Oriented Control System)
- the diagnostics section

One of the main complex parameters and development goal is the time structure of the laser beam shown in Fig. 2.

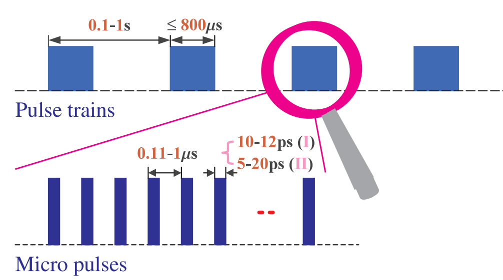


Figure 2: Schematic of the time structure of the laser beam. I) Phase I: GAUSSian-shape $\sigma \sim 6$ ps, II) Phase II: Rectangular shape with rise and fail time $< 1$ ps.

## 3 DIAGNOSTICS AT PITZ

### 3.1 Diagnostics of Laser Beam

- Time resolved bunch analysis of the laser beam by means of streak cameras.

  Two types of streak cameras (both from Hamamatsu)): FESCA-200 (time resolution $> 200$ fs), which is running only in single shot mode and C5680, running in single shot mode and synchroscan (time resolution $> 2$ ps) are available to analyse the time structure of

* baehr@ifh.de

[1] INFN Milano

# POSITION MONITORING OF ACCELERATOR COMPONENTS AS MAGNETS AND BEAM POSITION MONITORS

G. Schmidt, E. Kasel, D. Schirmer, D. Zimoch, K. Wille

DELTA, University of Dortmund, Germany

*Abstract*

In third generation light sources a large amount of heat load from synchrotron radiation must be dissipated from the vacuum chamber. The synchrotron radiation hits the outer chamber wall and leads to a bending of the vacuum chamber.

Due to the fact that very often beam position monitors are included into the vacuum chamber, they start to move with increased heat load onto the vacuum chamber.

An inexpensive and precise method to monitor this movement has been tested at the Dortmunder Electron Test Accelerator (DELTA). Commercially available Linear Variable Differential Transformers (LVDTs) have been used.

In addition it was possible to demonstrate that due to the vacuum chamber contact to quadrupole magnets the quadrupoles were moving with increasing beam current leading to a significant orbit drift.

## 1 DELTA STORAGE RING

The DELTA Storage Ring is a 1.5 GeV 3$^{rd}$ generation storage ring for synchrotron radiation production [1].

The stability and reproducibility of the storage ring, especially the beam orbit, is crucial for the operation as synchrotron light source. The stability of the measured beam orbit itself depends on the position of the beam position monitors and the focusing magnets. Therefore the position of quadrupole magnets and beam position monitors was measured.

## 2 POSITION SENSORS

To allow the monitoring of the large amount of components with sufficient resolution an inexpensive commercially available solution was searched, which allows the direct position measurement of the components. As a good compromise between cost, sensitivity and ease of use, Linear Variable Differential Transformers (LVDTs) were chosen. For the time being 5 sensors from Schlumberger [2] and TWK [3] have been used to make first tests. The next step will be the installation of 25 sensors to monitor quadrupoles and BPMs in one fourth of the DELTA storage ring. This will allow to study, survey and improve the mechanical stability of the components. After an efficient reduction of the movement of components the sensors will be mounted permanently on important BPMs to allow the correction of the BPM reading by the measured BPM position movement.

## 3 LINEAR VARIABLE DIFFERENTIAL TRANSFORMERS (LVDTS)

The position sensor works as an inductive half bridge. A position change of a Mu-Metall cylinder inside two solenoids induces an inductance change inside the two solenoids, which is transferred into a position proportional electrical signal (see Fig. 1). A standard measurement range of 5 mm was used. The sensor has a linearity of 0.25 % (10 μm).

The output signal is connected to the DELTA control system via standard ADC boards.

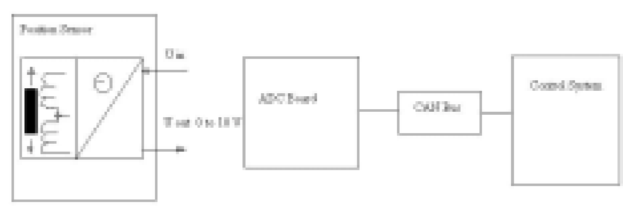

**Fig. 1: Working principle of the Linear Variable Differential Transformer (LVDT).**

## 4 FIRST MEASUREMENTS AND RESULTS

DELTA is only operated during the week from Monday morning to Friday afternoon. Especially on Mondays the reproducibility of the machine was difficult. The position monitoring of magnets showed a large movement of magnets during the Monday morning shift (see Fig. 2 ).

# SIGNAL PROCESSOR FOR SPring-8 LINAC BPM

K. Yanagida, T. Asaka, H. Dewa, H. Hanaki, T. Hori, T. Kobayashi, A. Mizuno,
S. Sasaki, S. Suzuki, T. Takashima, T. Taniuchi, H. Tomizawa,
Japan Synchrotron Radiation Research Institute, Mikazuki, Hyogo, 679-5198, Japan

*Abstract*

A signal processor of the single shot BPM system consists of a narrow-band BPF unit, a detector unit, a P/H circuit, an S/H IC and a 16-bit ADC. The BPF unit extracts a pure 2856-MHz RF signal component from a BPM and makes the pulse width longer than 100 ns. The detector unit that includes a demodulating logarithmic amplifier is used to detect an S-band RF amplitude. A wide dynamic range of beam current has been achieved; 0.01 $\sim$ 3.5 nC for below 100-ns input pulse width, or 0.06 $\sim$ 20 mA for above 100-ns input pulse width. The maximum acquisition rate with a VME system has been achieved up to 1 kHz.

## 1 INTRODUCTION

Beam operation of the SPring-8 linac began in 1996, but a BPM system was not equipped. Development of a BPM system started in 1990 and the conceptual design has been modified several times looking for the optimum BPM system for the SPring-8 linac. The guidelines for designing the BPM system were as follows.

- Bunch separation as short as 350 ps (2856 MHz).
- A wide range of beam pulse length; i.e., from a 1-ns (including a single bunch) beam to a 1-$\mu$s beam.
- A wide dynamic range of beam power; i.e., from a 1-ns - 10-mA (for the positron) beam to a 1-$\mu$s - 100-mA beam.
- Required resolution or beam-position measurement stability of $< 0.1$ mm (6 $\sigma$).
- A high acquisition rate of $\geq$ 60 Hz.
- Simple design and low cost manufacturing.

In the past decade, the conceptual design of the BPM system has been fixed. The detection frequency of 2856 MHz was determined in 1993. The electrostatic stripline pickup method for the BPM was chosen in 1998. Finally, a detection method based on a circuit using a demodulating logarithmic amplifier AD8313 (ANALOG DEVICES) was determined in 2000. After connection to the control system, the BPM system will be in operation in this year. The latest design of the BPM system was described in the previous paper [1].

## 2 SIGNAL PROCESSOR

The signal processor consists of two Nuclear Instrumentation Modules: the BPF (band pass filter) module, and the detector module. Both modules have four equivalent process channels. Figure 1 shows a block diagram of the signal processor.

There are two reasons to adopt the band pass filter. One is to extract a pure 2856-MHz RF signal component from the BPM or to eliminate noise (or higher harmonic) components. The other is to make the pulse width longer than 100 ns when an input pulse width is shorter than 100 ns. The pulse width of 100 ns was determined to match the response of the detector unit (the rise time of 40 ns).

A band pass filter is mounted in a case unit (the BPF unit), because characteristics of all BPF units cannot be adjusted precisely. This enables us to examine BPF units and to select four BPF units that have similar characteristics in order to get temperature stability. A component that includes the AD8313 is also mounted in a case unit (the detector unit) for the same reason.

### 2.1 BPF Module

The BPF unit is a second-order Butterworth cavity filter which has very flat transmission spectrum around center frequency. The center frequency is tuned to 2856 $\pm$ 0.01 MHz under the temperature of 33 $\pm$ 0.1 °C. These characteristics of the BPF unit are summarized in Table 1.

Table 1: Characteristics of the BPF unit

| | |
|---|---|
| Type of Filter | Second-Order Butterworth Cavity Filter |
| Material | Brass |
| Center Frequency | 2856 $\pm$ 0.01 MHz |
| Tuning Temperature | 33 $\pm$ 0.1 °C |
| Temperature Drift of Frequency | $\sim$ 50 kHz/°C |
| Flatness | $-$0.01 dB at $\pm$ 300 kHz |
| Band Width | $\sim$ 10 MHz |
| Insertion Loss | $\sim$ 1.5 dB |
| VSWR | $\leq$ 1.5 |
| Input/Output Impedance | 50 $\Omega$ |

### 2.2 Detector Module

The principal elements of the detector module are the detector unit that detects an S-band RF amplitude, a self-triggered peak hold (P/H) circuit, an externally triggered sample hold (S/H) IC and a 16-bit analog-to-digital converter (ADC). Although the signal processor needs an external trigger synchronizing with the input signal, the pulsed output (Detector Unit Output) can be used as the external trigger.

# Accuracy of the LEP Spectrometer Beam Orbit Monitors

E. Barbero, B. Dehning, J. Prochnow, CERN, Geneva, Switzerland
J. Bergoz, K. Unser, Bergoz Instrumentation, 01630 St. Genis Pouilly, France
J. Matheson, Rutherford Appleton Laboratory, Chilton, UK
E. Torrence, University of Chicaco, Chicago, IL60637, USA

*Abstract*

At the LEP e+/e- collider, a spectrometer is used to determine the beam energy with a target accuracy of $10^{-4}$. The spectrometer measures the lattice dipole bending angle of the beam using six beam position monitors (BPMs). The required calibration error imposes a BPM accuracy of 1 $\mu$m corresponding to a relative electrical signal variation of $2 \cdot 10^{-5}$. The operating parameters have been compared with beam simulator results and non-linear BPM response simulations. The relative beam current variations between 0.02 and 0.03 and position changes of 0.1 mm during the fills of last year lead to uncertainties in the orbit measurements of well below 1 $\mu$m. For accuracy tests absolute beam currents were varied by a factor of three. The environment magnetical field is introduced to correct orbit readings. The BPM linearity and calibration was checked using moveable supports and wire position sensors. The BPM triplet quantity is used to determine the orbit position monitors accuracy. The BPM triplet changed during the fills between 1 and 2 $\mu$m RMS, which indicates a single BPM orbit determination accuracy between 1 and 1.5 $\mu$m.

## 1 INTRODUCTION

The LEP energy calibration requires the determination of the beam energy ratio between 50 GeV and 93 GeV. The beam energy at 50 GeV is accurately calibrated using the spin polarization of the circulating electrons. Therefore only changes of the relevant quantities which occur during the calibration procedure have to be taken into account. The spectrometer measures the change in bending angle in a well-characterised dipole magnet as LEP is ramped [1, 2]. The beam trajectory is obtained using three beam position monitors (BPMs) on each side of the magnet. The BPMs used consist of an aluminium block with an elliptical aperture and four capacitive button pickup electrodes placed at the corners of a square with a length of 62 mm. The button signals are fed to customised electronics supplied by Bergoz Instrumentation. The electronics use time multiplexing of individual button signals through a single processing chain to optimise for long-term stability. The position of the BPM block is surveiled with wire position sensors [6]. Two independent wires are used to monitor the relative horizontal and vertical movements. The environmental magnetic field in the drift space is monitored with fluxgates.

The required BPM accuracy of 1 $\mu$m means that a orbit position determination at time $t_1$ and a second at $t_2$ should not differ more then 1 $\mu$m for the same beam position. In between of $t_1$ and $t_2$ the beam energy has to be changed from 50 to 93 GeV and several other parameters will change accordingly (for example: radiated synchrotron power, transverse and longitudinal beam size). A unobserved BPM support movement of 1 $\mu$m in between of $t_1$ and $t_2$ for the same beam position would be not acceptable.

An estimate of the influence of changing measurement conditions on the orbit determination accuracy is given in section 2 and 3. The absolute calibration of the BPMs with wire position sensors is explained in section 4. The orbit determination accuracy is estimated by using a beam position independent quantity (BPM triplet) and by calculating the difference of measurements taken at $t_1$ and $t_2$ (see section 5).

## 2 BEAM CURRENT AND BEAM ORBIT

During the operation, differences in the beam current in a fill were observed with a mean value of 55 $\mu$A and a RMS of 44.4 $\mu$A. The average beam current in a fill was 2050 $\mu$A. Estimating the position changes due to current variations, using the beam simulator results [3], an upper limit of position changes of 0.3 $\mu$m is calculated. The difference and the absolute value of the beam current during a fill as function of the fill number are shown in figure 1. The absolute beam currents in fill 7833, 8223 and 8443 were on purpose reduced.

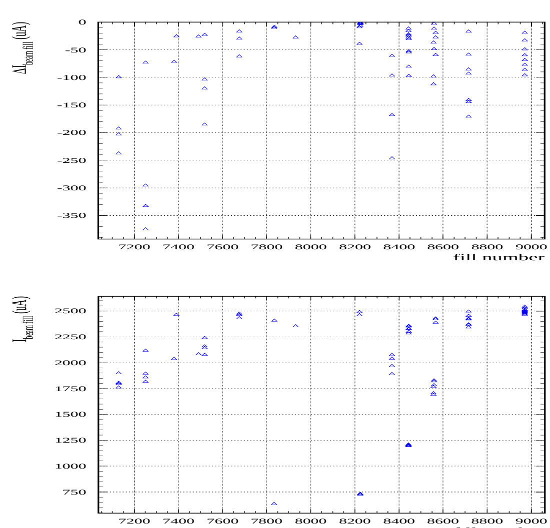


Figure 1: The beam current changes (top) and the absolute beam current (bottom) during a fill throughout the year.

# STRIPLINE BEAM POSITION MONITORS FOR "ELBE"

P.Evtushenko, A.Büchner, H.Büttig, P.Michel, R.Schurig, B.Wustmann, FZR, Germany
K. Jordan TJNAF, USA

*Abstract*

At the Forschungszentrum Rossendorf (FZR), the superconducting electron linear accelerator ELBE is under construction. It will deliver an electron beam with an energy of up to 40 MeV at an average beam current of up to 1mA. The accelerator uses standing wave DESY type RF cavities operating at 1.3 GHz. A non-destructive system for the measurement of the beam position at about 30 locations is needed. To obtain the required resolution of 100 µm, a system of stripline beam position monitors (BPM) is under design.

## 1 INTRODUCTION

There are some different applications of the electron beam of the ELBE accelerator. It will be used for experiments in radiation physics, nuclear physics and neutron physics. It also will be the driver for the infra red free electron laser (FEL). Obviously an accelerator needs a system for the beam position measurements. Also the position of the electron beam has to be controlled at the target in any experiment and inside the undulator of the FEL. In the case of the ELBE accelerator, the required resolution of the beam position measurements is about 100 µm. We decided to use stripline BPM, since it is well known that with the BPM one can easily achieve the resolution.

## 2 MECHANICAL DESIGN OF THE BPM

### *2.1 3λ/4 version of the ELBE BPM*

Two versions of the BPMs were designed. The BPM of the JLab FEL machine was the prototype for our first BPMs. The BPM is electron beam welded and it has four SMA feedthroughs which are also welded to the BPM. The transmission line which is formed by the strip and external pipe of the BPM has on impedance of 50 Ω. The length of the strip is an important item for BPM sensitivity and for the calibration of the whole BPM system. Usually the length is optimized so that the BPM has maximum sensitivity at the fundamental frequency of the accelerator, which leads to a strip length $(\lambda/4)\times(2n+1)$, where n is 0,1,2,… That means 57 mm, 173 mm and so on at 1.3 GHz. But because of the calibration procedure which we want to use the length of the strip of the BPM is 144 mm, instead of 173 mm.

### *2.2 Calibration of the BPM system*

For the calibration and verification of the BPM system we will use the procedure familiar with the JLab BPM system [1]. Before we explain the idea of the calibration we want to note, that during machining and welding of the BPM the X plane electrodes can be a little shifted in the X direction, but not in the Y direction. The procedure of the calibration is the following, if we want to calibrate, for instance, the Y plane of a BPM, we can inject a 1.3 GHz signal to the X plane electrode of the BPM. In this case the position which will be displayed in the corresponding BPM software is a result of two facts. First is the difference between the mechanical and electrical center of the BPM and second is that electrical chains of the two opposite channels can have slightly different gain and offset. All these facts can be taken in to account in the calibration. There is one more important item in the calibration. To enable such a method of calibration the $S_{21}$ from the X channel to a Y electrode has to be big enough. To increase the $S_{21}$ the strip length was reduced from 173 mm to 144 mm. Important is that such calibration can be done when the BPM detectors are already installed on the beam line.

### *2.3 Compact version of the BPM*

During the manufacturing of the first BPMs we faced some technological problems. For instance, some feedthroughs

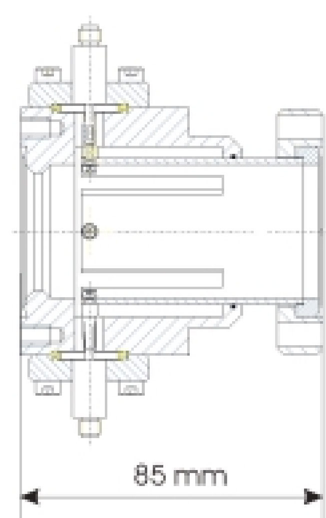


Figure 1: Compact BPM with strip length 40 mm

# FUNCTIONALITY ENHANCEMENT OF THE MULTIPLEXING BPM SYSTEM IN THE STORAGE OF SRRC

Jenny Chen, C. S. Chen, K. H. Hu, K. T. Hsu, C. H. Kuo, Demi Lee, K. K. Lin
Synchrotron Radiation Research Center, Hsinchu, Taiwan, R. O. C.

*Abstract*

An extension of existing multiplex BPM electronics to provide capability for turn-by-turn beam position and phase advance measurement is implemented. The system can be configured as turn-by-turn beam position measurement or phase advance and coupling measurement. For turn-by-turn mode, the system performed four consecutive measurements of four BPM buttons. Data acquisition is synchronize with beam excitation. Turn-by-turn beam position is reconstructed by these four independent measurements. This system was named as pseudo-turn-by-turn beam position monitor system (PTTBPM). Resonance excitation of the stored beam and adopting lock-in techniques can measure betatron phase and local coupling. Design considerations of the system and preliminary beam test results are presented in this report.

## 1 INTRODUCTION

Measured betatron function and phase advance information is essential for precision beam-based machine modelling and is helpful to achieve ultimate machine performance. The BPM system of SRRC is a multiplexing system for precision closed-orbit measurement [1]. Using all BPMs for machine optics measurement is highly desirable. However, at present stage, only a couple of BPMs are equipped with log-ratio processor for turn-by-turn beam position measurement. Based upon the ideas of ESRF's "Mille-Tour" BPM system [2], we made a simple functional extension of the SRRC BPM system. A log-amplifier video detector mezzanine is implementing and installing at all BPMs electronic. Accompany with beam excitation and data acquisition system, turn-by-turn beam position at all BPMs site can be acquired. The data from four measurement of individual button can be reconstructed as pseudo-turn-by-turn beam position. Averaging out time dependent information is its drawback. Using lock-in amplifier to detect coherent oscillation with resonance excitation can support fast betatron phase measurement. PTTBPM system can acquire a lot of information for various beam physics study. However, the data analysis is tedious. On the other hand, the lock-in detection techniques accompany with resonance excitation can also be used for betatron phase measurement, betatron functions measurement, local coupling parameter measurement, and determines the errors of the lattice.

## 2 MEZZANINE MODULE

The multiplexing BPM electronics is a commercial units (Bergoz's MX-BPM). It is designed for averaged beam position measurement with micron resolution. The electronics composed of low pass filter, GaAs RF switch, band pass filter, high performance mixer and IF amplifier, quasi-synchronous detector, analog de-multiplexer and position computation circuitry. To observe betatron oscillation, wide bandwidth detector is needed. The IF bandwidth of MX-BPM before quasi-synchronous detector is larger than 5 MHz which is sufficient for betatron oscillation observation. This simple log amplifier detector was implemented due to its simplicity, no need of gain control, and small component counts. This mezzanine supports more than 50 dB dynamic range. When mezzanine module is engaged, AGC function of MX-BPM is disabled and single button is enable. The mezzanine is installed near the IF amplifier and detector circuitry. Small signal sensitivity is limited to about – 60 dBm that is due to deteriorate of the operation of PLL in synchronous detector. The functional block diagram of the mezzanine is shown in Figure 1. The mezzanine demodulates bunches signal at IF frequency (21.4 MHz). Position error of reconstructed position due to log conformance is acceptable for small oscillation amplitude.

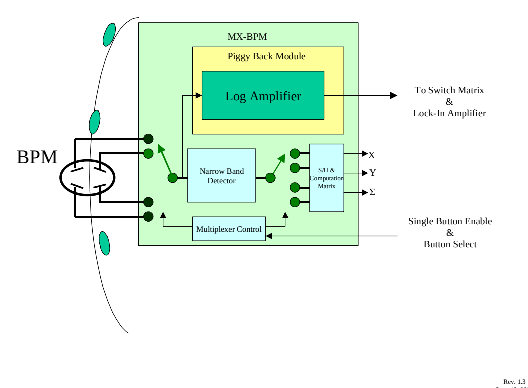


Figure 1. Functional block diagram of BPM processing electronics.

## 3 PTTBPM SYSTEM

The idea of PTTBPM is shown in Figure 2. Four measurements of individual BPM button signal can be reconstructed to obtain the turn-by-turn beam position.

# THE LOW GAP BPM SYSTEM AT ELETTRA: COMMISSIONING RESULTS

M.Ferianis, R. De Monte, Sincrotrone Trieste, Trieste, Italy

*Abstract*

Two Low Gap BPMs have been successfully installed at ELETTRA and have now completed the commissioning phase. The main purpose of these new devices is to provide stable beam position measurement, at sub-micron level, to monitor the stability of the light delivered to the Users. The improvements with respect to the normal BPM system have been obtained adopting both a new Low Gap BPM sensor and a new non-multiplexed BPM detector, the latter being developed in co-operation with the SLS diagnostic group at the PSI. Beside the Closed Orbit mode, thanks to the digitally selectable bandwidth, the new BPM detector can be operated also in the Turn-by-Turn mode and provide the position signal to feedback loops.

In this paper we first briefly review the system architecture, describing its mechanical and electronic parts. Then, we present the digital BPM detector set-up used at ELETTRA and the associated firmware required by the four-channel BPM detector to guarantee performance over the full dynamic range. The BPM-position monitoring system is also described and its integration in the BPM system presented. Laboratory tests confirmed sub-micron resolution at 10kHz data rate. A series of beam based measurements have been performed in order to test this system and to verify the improvement in performance. The system is presently used in the control room as a powerful beam quality monitor; its extension to other Storage Ring straight sections is under evaluation.

## 1 SYSTEM OVERVIEW

To provide a stable photon source point is a well-known challenge in third-generation synchrotron light sources. The stabilization over long time periods, typically 24-hours, of the position of the electron beam can be achieved only using high- resolution, high-stability beam position monitoring systems in feedback loops, high meaning here at the sub-micron level.

The Low Gap Beam Position Monitor (LG-BPM) system at ELETTRA [1] has been developed to provide both high resolution and high accuracy beam position measurements. Two main developments have been completed to satisfy the requirements: the new digital programmable detector and the new sensor with its dedicated support system. The new digital detector has been jointly developed between the Swiss Light Source (SLS) Diagnostic group, the Instrumentation Technology Company [2] and the ELETTRA diagnostic group. This is a completely new four-channel system using parallel processing of the four button signals, to avoid errors due to multiplexingand to improve read out rate. Furthermore, thanks to direct IF signal under-sampling and digital filtering, the receiver bandwidth can be tuned to any of the operation modes: closed orbit, feedback mode or turn-by-turn [3].

The new Low Gap BPM sensor has been developed at ELETTRA [4] and it has been designed taking full advantage of the 14mm, low gap, new aluminum ID chamber installed at ELETTRA. Furthermore, this new sensor is fitted with bellows on each side to reduce mechanical coupling to the vacuum chamber.

Two sensors have been located in straight section 2, close to the undulator, using a dedicated support system. The position of each sensor is monitored in real time with respect to a reference column made of carbon fiber. The absolute position of the electron beam is therefore measured at sub-micron accuracy with a suitable resolution.

## 2 DIGITAL DETECTOR AT ELETTRA

### *2.1 System configuration*

The Digital Detector system installed at ELETTRA relies on the Quad Digital Receiver (QDR) VME board and on the Front-End (FE) VME board. Both units are four channel devices for non-multiplexed acquisition of the button electrode signals and have been described in [3]. At ELETTRA two pairs of QDR+FE have been installed to acquire the signals of the LG-BPM.

### *2.2 Software Configuration*

Two different software environments have been created. The first one runs under the Windows operating system and it is written in ‘C’ language using National Instruments CVI. With this software it is possible to perform all the hardware settings and tests on the Digital Receiver VME boards. The results are graphically displayed in real-time. The second environment has a completely different architecture and is used for field operation with the same hardware. The requirements for field operation are: continuous real time data acquisition, network (Ethernet) connectivity, data reliability and compatibility with the Elettra Control System, remote control access capability (telnet). To meet all these requirements, Linux with real time extensions (RTAI) has

# ORBIT CONTROL AT THE ADVANCED PHOTON SOURCE*

Glenn Decker, Argonne National Laboratory, Argonne, Illinois 60439 USA

*Abstract*

The Advanced Photon Source (APS) began operation in 1995 with the objective of providing ultra-stable high-brightness hard x-rays to its user community. This paper will be a review of the instrumentation and software presently in use for orbit stabilization. Broad-band and narrow-band rf beam position monitors as well as x-ray beam position monitors supporting bending magnet and insertion device source points are used in an integrated system. Status and upgrade plans for the system will be discussed.

## 1 INTRODUCTION

Since the commissioning of the APS, there has been significant progress in the understanding of beam stabilization, with the result that a first round of hardware upgrades is near completion. The goal is ultimately to achieve better than 1 micron rms beam stability at all x-ray source points in a frequency band up to 30 Hz and extending at the low frequency end to 24 hours or longer, and to be able to prove it.

## 2 HARDWARE DESCRIPTION

The APS beam position monitor (BPM) systems consist of approximately 360 stations employing broad-band (monopulse) rf receivers [1], 48 narrow-band receivers [2] distributed among the 24 insertion device vacuum chambers, and 86 front-end x-ray BPMs [3,4].

Data from each of these BPM systems are provided to a distributed array of digital signal processors (DSPs) that have real-time (1.534 kHz) connections to as many as 317 combined function horizontal/vertical steering corrector magnet power supplies. For normal operation, this real-time feedback system [5] employs 160 broad-band rf BPMs and uses a singular value decomposition (SVD) algorithm to compute set points for writing to 38 corrector magnet power supplies.

The 38 corrector magnets employed by the real-time feedback system are mounted at spool piece locations and thus have faster response times than the other 279 units, which are mounted at locations with thick aluminum vacuum chamber walls that are subject to large eddy current effects. Each corrector is powered by an identical pulse-width-modulated power supply, which is interfaced both to the Experimental Physics and Industrial Control System (EPICS) network and the real-time feedback dedicated network. EPICS also reads the BPMs at up to a -Hz rate, after de-aliasing, for use in a separate DC correction algorithm.

* Work supported by U.S. Department of Energy, Office of Basic Energy Sciences under Contract No. W-31-109-ENG-38.

## 3 SYSTEMATIC EFFECTS

Virtually all of the orbit correction technique can be reduced to the study and compensation of systematic effects of one form or another. While space does not allow a detailed study of the many known effects, a listing of them should give some idea of the depth of this area. With regard to orbit correction, there are both intrinsic and extrinsic systematic effects. The extrinsic effects are those for which the BPM system was built to correct in the first place. The challenge in putting together an effective orbit correction strategy is to reduce the size of the intrinsic systematic effects to such a degree that the extrinsic perturbations can be reduced to an acceptable level.

### *3.1 Rf BPM systematic effects*

- Timing/trigger stability
- Intensity dependence
- Bunch pattern dependence
- The “rogue” microwave chamber modes [6]
- Electronics thermal drift

### *3.2 X-ray BPM systematic effects*

- Stray radiation striking X-BPM blade pickups [7]
- X-BPM blade misalignment
- Electronics thermal drift
- Gap-dependent effects (e.g., sensitivity, steering)

### *3.3 Extrinsic systematic effects (noise sources)*

- Magnet power supply noise/ripple
- Rf system high-voltage power supply ripple
- Mechanical vibration
- Thermal effects (tunnel air/water temperature)
- Earth tides
- Insertion device gap changes

Each of these systematic effects has its own spectrum, ranging from long-term drift effects of hours to days, up to motions of several kHz. Ultimately, one can speak of stabilizing turn-by-turn motions using rf frequency broad-band feedback systems, however this can be considered to impact beam size for most x-ray experiments that average over many turns, and is beyond the scope of the present

# ADVANCED PHOTON SOURCE RF BEAM POSITION MONITOR SYSTEM UPGRADE DESIGN AND COMMISSIONING

R. Lill, G. Decker, O. Singh
Advanced Photon Source, Argonne National Laboratory,
9700 South Cass Avenue, Argonne IL 60439 USA

*Abstract*

This paper describes the Advanced Photon Source (APS) storage ring monopulse rf beam position monitor (BPM) system upgrade. The present rf BPM system requires a large dead time of 400 ns between the measured bunch and upstream bunch. The bunch pattern is also constrained by the required target cluster of six bunches of 7 mA minimum necessary to operate the receiver near the top end of the dynamic range. The upgrade design objectives involve resolving bunches spaced as closely as 100 ns. These design objectives require us to reduce receiver front-end losses and reflections. An improved trigger scheme that minimizes systematic errors is also required. The upgrade is in the final phases of installation and commissioning at this time. The latest experimental and commissioning data and results will be presented.

## 1 INTRODUCTION

The measurement of the APS storage ring beam position is accomplished by 360 rf BPMs located approximately every degree around the 1104-m circumference ring [1]. The rf BPM signal processing topology used is a monopulse amplitude-to-phase (AM/PM) technique for measuring the beam position in the x and y axes. A logarithmic amplifier channel measures the beam intensity. The rf BPM upgrade was proposed at BIW 1998 [2].

## 2 SYSTEM DESIGN

Figure 1 is the block diagram for the monopulse rf BPM receiver front end. The matching networks are attached directly to 10-mm-diameter button electrodes [3]. The button matching network was designed to match the capacitively reactive button (0.25–j75 ohm) into 50 ohms in a 100-MHz, 3-dB bandwidth centered at 352 MHz. This matching network circuit has the response characteristics of a bandpass filter with the button's capacitance (4.8 pf) integrated as part of the filter design. To match the button's impedance, an inductor and resistor are placed in parallel with the capacitive electrode and the beam current source. The matching network circuit also includes a 3-pole, low-pass filter that attenuates the second harmonic (704 MHz) by 46 dB. The matching network typically improves the in-band signal strength by 5 dB. They also provide >25 dB return loss source match, in a 10-MHz bandwidth centered at 352 MHz.

The filter comparator (Figure 1) is to be located 42 inches away from the buttons via matched silicon dioxide cables. The system is matched in phase and amplitude to insure the vector addition and subtraction of the input signals. The 180-degree hybrid comparator network described in Figure 1 has been implemented using a rat race hybrid topology. The rat race hybrid consists of three $\lambda/4$ and one $3\lambda/4$ lengths of 70.7-ohm mini coax. The four lengths are connected together in a ring configuration yielding 50-ohm inputs and outputs. The bandwidth is extended from 20% to 30% by using a ferrite reversing coil on the $3\lambda/4$ leg of the bridge. The hybrid network provides a low loss sum of all four inputs and excellent return loss on all ports.

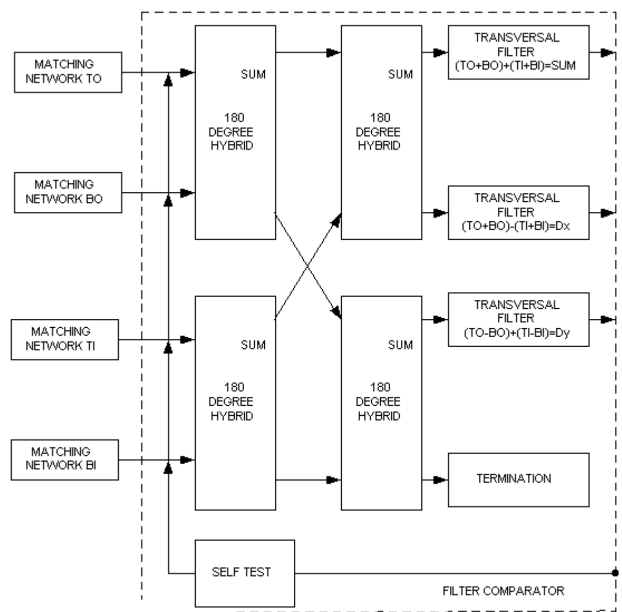


Figure 1: BPM receiver front-end block diagram.

The self-test input provides an input signal to test the comparator during maintenance periods. The input signal is split four ways and fed into the coupling arm of 15-dB directional couplers in each of the inputs. The new comparator can be operated with one input offset by 6 dB or with all inputs balanced. Resolving bunches spaced as closely as 100 ns and minimizing associated systematic errors required designing a bandpass filter that had nearly a rectangular time domain response. This $[\text{SIN F/F}]^2$ frequency response was realized using the technique illustrated in Figure 2. The transversal filter is best explained in the time domain. The transversal filter

# DESIGN OF A MULTI-BUNCH BPM FOR THE NEXT LINEAR COLLIDER[1]

Andrew Young, Scott D. Anderson, Douglas McCormick, Janice Nelson, Marc Ross, Stephen R. Smith, Tonee J. Smith, SLAC, Stanford, CA. USA,
Hayano, T. Naito, N. Terunuma, S. Araki, KEK, Ibaraki, Japan

*Abstract*

The Next Linear Collider (NLC) design requires precise control of colliding trains of high-intensity ($1.4x10^{10}$ particles/bunch) and low-emittance beams. High-resolution multi-bunch beam position monitors (BPMs) are required to ensure uniformity across the bunch trains with bunch spacing of 1.4ns. A high bandwidth (~350 MHz) multi-bunch BPM has been designed based on a custom-made stripline sum and difference hybrid on a Teflon-based material. High bandwidth RF couplers were included to allow injection of a calibration tone. Three prototype BPMs were fabricated at SLAC and tested in the Accelerator Test Facility at KEK and in the PEP-II ring at SLAC. Tone calibration data and single-bunch and multi-bunch beam data were taken with high-speed (5Gsa/s) digitisers. Offline analysis determined the deconvolution of individual bunches in the multi-bunch mode by using the measured single bunch response. The results of these measurements are presented in this paper.

## 1. OVERVIEW

The multi-bunch (MB) BPMs were designed to operate over a wide range of conditions (Table 1) allowing for testing to be performed at SLAC and KEK. The MB BPMs are used by the sub-train feedback, which applies a shaped pulse to a set of stripline kickers to straighten out a bunch train. These are qualitatively different from the quad (Q) and feedback (FB) BPMs due to their high bandwidth and relatively relaxed stability requirements. The primary requirement on the MB BPMs is a bunch train that generates a BPM signal, which is straight.

Table 1: BPM Specifications

| Parameters | Value | Comments |
|---|---|---|
| Resolution | 300 nm rms at $0.6x10^{10}$ $e^-$ /bunch | For bunch-bunch displacements freq. Below 300 MHz |
| Position range | $\pm$2mm | |
| Bunch spacing | 2.8 or 1.4 ns | |
| No. of bunches | 1-95<br>1-190 | 2.8ns<br>1.4ns |
| Beam current | 1 $x10^9$<br>1.4x $x10^{10}$ | Particles per bunch |
| No. of BPMs | 278 | |

## 2. IMPLEMENTATION

Figure 1 shows a simplified block diagram of the multi-bunch front-end chassis. The BPM chassis contains directional couplers, non-reflective switches for transfer function measurements, sum and difference hybrid, bandpass filters for noise rejection, and sold-state amplifies. The BPM chassis takes the two x or y inputs from the BPM buttons and takes the sum and difference. The BPM signal is then amplified in order to run it on a long cable to a digitiser outside the radiation area. The front-end has a feature where a single tone can be injected into the inputs of the sum and difference hybrid for calibration. Thus allowing the operators to perform a transfer function.

Figure 1 Block diagram of the BPM front-electronics

To obtain the bandwidth and performance requirements, several custom components were designed at SLAC. The first component is the heart of the front-end chassis, a stripline 5/4λ sum and difference hybrid illustrated in figure 2. The hybrid operates at 600MHz with a 300MHz bandwidth. The phase variation at the output across the bandwidth is $\pm$5 degrees.

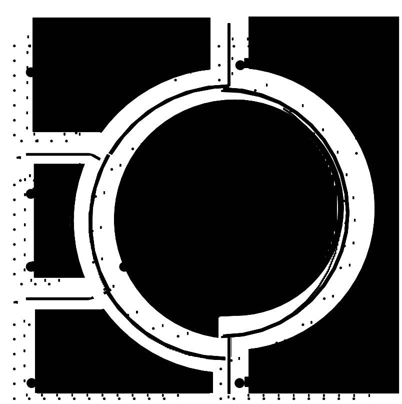

Figure 2 Stripline 5/4λ Hybrid

[1] Work supported by the Department of Energy, contract DE-AC03-76SF00515

# A logarithmic processor for beam position measurements applied to a transfer line at CERN

H. Schmickler, G. Vismara, CERN, Geneva, Switzerland


*Abstract*

The transfer line from the CERN proton synchrotron (PS) to the super proton synchrotron (SPS) requires a new beam position measurement system in view of the LHC.

In this line, the single passage of various beam types (up to 7), induces signals with a global signal dynamics of more than 100 dB and with a wide frequency spectral distribution.

Logarithmic amplifiers, have been chosen as technical solution for the challenges described above.

The paper describes the details of the adopted solutions to make beam position measurements, with a resolution down to few $10^{-4}$ of the full pickup aperture over more than 50 dB of the total signal dynamics.

The reported performances has been measured on the series production cards, already installed into the machine and on one pickup in the transfer line.


## 1 BEAM PARAMETERS

### 1.1 Beam types

Here is a non-exhaustive list of the transfer line beams.

Table 1: Transfer line beam types

| Beam Name | Number of bunches | Bunch width | Bunch spacing | Intensities (minimal) |
|---|---|---|---|---|
| Fix Target | 2000 | 1.7 | 5 | $1*10^9$ |
| LHC | 1 to 84 | 2.1 | 25 | $5*10^9$ |
| Special | 1,8,16 | 4.8 | 262 | $5*10^9$ |
| Heavy Ions | 16 | 6.2/15 | 131 | $2.6*10^8$ |
| | | ns | ns | Charges/b |

Due to the very low intensity of the heavy ions beams, long coupler pickups have been chosen. Their transfer impedance shows a maximum at about 100MHz, which is a good compromise for the various beams present in the transfer line. The position sensitivity corresponds to 0.54 dB/mm.

### 1.2 Signals spectral distribution

The signal spectra at the coupler's output are illustrated in fig. 1. In order to illustrate the large dynamic range, the most intense beams have been represented at their maximum intensity, while the weakest beams at their minimum intensity.

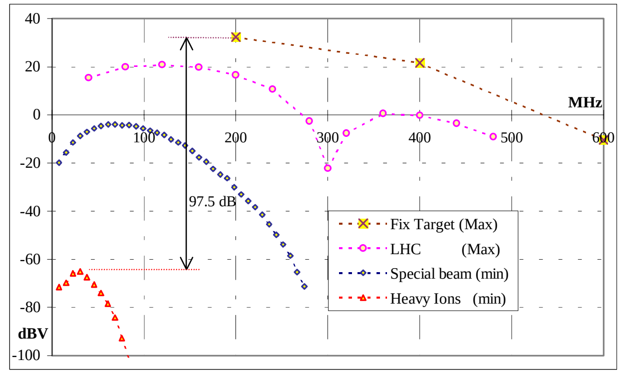


### 1.3 Global dynamic

The intensity dynamic corresponds to 97.5 dB, to which one should add a position dynamic of at least 25 dB.

Figure 1: Spectral distribution of various beam types

## 2 DESIGN CONSIDERATIONS

None of the existing electronic processors can cover the whole dynamic range.

Since the various beams are transferred at time interval in the range of seconds, it is acceptable to select a tailored processor to each individual beam. In practice, two processors can handle all the various situations.

The conditions associated to this choice are:

- No reliability reduction, hence no mechanical switching elements
- No significant power consumption increment
- Similar position resolution for the various beam
- Negligible costs increment

### 2.1 Beam grouping

#### *2.1.1 Narrow Band*

The most critical case corresponds to the "Heavy Ions" beam, which shows the largest spectral lines at 22.89 MHz. At this frequency, the "Special" beam is only 7 db below its maximum level and being over 40 dB larger, it can be treated by the same narrow band processor.

The bandwidth choice (BW = 1.3 MHz) is determined by the compromise between the time required to build up a stable signal level and the required long dumping time, to allow a proper measurement to be done, in the case of single LHC bunch.

#### *2.1.2 Wide Band*

The "Fix target" and "LHC" beams have respectively fundamental and 5th harmonics tuned at 200 MHz hence

# INJECTION MATCHING STUDIES USING TURN BY TURN BEAM PROFILE MEASUREMENTS IN THE CERN PS

M. Benedikt, Ch. Carli, Ch. Dutriat, A. Jansson, M. Giovannozzi, M. Martini, U. Raich,
CERN, Geneva, Switzerland

*Abstract*

The very small emittance beam needed for the LHC requires that the emittance blow-up in its injector machines must be kept to a minimum. Mismatch upon the beam transfer from one machine to the next is a potential source of such blow-up.
The CERN PS ring is equipped with 3 Secondary Emission Grids (SEM-Grids) which are used for emittance measurement at injection. One of these has been converted to a multi-turn mode, in which several tens of consecutive beam passages can be observed. This allows the study of mismatch between the PS-Booster and the PS.
This paper describes the instrument and experimental results obtained during the last year.

## 1 MOTIVATION

Since the construction of the PS Booster (PSB) the transfer line between the PSB and the PS has been operated with a rather large dispersion mismatch. This was acceptable for beams with relatively large transverse emittance and small momentum spread. For LHC-type beams however, due to their low emittance requirements, it is essential to improve the dispersion matching.

The method described was used to measure this mismatch and to investigate new quadrupole settings in the transfer line in order to reduce it[1].

## 2 EXPERIMENTAL SETUP

Three SEM-Grids are installed in the PS ring in order to measure beam emittance at injection into the machine. After traversal of the detectors, the beam is normally stopped by an internal dump in order to prevent multiple passages, heating the SEM-Grid wires and destroying the detectors. Slow charge integrating electronics is used for the measurements.

However for the measurements reported here, one of the SEM-Grids has been equipped with a fast amplifier (100 ns rise-time) and 40 MHz Flash-ADC associated with 2 kbytes of memory for each SEM-Grid wire. The injection kicker is pulsed twice at 60 µs time interval. The second kick destroys the beam after 28 turns (revolution period in the PS at 1.4 GeV is 2.2 µs) in the machine, thus avoiding unnecessary heating of the SEM-Grid wires.

The ADCs are triggered a few µs before injection and the wire signals are converted and stored in memory at the ADC's internal clock frequency of 40 MHz.

An acquisition program reads out the ADC channels and saves the results onto a disk file for offline evaluation.

The beams used for the measurement had a bunch length of ~ 80ns, an intensity of $10^{11}$ protons and a small momentum spread in order to ease the evaluation of the betatron mismatch. The method has been first proposed in [2] and preliminary results presented in [3].

## 3 DATA EVALUATION

A *Mathematica* [4] program reads the disk file and evaluates the data.

### *3.1 The Raw Data*

The raw data correspond to a copy of the ADC memory contents consisting of 2048 samples (one sample every 25 ns) for each of the 20 wires.
Figure 1 shows the signal seen on a single SEM-Grid wire in the centre of the SEM-Grid (wire 11).

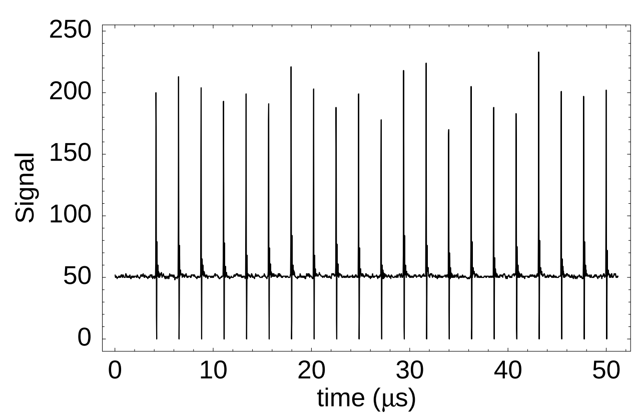


Figure 1: Raw data on a single wire

The raw data from 20 wires around a single beam passage is shown in fig. 2. Here 12 samples of the wire signals from all wires is plotted.

# THE SPS INDIVIDUAL BUNCH MEASUREMENT SYSTEM

A. Guerrero, H. Jakob, R. Jones, J.J. Savioz.
SL Division CERN Laboratory - CH - 1211 Geneva 23

*Abstract*

The Individual Bunch Measurement System (IBMS) allows the intensity of each bunch in an LHC batch to be the measured both in the PS to SPS transfer lines and in the SPS ring itself. The method is based on measuring the peak and valley of the analogue signal supplied by a Fast Beam Current Transformer at a frequency of 40MHz. A 12 bit acquisition system is required to obtain a 1% resolution for the intensity range of $5\times10^{9}$ to $1.7\times10^{11}$ protons per bunch, corresponding to the pilot and ultimate LHC bunch intensities. The acquisition selection and external trigger adjustment system is driven by the 200MHz RF, which is distributed using a single-mode fibre-optic link. A local oscilloscope, controlled via a GPIB interface, allows the remote adjustment of the timing signals. The low-level software consists of a real-time task and a communication server run on a VME Power PC, which is accessed using a graphical user interface. This paper describes the system as a whole and presents some recent uses and results from the SPS run in 2000.

## 1. INTRODUCTION

Since 1999 the PS pre-injector complex has been able to produce proton beams for LHC [1]. The LHC batch, consisting of 72 bunches spaced by 25ns is generated in the PS at 26 GeV/c and transferred to the SPS. Following three or four of such injections, the SPS is ramped in energy to 450 GeV/c, after which injection to the LHC will take place (see Fig. 1).

The Individual Bunch Measurement System (IBMS) was designed for a continuous monitoring of the intensity of each bunch of each LHC batch. The total range of intensities involved is summarised in Table 1.

| Beam Type | Intensity per bunch ($\times10^{11}$ppb) | Max Nb of Bunches | Total Current (mA) |
|---|---|---|---|
| Pilot | 0.03 | 1 | 0.05 |
| Set-up | 0.03 | 72 | 3.6 |
| Commissioning | 0.17 | 288 | 34 |
| Nominal | 1.05 | 288 | 209 |
| Ultimate | 1.7 | 288 | 340 |

Table 1: Bunch intensity for LHC type beams.

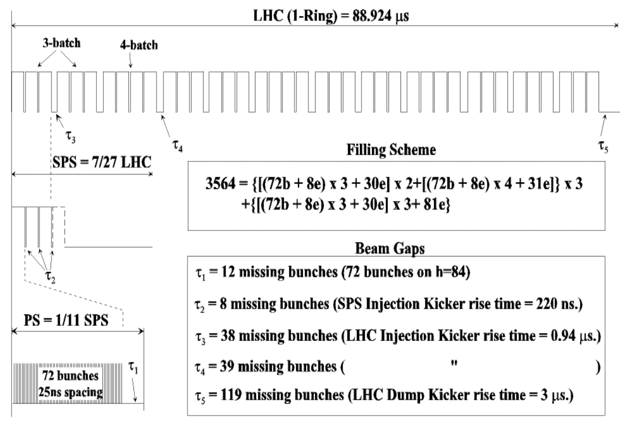


Figure 1: Bunch disposition in the LHC, SPS and PS.

The system is able to measure all bunches for all injected batches in the PS to SPS transfer lines, and a selected number of turns in the SPS ring, or up to 16 selected bunches for all turns in the SPS.

## 2. INSTALLATION

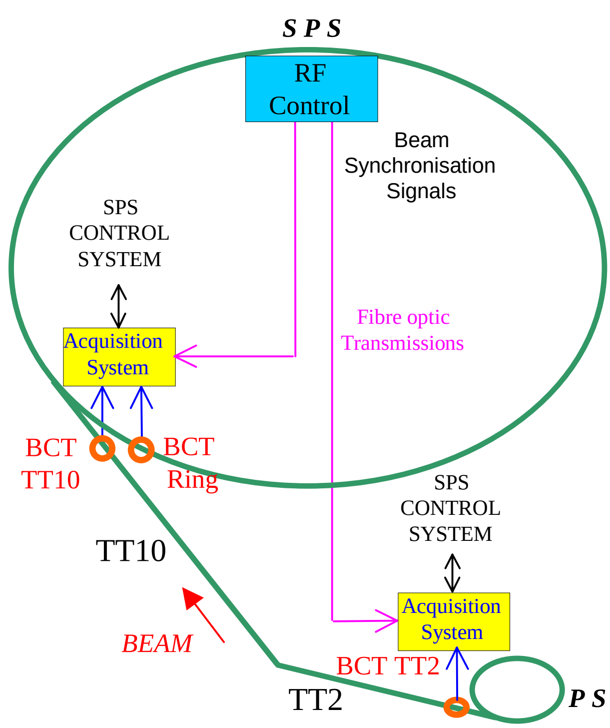


Figure 2: Layout of the installation.

# CONTROL MODULES FOR SCINTILLATION COUNTERS IN THE SPS EXPERIMENTAL AREAS

G. Baribaud, C. Beugnet, A. Cojan, G.P. Ferri, J. Fullerton,
A. Manarin, J. Spanggaard
CERN Laboratory - CH - 1211 Geneva 23

*Abstract*

The hardware used in the SPS Experimental Areas to control the beam instrumentation electronics and mechanics of the particle detectors is based on CAMAC and NIM modules. The maintenance of this hardware now presents very serious problems. The modules used to operate the Experimental Areas are numerous and older than 20 years so many of them cannot be repaired any more and CAMAC is no longer well supported by industry. The fast evolution of technology and a better understanding of the detectors allow a new equipment-oriented approach, which is more favourable for maintenance purposes and presents fewer data handling problems. VME and IP Modules were selected as standard components to implement the new electronics to control and read out the particle detectors. The first application implemented in this way concerns the instrumentation for the Scintillation Counters (formerly referred to as triggers). The fundamental options and the design features will be presented.

## 1 MOTIVATION AND HISTORY

Most of the detectors in the Experimental Areas of the SPS were implemented more than twenty years ago. At that time many detectors were at an experimental stage and the implementation of their control electronics and data acquisition were not yet in a final state. It was therefore convenient to have building blocks that made it easy to add new features whenever needed. The electronics were therefore implemented in a function-oriented way (see chapter 2), where many different systems, often located in different racks, constituted the building blocks of the detector control.

Our detectors are now well known and implemented in a well-defined manner. The advantage of the function-oriented approach has now vanished and has turned into a time consuming problem when it comes to maintenance and troubleshooting. For some detectors more than hundred cables are needed to interconnect their functional building blocks making fault finding very difficult.

Scintillation Counters are rather simple devices used to count the number of particles in a beam. They are made up of a scintillator that can be moved in or out of the beam and a photomultiplier to pick-up the scintillation light produced by each charged particle. When put in coincidence two Scintillation Counters are often used to strobe a more complex detector (see Fig. 1). The old function-oriented approach presently implemented for the Scintillation Counters requires the interconnection of seventeen different electronic modules for their control and data acquisition (see chapter 2.1).

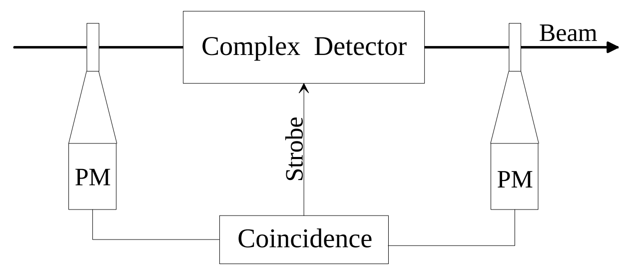


Figure 1: Scintillation Counters in coincidence.

## 2 FUNCTION ORIENTED APPROACH

### *2.1 Modules used for the old implementation*

In the old function-oriented approach the different systems like Discriminators, Delays, DACs and ADCs have many channels connected to signals from many different types of equipment.

For the Scintillation Counter the electronic modules needed to implement the old function-oriented systems are listed below:

- Discriminator. 8 ch NIM module.
- Delay Driver. 64 ch CAMAC module.
- Quad Delay. 4 channel 19” chassis.
- Coincidence. 4 ch NIM module.
- Scaler. 6 ch CAMAC module.
- Programmable Fan Out. 16 ch Camac module.
- Led Driver. 16 ch NIM module.
- ADC. CAMAC module.
- Multiplexer Driver. 1024 ch CAMAC module.
- ADC multiplexer. 64 ch 19” chassis.
- Analogue MPX PP. 32 ch 19” chassis.
- DAC. 12 ch. CAMAC module.
- Output Register. 128 ch CAMAC module.
- Input Gate. 256 ch CAMAC module.
- Timing Repeater. 4 ch NIM module.
- Line Survey. 128 ch CAMAC module.
- I/O Motor Driver. Two ch NIM module.

# LHC BEAM LOSS MONITORS

A. Arauzo Garcia, B. Dehning, G. Ferioli, E. Gschwendtner, CERN, Geneva, Switzerland

*Abstract*

At the Large Hadron Collider (LHC) a beam loss system will be installed for a continuous surveillance of particle losses. These beam particles deposit their energy in the super-conducting coils leading to temperature increase, possible magnet quenches and damages. Detailed simulations have shown that a set of six detectors outside the cryostats of the quadrupole magnets in the regular arc cells are needed to completely diagnose the expected beam losses and hence protect the magnets.

To characterize the quench levels different loss rates are identified. In order to cover all possible quench scenarios the dynamic range of the beam loss monitors has to be matched to the simulated loss rates. For that purpose different detector systems (PIN-diodes and ionization chambers) are compared.

## 1 LHC PARAMETERS

### *1.1 Quench levels*

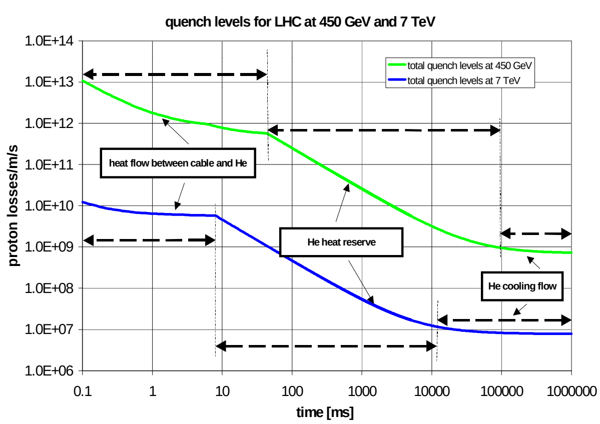


Figure 1: Different quench levels for 450GeV and 7TeV.

Super-conducting magnets can quench if a local deposition of energy due to beam particle losses increases the temperature to a critical value. Figure 1 shows the maximal allowed proton losses/m/s at 450GeV and 7TeV for quenches being reached after different time scales. These quench levels are determined by the coil materials and the coil cooling. The main effects are[1]:

1. At short time scales ($\tau$<50ms at 450GeV, $\tau$<8ms at 7TeV) the maximal allowed proton loss rate is limited by the heat reserve of the cables as well as by the heat flow between the super-conducting cables and the helium.
2. At intermediate time-scales ($\tau$>50ms at 450GeV, $\tau$>10ms at 7TeV) the limited heat reserve of the helium determines the quench levels.
3. The maximal helium flow to evacuate the heat across the insulation defines the allowed proton losses at times above seconds.

The proton loss rate extends over six orders of magnitude. An uncertainty of 50% is considered for the levels.

### *1.2 Operation conditions*

The magnet protection must cover the different filling schemes for LHC shown in Table 1 at injection, ramping and top energy.

Table 1: Different filling schemes for the LHC.

| filling scheme | Number of bunches | number of protons/bunch |
|---|---|---|
| **pilot bunch** | 1 | $5\cdot10^{9}$ |
| **TOTEM** | 36 | $1\cdot10^{10}$ |
| **batch** | 243 | $1\cdot10^{11}$ |
| **nominal** | 2835 | $1.1\cdot10^{11}$ |

## 2 SIMULATION OF BEAM LOSSES AND DETECTOR LOCATIONS

With the Monte Carlo code GEANT 3.21 the impact of beam protons on the aperture of the super-conducting magnets has been simulated[2]. In order to detect the beam losses outside the cryostat the shower development in the magnets has been computed in consideration of the main different geometries and magnetic field configurations. These calculations allow determining the suitable positions of the beam loss detectors as well as the needed number of monitors. The results show that a set of six monitors outside the cryostat of the quadrupole magnets in the arc cells are needed to completely diagnose the expected beam loss.

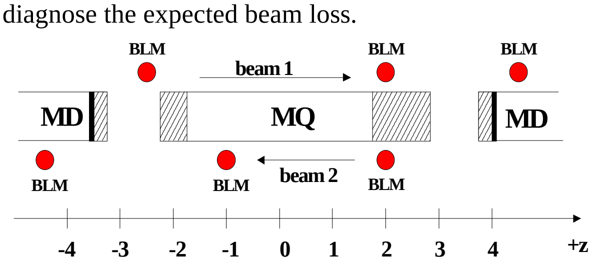


Figure 2: Proposed beam loss monitor locations around the quadrupoles.

The proposed beam loss detector locations in the arc shown in Figure 2 cover aperture limitations in the

# SENSITIVITY STUDIES WITH THE SPS REST GAS PROFILE MONITOR

G. Ferioli, C. Fischer, J. Koopman, M. Sillanoli, CERN, Geneva, Switzerland


*Abstract*

During the SPS run in the year 2000 further test measurements were performed with the rest gas monitor.

First, profiles of single circulating proton bunches were measured and the bunch charge progressively reduced, in order to determine the smallest bunch intensity which can be scanned under the present operating conditions. The image detector in this case was a CMOS camera.

Using a multi-anode strip photo-multiplier with fast read-out electronics, the possibility to record profiles on a single beam passage and on consecutive turns was also investigated. This paper presents the results of these tests and discusses the expected improvements for the operation in 2001.

Moreover, the issue of micro channel plate ageing effects was tackled and a calibration system based on electron emission from a heating wire is proposed. The gained experience will be used for the specification of a new monitor with optimised design, to be operated both in the SPS and in the LHC.


## 1 INTRODUCTION

A residual gas ionisation beam profile monitor (IPM) is considered as one of the instruments for measuring the transverse beam size of the proton beams in the SPS and in the LHC. A monitor from DESY has been modified and is under test in the SPS [1][2]. Previous measurement campaigns have shown that adequate accuracy and resolution can be achieved. During 2000 the sensitivity limit of the monitor was probed. It was operated in both a high spatial resolution read-out mode, using a standard CMOS camera, and a high speed read-out mode, employing a miniature photo-multiplier tube with 16 anode strips.

In the LHC the instrument will have to deal with beam intensities varying from one pilot bunch, ($5\times10^9$ protons), up to 2808 bunches of $1.67\times10^{11}$ protons each (ultimate current): a dynamic range in the order of $10^5$.

The acquisition speed is another important issue, since the device may also be used to verify the quality of the betatron matching at injection into the SPS and the LHC [3]. For that purpose a single nominal bunch, ($1.1\times10^{11}$ protons), should be measured on a turn by turn basis (23.1 µs in the SPS and 88.9 µs in the LHC).

One of the problems encountered, when exploiting IPM monitors, is the ageing of the micro channel plate (MCP). This ageing affects the area of the MCP where the beam is imaged. To track this effect and correct for it, a remote controlled built-in calibration system would be very useful. A method is proposed using a heating wire acting as an electron source. The feasibility of such a correction system has been checked in a dedicated laboratory set-up.

## 2 SENSITIVITY LIMIT

### *2.1 High spatial resolution read-out set-up.*

In the first half of the 2000 SPS run, a read-out system integrating a standard CMOS camera, with a 25 Hz frame rate associated to CERN designed acquisition electronics, was installed. Beam profiles, integrated over 866 SPS turns, were provided every 40 ms. Figure 1 shows 108 consecutive horizontal profiles acquired during the SPS acceleration cycle, starting at injection.

These measurements are performed on a single bunch

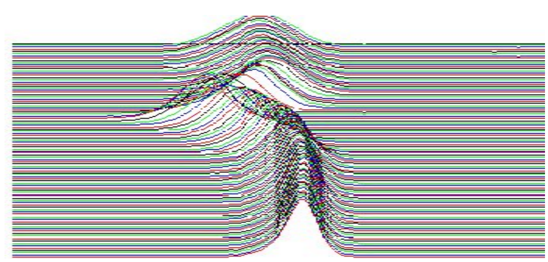

Figure 1: 108 consecutive horizontal profiles of a bunch of $6\times10^{10}$ protons accelerated in the SPS.

of $6\times10^{10}$ protons, (half the nominal LHC intensity). Profiles are very well defined, as can be seen in Figure 2, and the shrinking of the r.m.s. beam size (from 1.2 to 0.7 mm) during acceleration can be easily distinguished.

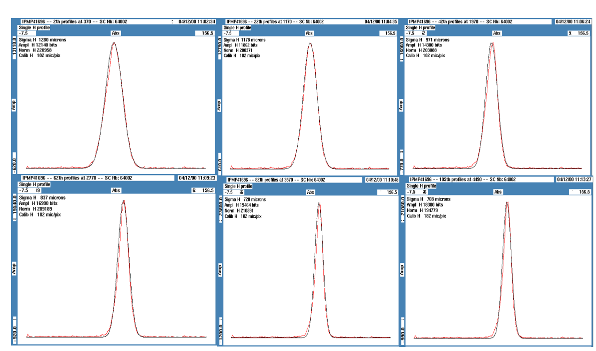

Figure 2: Six horizontal individual bunch profiles of a bunch of $6\times10^{10}$ protons accelerated in the SPS.

The profile of a bunch of $6.10^9$ protons, nearly an LHC pilot bunch, is displayed in Figure 3. This measurement was performed with all gains set at maximum, while maintaining the nominal SPS rest gas pressure of $10^{-8}$ hPa. The signal, although rather noisy, is still exploitable. This confirms that this set-up is suitable for transverse profile

# THE MEASUREMENT AND OPTIMISATION OF LATTICE PARAMETERS ON THE ISIS SYNCHROTRON

D.J. Adams, K.Tilley, C.M.Warsop, Rutherford Appleton Laboratory, Oxfordshire, UK.

*Abstract*

The ISIS Synchrotron accelerates a high intensity proton beam from 70 to 800 MeV at 50 Hz. Recent hardware upgrades to the diagnostics, instrumentation and computing have allowed turn by turn transverse position measurements to be made. A special low intensity beam can also be injected for detailed diagnostic measurements. The analysis of such data at many points around the ring has allowed the extraction of lattice parameters. This information will have significant application for improved beam control. The methods of analysis as well as some applications for setting up and optimising the machine are described in this paper. Future plans and relevance for high intensity performance is also given.

## 1 INTRODUCTION

The ISIS Synchrotron [1] accelerates $2.5\times10^{13}$ protons per pulse at 50 Hz, corresponding to a mean current of 200 µA. To establish high intensity beam, particles are accumulated via charge exchange injection over 120 turns. Beam is then bunched and accelerated from 70 to 800 MeV in 10 ms, extracted in a single turn and transported to the target.

In optimising the machine, extensive use is made of special low intensity 'diagnostic' beams [2]. These are provided by 'chopping' the normal 200 µs injection pulse to ~100 ns (less than one turn) with an electrostatic kicker. The injection painting provides the initial 'kick', and measurement of the turn by turn, transverse motion at a position monitor then allows extraction of numerous ring parameters. Allowance has to be made for the apparent damping caused by the finite Q-spread in the beam. Fitting a suitable function allows the centroid betatron amplitude, the closed orbit position, the betatron Q and phase to be extracted.

This paper describes new measurements and beam control applications, made possible with recent upgrades to the synchrotron diagnostics data acquisition system [3]. These use the low intensity beam at injection together with the new facility to take turn by turn measurements at many position monitors around the ring. The relevance of these measurements to high intensity operation is described in Section 5.

## 2 PHASE SPACE MEASUREMENTS

### 2.1 Basic Measurements

On the ISIS Synchrotron we have two sets of beam position monitors separated by drift spaces, one set per transverse plane. By using the signals from these monitors, it is possible to reconstruct $(y_n, y_n')$ on each turn. The apparent Q-spread damping over many turns can be removed with appropriate use of fitted parameters. The 'corrected' $(y_n, y_n')$ are then fitted with a suitable ellipse to extract alpha, beta and centroid emittance.

Measured phase space ellipses for the vertical plane are shown in Figure 1. In this case measurements were taken with the lattice in two distinct configurations. The first under normal configuration, and the second, with a low field tuning (trim) quadrupole switched off.

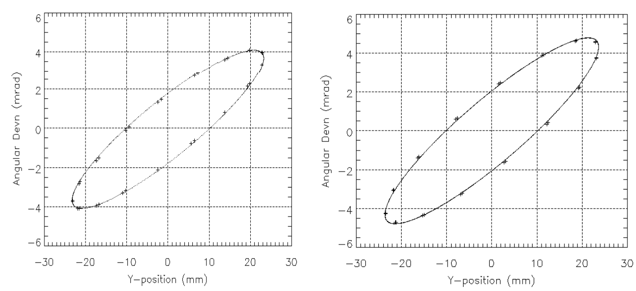


Figure 1. Measured Vertical Phase Space Ellipse.
Left: Normal. Right: Trim Quad off.

To check the measurement, the extracted parameters were compared with the results of a MAD model [4]. The results are shown in Table 1.

Table 1: Fitted parameters and MAD predictions.

| | Alpha | | Beta (m) | |
|---|---|---|---|---|
| **Optics** | **MAD** | **Measured** | **MAD** | **Measured** |
| Normal | -2.09 | -2.05+/-0.2 | 13.37 | 13+/-1.0 |
| TQ Off | -1.92 | -2.1+/-0.2 | 12.43 | 11.5+/-1.0 |

This shows the measurement gives good agreement with theory. Systematic differences are consistent with measured lattice errors, see Section 4.

# FIRST BEAM TESTS FOR THE PROTOTYPE LHC ORBIT AND TRAJECTORY SYSTEM IN THE CERN-SPS

D. Cocq, L. Jensen, R. Jones, J.J. Savioz, CERN, Geneva, Switzerland
D. Bishop, B. Roberts, G. Waters, TRIUMF, Vancouver, Canada

*Abstract*

The first beam tests for the prototype LHC orbit and trajectory system were performed during the year 2000 in the CERN-SPS. The system is composed of a wide-band time normaliser, which converts the analogue pick-up signals into a 10 bit position at 40MHz, and a digital acquisition board, which is used to process and store the relevant data. This paper describes the hardware involved and presents the results of the first tests with beam.

## 1 INTRODUCTION

The LHC Orbit and trajectory prototype system is divided into two parts; an analogue front-end module (WBTN) that processes the signal from the four-button pick-up to produce digitised position data at 40MHz and a Digital Acquisition Board (DAB) that selects, stores and pre-processes the position data. The DAB module is developed at TRIUMF (Vancouver, Canada) using CERN specifications as part of the Canadian contribution to the LHC whereas the WBTN is developed entirely at CERN. An overview of the whole system is shown in Fig. 1. The initial signal is provided by a button pick-up, which is then processed by a wide-band time normaliser, converting the beam position into a pulse modulation at 40MHz. A 10-bit ADC then digitises this signal before a digital acquisition board is used to sort and store the data in memory.

## 2 WIDE BAND TIME NORMALISER

The principle of the Wide-Band Time Normaliser (WBTN) is explained in [1]. The WBTN is used to convert the amplitude ratios of the two signals provided by a pair of electrodes, into a variation in time. In this application an excursion over the full aperture of the BPM corresponds to a pulse width modulation of ~3ns. This variation is measured with an integrator and digitised with a 10-bit ADC at 40MHz. Within a dynamic range in intensity of 40dB, the systematic error measured at the centre is less than 1% (see Fig. 2). This covers the foreseen operating bunch intensities of the LHC, from the pilot bunch at $5\times10^{9}$ protons per bunch to the ultimate $1.7\times10^{11}$ protons per bunch. As the system works at 40MHz, measuring each individual bunch, there is no need to take into account the filling pattern when considering the dynamic range. The RMS random error due to noise remains well below 1% for the nominal and ultimate bunch intensities, rising to 1.3% for the pilot bunch, as can be seen in Fig. 3. The measured position is corrected using a 3rd order polynomial following the theory outlined in [1]. The systematic error can thereby be reduced to around 1% (see Fig. 4).

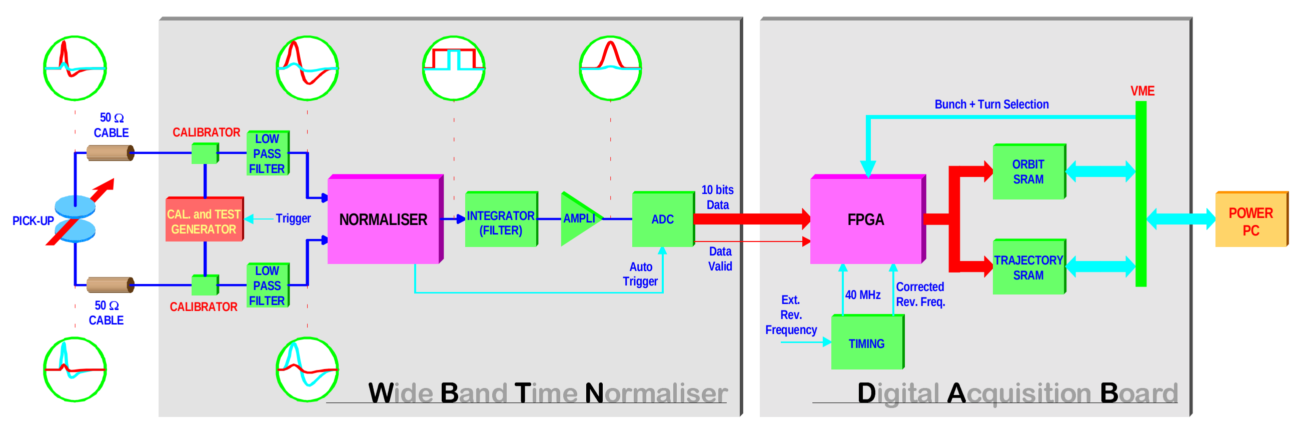


Figure 1: Schematic of the prototype LHC beam position system installed in the CERN-SPS

# BEAM DIAGNOSTICS FOR LOW-INTENSITY RADIOACTIVE BEAMS

L.Cosentino, P.Finocchiaro, LNS - INFN, Catania, Italy

*Abstract*

In order to perform imaging, profiling and identification of low intensity ($I_{beam}<10^5$ pps) Radioactive Ion Beams (RIB), we have developed a series of diagnostics devices, operating in a range of beam energy from 50 keV up to 8 MeV/A. These characteristics do them especially suitable for ISOL RIB facilities.

## 1 INTRODUCTION

At INFN - LNS Catania the ISOL (Isotope Separator On-Line) EXCYT facility (EXotics with CYclotron and Tandem) is under development [1]. It allows the production of radioactive beams with energies from 0.2 up to 8 MeV/A, emittance less than 1π mm·mrad and energy spread below $10^{-4}$.

The radioactive beam is produced by stopping a stable primary beam (A < 48, E $\leq$ 80 MeV/A) inside a thick target. The produced radioactive species are extracted and transported to a high resolution magnetic isobar separator ($\Delta M/M$ = 1/20000), which separates the ions of interest from the isobaric contaminants. The separator consists of two main stages composed of two magnetic dipoles each one, arranged so that the first stage is placed on a 250 kV platform, while the second is grounded. After it the radioactive beam has a kinetic energy of 300 keV and can be directly used for the experiments or accelerated by the 15 MV Tandem. Its intensity falls in a range from $10^3$ pps up to $10^8$ pps, depending on the intensity of the primary beam (< 1 pμA), on the production cross section in the target and on the overall extraction efficiency from the ion source.

In this paper we report on diagnostics devices developed for the beam pipe before the acceleration (kinetic energy from 50 keV to 300 keV), and for the accelerated beams (up to 8 MeV/A).

For the low energy regime, a device for imaging/identification of the beam has been developed. It is based on a CsI(Tl) scintillator plate and exploits the decay of radioactive ions of the beam, since the energy of the emitted radiation (β and γ) is typically above 1 MeV, enough to produce a detectable signal.

Regarding the high energy range, we make use of a couple of devices, capable of identifying and profiling the beam by directly detecting the accelerated ions. The background due to radioactive ions implanted inside the devices does not represent a problem, since its contribution to the overall signal is negligible.

## 2 PREACCELERATION BEAM IMAGING AND IDENTIFICATION

### 2.1 The LEBI device

The beam diagnostics in the preacceleration stage (low energy) is a crucial point, since a quick beam tuning needs an efficient real-time check of the beam properties. The devices should be able to locate the beam position, to measure its transversal size and to identify its nuclear composition. The device named LEBI (Low Energy Beam Imager / Identifier) permits to attain the beam imaging and identification by exploiting the radiation emitted by the radioactive ions, Fig. 1. The core of this system is a scintillator plate of CsI(Tl) and a thin mylar tape arranged in front of the plate. When the film and the scintillator are placed along the beam line in order to intercept the beam, the ions get implanted onto a small film area, which thus becomes a radioactive source. The emitted radiation (mainly β and γ rays) crosses the plate, so producing a light spot. A CCD camera watching the plate allows to determine the beam location and roughly measure its transversal size.

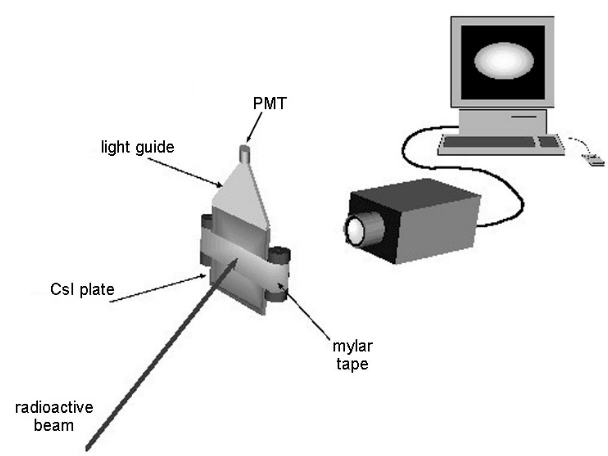


Figure 1: Sketch of the LEBI device for low energy beam imaging and identification.

In order to get as much information as possible to identify the beam, a small photomultiplier (Hamamatsu R7400) used in pulse counting mode is optically coupled to a side of the plate, by means of a light guide. Its main application concerns the identification of implanted nuclear species, by measuring the particle count rate at fixed time intervals, in order to estimate the decay constant λ.

# THE DYNAMIC TRACKING ACQUISITION SYSTEM FOR DAΦNE E+ / E- COLLIDER

A. Drago, A. Stella, Istituto Nazionale di Fisica Nucleare, Laboratori Nazionali di Frascati, Italy

*Abstract*

The goal of this paper is to describe the dynamic tracking acquisition system implemented for the DaΦne e+/e- collider at LNF/INFN. We have been using the system since last year and it has been possible to collect useful information to tune-up the machine.

A four-button BPM is used to obtain the sum and difference signals in both the transverse planes. The signals are acquired and recorded by a LeCroy LC574A oscilloscope with the capability to sample the input waveforms using a beam synchronous external clock generated by the DaΦne Timing System. The start of acquisition is synchronised to a horizontal kick given by an injection kicker. After capturing up to 5000 consecutive turns, data are sent through a GPIB interface to a PC, for processing, presentation and storage. A calibration routine permits to convert voltage data to millimetres values. The acquisition and control program first shows the decay time in number of turns. Then it draws a trajectory in the phase space (position and speed) in both the transverse planes. To do this the software builds a data vector relative to a second "virtual" monitor advanced by 90 degrees. This is done by two alternative ways: applying the Hilbert transform or using the transport matrix method. Examples of data acquired during the collider tune-up are shown.

## 1 INTRODUCTION

DaΦne is a Φ factory presently in operation at the Laboratori Nazionali di Frascati of I.N.F.N. In the last two years it alternated machine development and data taking shifts: during these periods it produces e+/e- collisions to give luminosity to one of the two installed experiments, KLOE in the Interaction Point 1 and DEAR in the Interaction Point 2. Recently DaΦne has reached in the IP1 a peak luminosity of $2.1 \cdot 10^{31}$ $cm^{-2}$ $sec^{-1}$, with an integrated luminosity up to 1.3 $pbarn^{-1}$ per day. The maximum stored current is more than 1 A for electrons and for positrons.

For the non-linear optics studies, a transverse monitor has been installed to record and analyze the dynamic characteristics of the beam by varying the machine parameters.

In this paper we describe the dynamic tracking monitor and acquisition system implemented for DaΦne and show some example of taken data. The system has been used since last year allowing collecting useful information to tune-up the machine.

## 2 DYNAMIC TRACKING

A coherent signal proportional to the transverse displacement of the bunch can be obtained by processing the signal from the beam position monitor electrodes.

The method of dynamic tracking [1] consists in exciting a free transverse betatron oscillation by kicking the beam and recording the transverse displacements at two different azimuths in the storage ring. If the two monitors have π/2 betatron phase difference, then the transverse beam position at the second monitor is proportional to the angle of the beam at the first monitor. Plotting the first monitor data versus the second ones (on turn by turn basis) is equivalent to a phase space plot at the azimuth of the first monitor. A dynamic tracking system makes possible to perform studies on the non-linear beam dynamics [2]. In particular, the tune dependence on amplitude is found by fitting the decay of the coherent signal as a function of the number of turns (an example of a recorded data sequence is shown in Fig.1). The dynamic aperture is defined as the maximum displacement amplitude (the stable acceptance) without intensity loss.

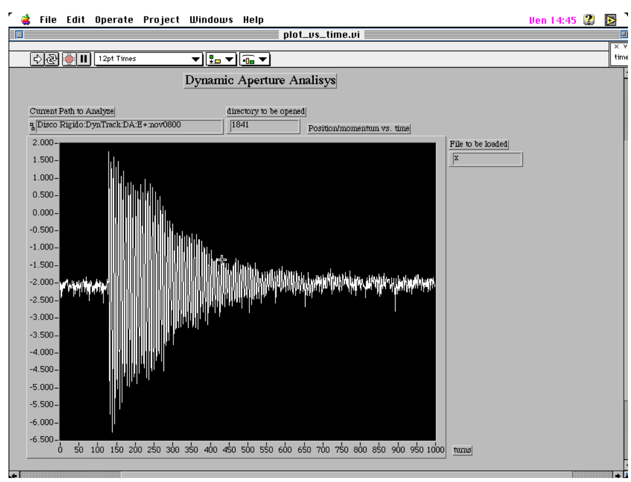


Figure 1: Horizontal displacement (in mm) after a kick versus number of turns.

## 3 SYSTEM DESCRIPTION

### 3.1 *Signal acquisition*

A four-button Beam Position Monitor is used to obtain transverse signals at the passage of a beam. Using hybrid junction components, it is possible to produce sum and

# A HIGH DYNAMIC RANGE BUNCH PURITY TOOL

B.Joly, G.A.Naylor. ESRF, Grenoble, France.

*Abstract*

The European synchrotron radiation facility uses a stored electron beam in order to produce x-rays for the study of matter. Some experiments make use of the time structure of the x-ray beam which is a direct reflection of the time structure in the electron beam itself. Avalanche photo-diodes have been used in an x-ray beam in a photon counting arrangement to measure the purity of single or few bunch filling modes. Conventional techniques measuring the photon arrival times with a time to analogue converter (TAC) achieve dynamic ranges in the $10^{-6}$ range. We report here the use of a gated high count rate device achieving a measurement capability of $10^{-10}$. Such high purity filling modes are required in synchrotron light sources producing x-ray pulses for experiments looking at very weak decay signals as seen in Mossbauer experiments..

## 1 INTRODUCTION

An avalanche photodiode, collects scattered x-ray photons from an x-ray absorber on an unused bending magnet beam-line (fig 1, 2) and is used to measure bunch purity in few bunch modes. The x-ray photons collected by the photodiode create a hundred to a thousand carriers which are then multiplied by avalanche in the junction. An avalanche photodiode is chosen with a thin (10µm) depletion layer to achieve a fast time response (HAMAMATSU model S5343SPL, ref 1). The subsequent electric pulse is amplified (fig 3) and sent to a photon arrival time electronic acquisition time (fig 4).

Such an acquisition system is frequently used in high dynamic range time resolved user experiments (ref 2) and can be used in two different operating regimes:

1) Low count rate mode where the probability of detecting a photon is much less than one per main pulse revolution. The arrival time of all photons is stored and a profile of the time dependent x-ray emission is determined and hence the electron bunch intensity profile as a function of time determined with a very high dynamic range (fig 4). Since photon pile up is rare the plot is fairly linear and accurate with moderate acquisition times (a few minutes) over around 6 orders of magnitude. This is an important diagnostic tool in determining the purity of the main bunch with respect to neighbouring bunches.

2) High count rate where the probability of detecting a photon from the main pulse is much more than one. In this case there is a great non-linearity between the measurement of the main pulse and subsequent pulses. By applying a gate to the discriminator the incoming photon counts can be accepted or de-validated. A gate can then be applied to only allow counts during a specified period after the main pulse. These validated counts are then at a rate much less than 1 per revolution and so the trace becomes linear again but with a much greater sensitivity (up to 10 orders of magnitude below the intensity of the main pulse. Since the main pulse now has an amplitude much higher than the subsequent pulses to be counted (due to the fact that it represents many photons) the gate can only be applied some 10-20ns after the main pulse due to the decay and possible oscillations following the main pulse. Such a diagnostic is then not useable for determining the population in neighbouring electron bunches but is very sensitive to occupancy in bunches more than 20ns following the main pulse up until the neighbouring pulse prior to the next main pulse.

## 2 DIAGNOSTIC CONFIGURATION

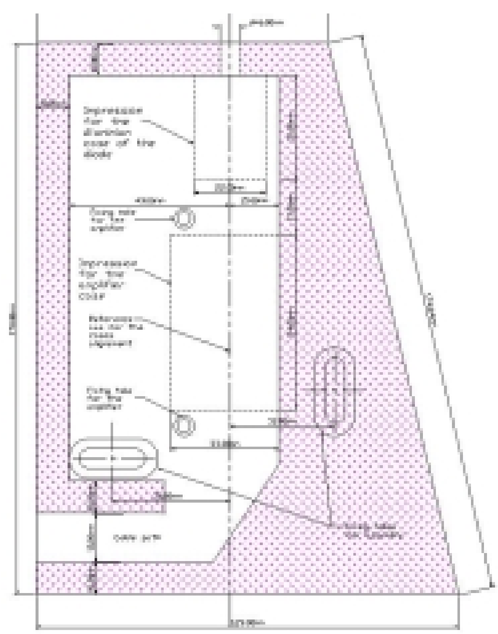

Figure 1: Avalanche photo-diode in lead shielding

A bunch purity diagnostic tool using the first mode of operation is installed on beam line D19. This paper concerns the performance of a bunch purity diagnostic used in the second counting mode. A high count rate is achieved on the D4 beam line (fig 1) using a beryllium window to allow the high flux of Cu K alpha fluorescence photons to be detected. As seen in figure 5, an aluminium

# DSP AND FPGA BASED BUNCH CURRENT SIGNAL PROCESSING

G.A.Naylor ESRF, Grenoble, FRANCE

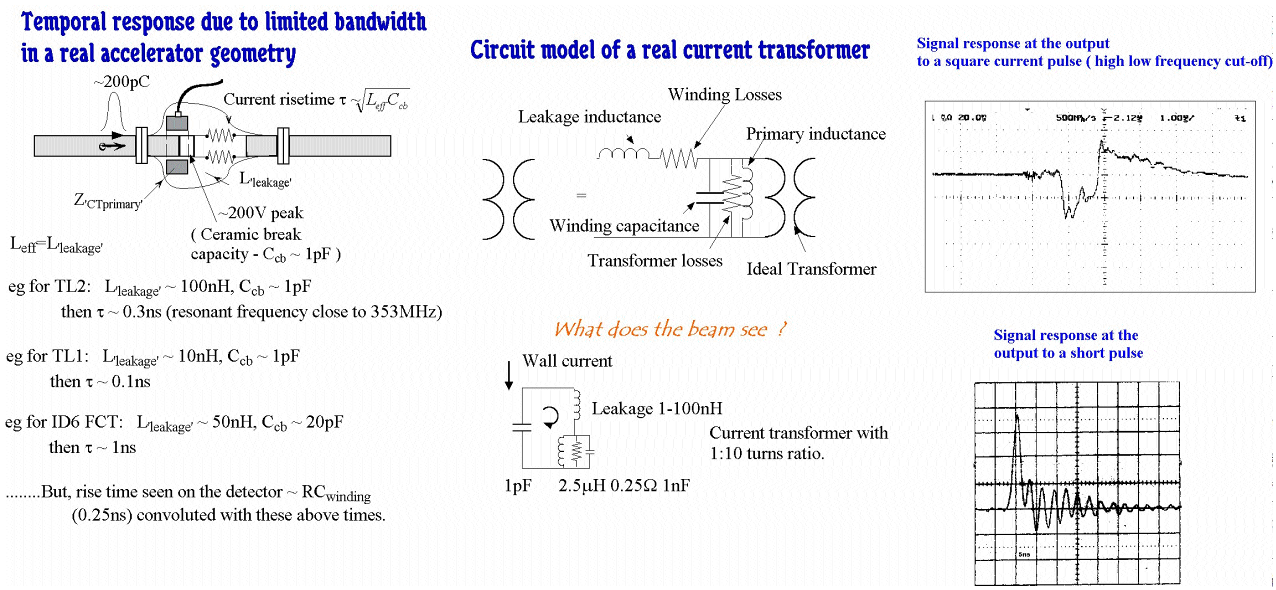


Figure 1 Principles of a fast current transformer to resolve a complex filling pattern


*Abstract*

The current in electron storage rings used as synchrotron light sources must be measured to a very high precision in order to determine the stored beam lifetime. This is especially so in high-energy machines in which the lifetime may be very high. Parametric current transformers (PCT) have traditionally been used to measure the DC or average current in the machine, which offer a very high resolution. Unfortunately these do not allow the different components of a complex filling pattern to be measured separately. A hybrid filling mode delivered at the ESRF consists of one third of the ring filled with bunches with a single highly populated bunch in the middle of the two-thirds gap. The lifetime of these two components may be very different. Similarly the two components are injected separately and can be monitored separately using a fast current transformer (FCT) or an integrating current transformer (ICT). The signals from these devices can be analysed using high speed analogue to digital converters operating at up to 100MHz and digital signal processing (DSP) techniques involving the use of field programmable gate arrays (FPGAs) in order to process the continuous data stream from the converters.


## 1 A NEW CURRENT TRANSFORMER ACQUISITION SYSTEM

There is a need at the ESRF to improve the data acquisition system measuring the current in the various elements of the injection system as well as the storage ring. The requirement is to measure the injection efficiency with a greater precision and reliability in order to provide an interlock against too low an injection efficiency.

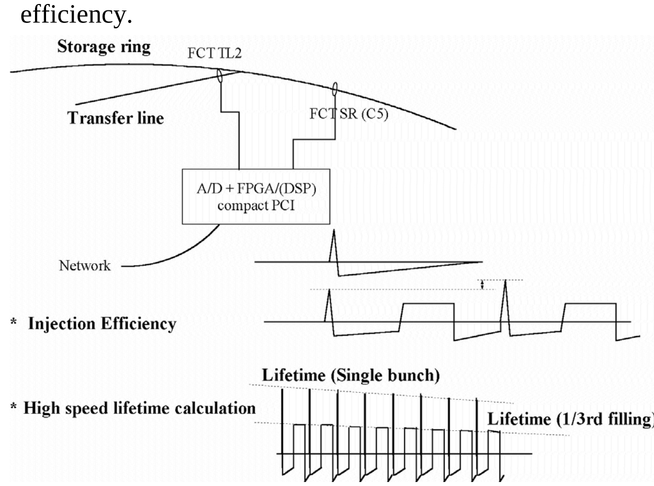


Figure 2 Fast current transformers to compare beam in the transfer line and storage ring

The machine division is examining the feasibility of operating the machine in a ‘topping up’ mode, for which a reliable and accurate measure of the injection efficiency is required. The existing diagnostic acquisition chain based on analogue gating techniques does not provide a

**DISCUSSION 1 : MONDAY AFTERNOON (16.30HRS - 18.00HRS)**

# Orbit Feedbacks for Synchrotron Light Sources

**Discussion animators: Micha Dehler, Daniele Bulfone**

The session is meant to serve as a survey giving an overview on the current status of closed orbit stabilisation and on future needs. Therefore we would be interested to have from each laboratory/project, where appropriate, transparencies on the following discussion topics.

The first general part are noise sources for the beam and requirements with the following items

?? Ground spectra at the different labs, e.g. function of ground humidity, natural seismic noise, man made noise by e.g. external traffic.
?? Transfer function between ground noise and resulting beam movement influenced by the girder design and magnet movement.
?? Beam coupling values, theoretical and real.
?? Thermal drifts due to cooling and variations in the air temperature.
?? Noise from the mains via e.g. the corrector power supplies requiring feedback at 50 Hz and upper harmonics.
?? Other sources of high frequency noise.
?? Resulting bandwidth requirements for feedbacks
?? Feedback compensating for loose and cheap design?

The second part concentrates on closed orbit feedbacks including components and is meant to cover:
?? Requirements for the BPM system: Sampling rates, fast interfacing, self calibration and compensation of e.g. current dependencies.
?? Use of photon BPMs
?? Power supplies: Mains rejection, bandwidth, resolution.
?? Performance of current systems as well features of planned systems.
?? Strategies: Local vs. global feedback systems
?? Feed forward techniques
?? Interference between orbit feedbacks and other feedbacks, e.g. local ones for the stabilisation of optical beam lines or experiments.

## DISCUSSION 2 : MONDAY AFTERNOON (16.30HRS - 18.00HRS)

# Emittance Measurement Techniques

### I. Physical questions.

Short review of the existing techniques, methods and approaches (imaging, interference, projection, betatron coupling) with their advantages and limitations.

New promising methods of emittance diagnostics (short contributions / messages from participants are expected).

How to go from beam profile (size, divergence, etc.) measurements to emittance ? Problems of indirect measurements.

### II. Practical questions.

Emittance, brightness (brilliance), luminosity are very important "passport" characteristics of an accelerator.
In practice, however, lack of time, man-power, sometimes low priority, make it not so easy to construct and maintain a good, reliable emittance diagnostic system.
How this situation can be improved ?

What can be shared (ideas, software, hardware, personnel) ?

How to shorten a long way from a bright idea to a reliable system ?

Can final beam users (e.g. SR users) contribute / share their diagnostics systems or data ?

**DISCUSSION 3 : MONDAY AFTERNOON (16.30HRS - 18.00HRS)**

# Industrial Products for Beam Instrumentation

In various branches of high technology industry there has been considerable progress in the past years which could be used for beam instrumentation.

**The subject will be introduced by two short demonstrations:**

## 1) a demonstration of modern audio electronics

with 24bit-96kHz ADC, digital signal electronics and application programs under windows on a PC, which allow to change the parameters of the signal treatment.

Potential applications are data monitoring at constant sampling frequency, orbit feedbacks (including high power audio amplifiers), noise reduction on beam current transformers....

## 2) digital treatment of video signals

webcams, frame grabbers, CCD-data via USB, all one needs for image acquisitions, in particular interesting for profile measurements.

These introductory demonstrations will not last longer than 30 minutes.

The remaining time will be used to pass through the audience collecting information into a two dimensional table, which shall contain as row index the accelerator and as column index the type of measurement.

The contents of the table will be the "of the shelf" industrial product, that has been used/will be used to perform the task.

This table with some explanation will be put into the conference proceedings, such that the interested parties can take the necessary contacts.

**DISCUSSION 4 : TUESDAY MORNING (11.30HRS - 13.00HRS)**

# Calibration and Stability of Diagnostics Equipment

Topics are divided in 3 categories: *BPMs*, *Current Monitors* and *Optical Monitors*. The animators, Volker Schlott (volker.schlott@psi.ch) and Laurent Farvacque (laurent@esrf.fr) have here below listed issues as a basis for discussion.
Further suggestions and/or contributions are welcome and can be communicated to the animators (preferably before DIPAC in order to adapt the schedule and to allow a proper planning of the discussion session).

## Beam Position Monitors (BPMs):

- Is there a need for calibration of BPM chambers on a test bench?
- Are mechanical resp. machining tolerances (< 0.05 mm) good enough to simply apply theoretical calibration factors, which are derived from EM-simulation codes like MAFIA, POISSON etc…?
- Is the initial error on the complete BPM system, including mechanics and electronics, low enough to store beam (in case of a storage ring) and simply apply the method of *beam based alignment* (BBA) to solve all further calibration issues of the system?
- To what accuracy leads BBA? How often should it be repeated in order to guarantee always a well “calibrated” system?
- How is BBA actually implemented in the different labs?
- Is online calibration of BPM electronics necessary (e.g.: new calibration for each change in gain settings)?
- How often should this procedure be repeated and to what level of accuracy? Is a (short) “time-out” in the position measurement tolerable?
- Are BPM electronics in general stable enough to be only calibrated once (before installation)?
- How important are *absolute* position measurements (with respect to the magnetic center of an accelerator)?
- How important is the reproducibility of a (absolute) “golden orbit”? How close is such a “golden orbit” to a calibrated “BBA” orbit?
- How are drifts resp. movements of the vacuum system (BPM block) considered in determination of beam positions (golden orbits)?
- Usually drifts occur in case of temperature gradients in the vacuum chamber (heat load from the beam) and/or changes in the ambient (tunnel) temperature - locally and globally after a shut-down.
  Should these mechanical drift be monitored and corrected?

## DISCUSSION 5 : TUESDAY MORNING (11:30HRS – 13:00HRS)

# Digital Signal Treatment in Beam Instrumentation

Digital Signal Processing has grown dramatically over the last five years. The evolution of digital logic and processors has opened up the use of digital signal processing in domains, which were reserved to analog signal processing.

In this discussion session we would like to review digital signal treatment for beam diagnostics application.

*Participants are encouraged to present their different approaches and their motivation to do it in one or the other way.*

**Emphasis shall be put on the following subjects:**

?? **Digital Signal Processing for :**

| | | |
|---|---|---|
| **- image processing** | **- BPMs** | **- current monitors** |
| **- beam loss monitors** | **- feedback systems** | **- others** |

**What are the advantages/disadvantages with respect to their analog counterpart?**

?? Digital Signal Processing – Overkill versus more flexibility?

?? Can digital signal processing provide better calibration methods?

?? Do commercial products suit the beam diagnostic needs or are in-house developments inevitable?

?? The fields of digital systems are manifold, different expertise on different levels is needed. Does a digital system need more manpower than a conventional analog system?

?? Trend in digital signal processing:
DSP / General Purpose Processor (PowerPC, Pentium MMX, etc.) / Field Programmable Gate Arrays (FPGA)?

?? Coding dilemma in DSP based systems:
- benefits and drawbacks of low- and high-level programming?
- benefits and drawbacks of using an operating system?

?? How risky is the use of newest commercial products or should one better rely on established hardware/tools with better software environment?

?? Integration into control systems:
What are the possibilities today for the communication with the 'control room'?
How easy is remote debugging?

?? Next generation of diagnostic devices: Could a modular design of a digital signal processing device (general processing unit + customizable signal conditioning hardware) be used as a general purpose diagnostic device?

## DISCUSSION 6 : TUESDAY MORNING (11.30HRS - 13.00HRS)

# Beam Loss Monitors

### 1) A very brief review of different beam loss monitors.

Which, how fast, sensitivity, experiences, reliability, ...

### 2) Where can beam loss monitors help us?

Beside of the information about the intensity and the position of beam losses, what else can beam loss monitors tell us?
BLMs are used for very different kinds of measurements: Tail scans, beam orbit oscillations, ground spectra, tune scans, protection of superconducting magnets, beam lifetime, beam steering, 'dust' detection, dosimetry, beam energy, transversal and longitudinal beam dynamics...

Typically, BLMs are required in case of unwanted beam conditions. However, BLM systems might give a lot of more information.

This discussion session should give a forum for ideas to use the special information from BLM systems to improve and/or understand the behavior of accelerators/storage rings/extraction lines.

Therefore we would be interested to have from different laboratories and projects a short presentation of their use of BLMs and what kind of (beam related) information is extracted.

Further suggestions and/or contributions are welcome and can be communicated to the animators. (Kay.Wittenburg@desy.de)